IBM quantum computers: evolution, performance, and future directions

Muhammad AbuGhanem[1]

Abstract

Quantum computers represent a transformative frontier in computational technology, promising exponential speedups beyond classical computing limits. IBM Quantum has led significant advancements in both hardware and software, providing access to quantum hardware via IBM Cloud® since 2016 and achieving a milestone with the world's first accessible quantum computer. This paper explores IBM's journey in quantum computing, focusing on its contributions to both hardware and software, as well as the development of practical quantum computers. We trace the evolution of IBM Quantum's processors, from the early *canary* processors to the milestone of surpassing the 1000-qubit barrier. In addition to these technological strides, we delve into the practical applications of quantum computing, particularly within nine key industries: airlines, banking, healthcare, electronics, life sciences, and more. We also explore IBM Quantum's case studies and strategic partnerships with organizations such as Boeing, CERN, ExxonMobil, and Cleveland Clinic, which are helping to bridge the gap between theoretical research and real-world applications. Further, we examine the key challenges and solutions in scaling quantum systems and achieving fault tolerance, highlighting IBM's efforts toward building practical, fault-tolerant quantum systems capable of addressing real-world problems.

Keywords IBM Quantum computers · The practical applications of quantum computation · Superconducting quantum computers · Performance of IBM's quantum computers · 1000-qubit processor · Quantum hardware · Quantum computing case studies · Heron · Condor · Qiskit · Boeing · CERN · ExxonMobil · Quantum supremacy

✉ Muhammad AbuGhanem
    gaa1nem@gmail.com

[1] Faculty of Science, Ain Shams University, Cairo 11566, Egypt

🖄 Springer

1 Introduction

Quantum computers represent a revolutionary approach to computation [1], leveraging the principles of quantum mechanics [2, 3] to potentially solve problems that are beyond the reach of classical computers [4–6]. The NISQ era [7] marks a pivotal phase in quantum computing, characterized by rapid advancements and challenges in achieving practical quantum applications [1].

Industry has been facilitating access to quantum computers for both academic and commercial users. Companies such as IBM (2016), Rigetti Computing (2017), IonQ (2020), Honeywell (2020), Google (2020), Xanadu (2020), Oxford Quantum Circuits OQC (2021), PASQAL (2022), QuEra (2022), and Quandela (2022). While others have adopted a reseller model through web-based services. As a result, research on quantum computers has increased significantly. For instance, scientific papers utilizing IBM Quantum's quantum systems via cloud service have reached approximately 2800 as of February 2024, with over 3 trillion circuits executed through IBM Quantum platform [8].

IBM Quantum [9] has emerged as a key player in the quantum computing landscape, leading efforts to advance both quantum hardware and software capabilities. The development of scalable quantum processors based on superconducting qubits has been central to IBM Quantum's research and development efforts. Over the years, IBM has made significant strides in increasing qubit counts, improving qubit coherence times, and implementing error correction techniques necessary for reliable quantum computation [10, 11]. These advancements have positioned IBM Quantum as a leader in quantum computing research, with broad implications ranging from computational chemistry and optimization to cryptography and machine learning [10–13].

This paper explores IBM Quantum's journey in quantum computing, highlighting key technological achievements, current challenges, and future prospects. The study aims to present a comprehensive review of detailed performance metrics across IBM Quantum's quantum computers, crucial for historical documentation within the NISQ era literature. Metrics examined include relaxation times, qubit frequency and anharmonicity, readout assignment errors and readout length, single-qubit gate errors, connection errors, and gate times.

2 Design philosophy

This paper is structured as follows: Sect. 3 offers an overview of IBM Quantum's quantum computing initiative. Section 4 explores the practical applications of quantum computing, focusing specifically on IBM Quantum's quantum systems. In this section, we examine how quantum technology is being adopted across nine major industries: airlines, banking, chemicals, electronics, government, healthcare, insurance, life sciences, and logistics. For each industry, we highlight three real-world use cases that demonstrate the transformative potential of quantum solutions.

In Sect. 5, we discuss three critical metrics-Scale, Quality, and Speed-that are essential for assessing the performance of quantum computing systems. These

metrics serve as vital benchmarks for evaluating progress in near-term hardware capabilities. Section 6 traces the evolution of IBM Quantum's hardware, from the early 5-qubit *Canary* processor to the achievement of the 1000-qubit milestone with the *Condor* processor. In Sect. 7, we summarize the performance and characteristics of IBM Quantum's quantum computers, reviewing both current systems and their capabilities, as well as retired systems and simulators.

Moving to Sect. 8, the focus shifts to IBM Quantum's software and tools, examining key technologies such as Qiskit, Qiskit Patterns, and Qiskit Circuits, alongside advanced features like quantum serverless computing and circuit design tools. Section 9 delves into IBM Quantum's strategic partnerships and use cases, highlighting collaborations with major organizations such as Boeing, CERN, ExxonMobil, Cleveland Clinic, E.ON, Mitsubishi Chemical, JSR, Keio University, and Mercedes-Benz. These partnerships are crucial to advancing quantum computing applications across a range of industries and bringing us closer to achieving a quantum advantage.

While IBM Quantum's contributions are undeniably significant, they represent just one facet of the broader and rapidly evolving quantum landscape. To gain a fuller perspective, Sect. 10 explores the efforts of other leading companies and research institutions in the field, such as Google Quantum AI, Rigetti Computing, IonQ, Quantinuum, Xanadu, Oxford Quantum Circuits, QuEra, Quandela Cloud, Microsoft, Alibaba Quantum, Intel Quantum, UST China, and TU Delft. By examining these developments, we deepen our understanding of the global push toward scalable, fault-tolerant quantum systems.

Section 11 outlines IBM Quantum's Technology Roadmap and its ongoing initiatives to make practical quantum computing a reality (Sect. 11.1). This includes a focus on quantum safety, along with a detailed look at IBM Quantum's Hardware Development Roadmap: Milestones $(2016 - 2033+)$ in Sect. 11.3. Each milestone is presented in three parts: (1) Strategy Overview, (2) Significance for clients and society, and (3) Innovations that will drive progress, with an emphasis on the delivery of solutions to clients and partners.

Despite IBM Quantum's significant progress, challenges remain in developing fault-tolerant quantum systems (Sect. 12), particularly concerning issues like noise, error correction, qubit connectivity, and scalability. Section 12.1 discusses these scalability challenges in detail, while Sect. 12.2 explores IBM Quantum's strategies for addressing them. These strategies include a combination of hardware innovations, modular architectures, and advanced error correction techniques [14].

IBM Quantum's long-term vision for quantum computing-particularly using superconducting qubits-highlights both the complexity of these challenges and the approaches required to overcome them [15]. To achieve a computational advantage, substantial advancements in quantum error correction will be necessary to address issues such as noise and qubit connectivity, along with other hardware limitations [7]. Section 12.3 discusses IBM Quantum's work on quantum error mitigation and quantum error correction (QEC), while Sect. 12.4 explores IBM Quantum's plans for building fully fault-tolerant quantum systems that can address real-world problems.

Finally, Sect. 13 presents the conclusion, synthesizing the key findings and their implications for the future of IBM Quantum technology.

3 IBM quantum

3.1 Overview

IBM Quantum is a leading provider of quantum computing resources, offering access to top-of-the-line quantum hardware that is built with the latest technology to meet the needs of researchers, industry professionals, and developers.

IBM Quantum operates the most sophisticated collection of quantum systems globally, currently featuring seven utility-scale systems, with additional systems in development. These systems are known for their exceptional reliability, boasting over 95% uptime collectively. They also demonstrate remarkable stability, with minimal fluctuations in two-qubit gate errors, which do not exceed 0.001 over periods spanning several months (median 2-qubit gate errors measured across all accessible *Eagle* processors from July 20 to September 20, 2023) [16].

In 2023, IBM has introduced its latest quantum computing milestone with the unveiling of *Condor*, a quantum processor featuring 1121 superconducting qubits arranged in a honeycomb configuration [17]. This follows the pattern set by earlier record-breaking machines such as *Eagle*, a 127-qubit chip launched in 2021 [16, 18], and *Osprey*, a 433-qubit processor announced November 2022 [19]. As part of its strategy, IBM also introduced a new quantum chip named *Heron*, boasting 133 qubits and achieving a remarkable record-low error rate that is three times lower than that of IBM's previous quantum processor. This achievement marks a departure from IBM's previous strategy of doubling qubit counts annually, signaling a shift toward prioritizing enhanced error resistance over further qubit scalability [11, 17].

IBM Quantum offers a wide range of hardware and software resources that support learning, experimentation, and collaboration in the field of quantum computing, as detailed in this paper, with promising implications for accelerating scientific discovery, enhancing computational efficiency, and addressing complex real-world problems.

3.2 Breaking the 1000-qubit barrier

IBM Quantum has introduced IBM *Condor*, a quantum processor with 1121 superconducting qubits based on IBM Quantum's cross-resonance gate technology [17]. *Condor* sets new standards in chip design (see Fig. 1), featuring a 50% increase in qubit density, enhancements in qubit fabrication and laminate size, and over a mile of high-density cryogenic flex I/O wiring within a single dilution refrigerator.

Moving to high performing quantum processors, IBM Quantum introduced the first IBM Quantum *Heron* processor on the *ibm_torino* quantum system. Featuring

Fig. 1 IBM's latest quantum processor *Condor*, unveiled in 2023, features 1121 superconducting qubits arranged in a honeycomb configuration. (Credit: Ryan Lavine, IBM)
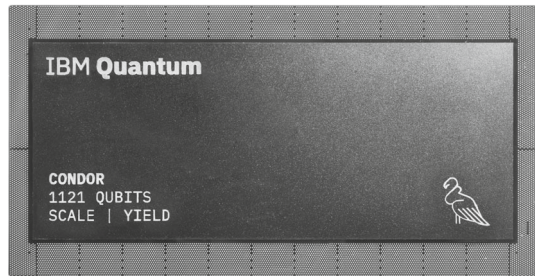
133 fixed-frequency qubits with tunable couplers. *Heron* delivers significant improvements in device performance (a 3-5x improvement in device performance) compared to IBM Quantum's previous flagship 127-qubit *Eagle* processors [16, 18], while virtually eliminating cross-talk. With *Heron*, IBM Quantum has developed qubit and gate technology that forms the foundation of IBM Quantum's hardware roadmap moving forward.

3.3 IBM quantum's system two

IBM Quantum System Two serves as the foundation for scalable quantum computation and is currently operational at the IBM lab in Yorktown Heights, NY. Housing three IBM Quantum *Heron* processors, integrating cryogenic infrastructure with third-generation control electronics and classical runtime servers (see Fig. 2). IBM Quantum System Two features a modular architecture designed to facilitate parallel circuit executions, which are essential for achieving quantum-centric supercomputing [15].

4 The practical applications of quantum computation

Quantum computing offers transformative potential for industries by solving complex problems more efficiently, cost-effectively, and with greater precision than classical systems. The true power of quantum computing lies in its ability to complement and enhance classical computing, creating a synergy that can unlock new possibilities. As advancements in quantum hardware, software, and algorithms converge, industries can expect significant breakthroughs that go beyond the capabilities of traditional systems [1]. This section explores how quantum computing is being adopted across various sectors, including airlines, banking, healthcare, and more, highlighting industry-specific use cases and insights. While the path to achieving "Quantum Advantage" may take time, businesses can already begin to benefit from the exponential progress and learning that quantum computing promises.
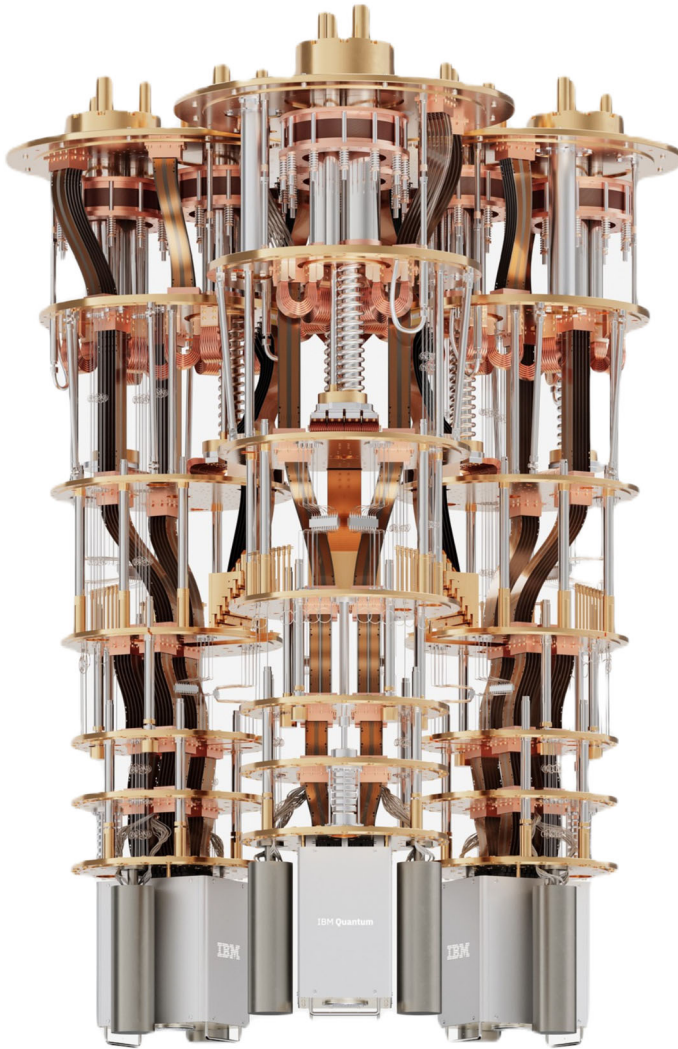
Fig. 2 IBM Quantum System Two, unveiled at the IBM Quantum Summit 2023, represents IBM's first modular quantum computer and serves as a foundational element in IBM's quantum-centric supercomputing architecture. (Image source: IBM Quantum)

4.1 Airline

Quantum computing is revolutionizing the airline industry by addressing complex operational challenges and enhancing customer experiences. As global travel recovers from the COVID-19 pandemic, airlines are leveraging quantum technologies to tackle inefficiencies in operations, improve personalization, and optimize planning. The computational power of quantum systems provides faster decision-

making and more advanced algorithms, enabling the industry to remain competitive in an increasingly dynamic environment.

Use Cases Quantum computing helps airlines manage Irregular Operations (IROPS) by enabling integrated recovery models and enhancing customer satisfaction with rapid solutions [20]. It also enhances personalized customer services by analyzing multidimensional data to refine customer segmentation and improve marketing strategie [21]. Additionally, quantum systems optimize global network planning by unifying fleet, crew, fuel, and revenue management into a single model, ensuring cost-effective and efficient operations. These advancements position airlines to offer streamlined and customer-focused services while boosting profitability [22].

4.2 Banking and financial markets

Quantum computing holds the potential to revolutionize the banking and financial markets by tackling complex challenges such as market uncertainty, constrained system optimization, and profitable opportunity identification. This technology enhances traditional financial models, enabling faster and more accurate assessments of market risks, responses to volatility, and utilization of behavioral data for superior customer engagement. While widespread applications may take time, financial institutions are already exploring quantum computing to transform operations like client management, trading, asset management, and compliance, offering a competitive edge in an increasingly dynamic market [20].

Use Cases Quantum computing aids financial institutions in targeting and prediction by improving data modeling for personalized services, fraud detection, and customer acquisition [23]. It enhances risk profiling by accelerating scenario simulations and refining compliance with regulatory standards like Basel III. Additionally, quantum algorithms optimize trading by enabling more effective portfolio diversification, rebalancing, and scenario analysis, reducing costs and boosting portfolio performance. Together, these advancements streamline operations and position financial institutions to better navigate market complexities and customer demands.

4.3 Chemicals and petroleum

Quantum computing is set to transform the chemicals and petroleum industries by addressing challenges such as complex molecular modeling, optimizing refining processes, and improving resource extraction. These industries, crucial to the global economy (contributing approximately 5.7 trillion to global GDP and supporting over 120 million jobs [24]), face computational bottlenecks when simulating molecular behaviors or managing supply chain logistics. For instance, the simple hydrocarbon Naphthalene ($C_{10} H_8$) can be simulated using approximately 116 qubits. In contrast, a classical computer would need around 10^{34} bits to perform the same simulation [25]. To put this into perspective, 10^{34} bits is roughly 7.1 billion times the amount of data expected to be stored electronically by 2025, which is estimated to be

around 175 zettabytes [26]. Quantum algorithms offer a scalable and efficient solution, enabling precise molecular simulations, refined operations, and innovative methods for expanding resource production. This technology has the potential to reduce costs, enhance efficiency, and drive sustainable innovations across the value chain.

Use Cases Quantum computing accelerates chemical product development by enabling accurate simulations for catalysts and surfactants, revolutionizing product design and emissions reduction efforts [27]. It optimizes feed-stock routing and refining processes, reducing inefficiencies such as octane giveaways, which cost billions annually [28]. Additionally, it enhances reservoir production by modeling molecular-scale subsurface interactions, improving resource extraction efficiency and boosting profitability [25]. These applications demonstrate the profound impact of quantum computing on operational efficiency and industry sustainability.

4.4 Electronics

The electronics sector, a linchpin of modern technology and the global economy, faces mounting challenges, including the escalating costs of semiconductor manufacturing, plateauing advancements in product performance, and inefficiencies in design and production processes. As Moore's Law slows, traditional approaches to driving innovation and efficiency are becoming less effective. Quantum computing presents a groundbreaking alternative, offering solutions to complex problems in materials science, product design, and manufacturing optimization. By leveraging its computational advantages, quantum technology can help the industry overcome current barriers, ensuring continued progress and competitiveness.

Use Cases Quantum computing holds transformative potential for the electronics industry across materials development, product design, and manufacturing. It can revolutionize materials research by accurately simulating molecular interactions, enabling breakthroughs like more efficient displays and eco-friendly manufacturing chemicals [29]. In product design, quantum optimization accelerates development by solving complex challenges, such as optimizing chip layouts and enhancing bug detection, reducing time-to-market and improving reliability [30]. For manufacturing, quantum-enhanced AI significantly improves defect detection accuracy, reducing false positives and minimizing financial losses, while optimizing production processes sustainably [31, 32]. Together, these capabilities position quantum computing as a pivotal driver of innovation and efficiency in electronics.

4.5 Government

Governments are under growing pressure to address complex challenges, such as climate change, social program sustainability, and transportation infrastructure strain, while balancing limited resources. Quantum computing offers a transformative solution by enabling more efficient problem-solving, accelerating decision-making, and reducing costs. With the ability to tackle intricate simulations and optimization tasks, quantum computing holds the promise of enhancing public services, improving

emergency responses, and supporting sustainable development across various sectors.

Use Cases Quantum computing can revolutionize government operations through enhanced emergency preparedness, transportation management, and fraud detection. It can optimize disaster response by improving real-time analysis and resource allocation, as seen in wildfire evacuation planning [33]. In transportation, quantum algorithms can streamline traffic management, reducing congestion and enhancing flow efficiency, leading to significant economic benefits [25, 34]. For social programs, quantum-enhanced machine learning can improve fraud detection, saving billions annually while ensuring resources are directed to those in need [35]. These advancements demonstrate quantum computing's potential to elevate government efficiency and service delivery.

4.6 Healthcare

Healthcare is increasingly driven by data, with rapidly growing volumes from clinical trials, electronic health records, and medical devices. These data are pivotal in achieving healthcare's "quadruple aim": enhancing outcomes, reducing costs, improving patient experiences, and supporting practitioners [36]. However, classical computing systems struggle with the scale and complexity of this data. Quantum computing offers transformative potential, promising faster processing, deeper insights, and improved efficiency across various applications. While its adoption requires significant investment and innovation, quantum computing could reshape healthcare by augmenting classical systems and addressing critical challenges.

Use Cases Quantum computing can transform healthcare in diagnostics, insurance, and precision medicine [37]. In diagnostics, it can enhance medical imaging and biomarker discovery, improving early detection and accuracy [38, 39]. For insurance, quantum algorithms enable more precise risk assessments, fraud detection, and tailored pricing, lowering premiums and increasing transparency [20, 40]. In precision medicine [37], quantum models can better predict disease risks and optimize treatment plans by analyzing complex genetic and molecular data [41–43]. These advancements promise personalized care, lower costs, and better patient outcomes, positioning quantum computing as a cornerstone of future healthcare innovation.

4.7 Insurance

The insurance industry faces significant challenges in maintaining competitiveness amid technological advancements and economic uncertainty. To keep pace, insurers require more sophisticated models for pricing, risk management, and claims processing-tasks that often exceed the capabilities of classical computing. Quantum computing promises to deliver enhanced computational power, enabling insurers to improve decision-making, adapt to market changes, and better manage large-scale risks. By complementing AI and machine learning techniques, quantum technology could optimize underwriting, customer segmentation, pricing, and overall portfolio

management, opening new opportunities for innovation and more personalized services [34, 44].

Use Cases Quantum computing holds great potential to revolutionize the insurance sector through three key use cases: customer and risk classification, risk concentration analysis, and catastrophe and mortality protection. In customer and risk classification, quantum-enhanced machine learning can improve data analysis and uncover deeper insights, enabling more precise pricing and personalized policies [44]. In risk concentration analysis, quantum optimization could help insurers balance policy design and pricing more effectively while managing risks [44]. Lastly, quantum computing can enhance the forecasting of catastrophic events and mortality risks, improving the accuracy and speed of scenario modeling, leading to better risk management, capital allocation, and regulatory compliance [25].

4.8 Life sciences

Quantum computing holds transformative potential in life sciences, particularly in addressing the industry's most computationally demanding challenges. It could significantly advance genomics, drug discovery, and protein folding predictions, unlocking new opportunities in precision medicine. By providing enhanced computational power, quantum algorithms can model complex molecular interactions, analyze vast datasets more efficiently, and predict biological phenomena with greater accuracy. This could lead to breakthroughs in personalized treatments, faster drug development, and better understanding of protein functions, all of which are critical to improving patient outcomes and advancing healthcare.

Use cases The application of quantum computing in life sciences spans several key areas. First, in precision medicine, quantum computing can link genomic data with health outcomes to create highly personalized therapies, improving treatment efficacy [45–48]. In drug discovery, quantum algorithms can simulate molecular interactions with greater precision, reducing development time and costs while identifying more effective drug candidates [49–51]. Lastly, protein folding predictions could be revolutionized by quantum computing, enabling more accurate predictions of protein structures, which are essential for designing biologic drugs like antibodies and vaccines [52–57]. These advancements could lead to more effective, targeted therapies and improve the overall drug development process.

4.9 Logistics

Quantum computing holds significant potential to address the complexities and challenges faced by the logistics sector. As globalization continues to increase the scale and scope of supply chain networks, logistics companies need advanced computational tools to optimize operations, reduce costs, and improve efficiency. Traditional computing methods often struggle to handle the enormous data volumes and complexities involved in logistics management, particularly as demand for faster and more sustainable solutions rises. Quantum computing can provide the required computational power to enhance solutions for issues such as last-mile delivery,

disruption management, and sustainable maritime routing, ultimately leading to improved service and cost savings.

Use cases Quantum computing can be applied to logistics in several impactful ways. In last-mile delivery, quantum algorithms could optimize routing and fleet management, enabling more frequent re-optimization and improved efficiency, reducing transportation costs significantly [58]. In disruption management, quantum computing could enhance decision-making by simulating multiple disruption scenarios, improving recovery times and lowering operational costs [59]. Lastly, in sustainable maritime routing, quantum algorithms could help optimize global shipping operations by forecasting demand more accurately and improving container repositioning, resulting in cost savings and reduced carbon emissions [57]. These applications demonstrate the transformative potential of quantum computing in the logistics sector, enabling faster, more sustainable, and cost-effective operations.

5 Scale, quality, and speed

Quantum computing performance can be measured by the amount of meaningful work a quantum computer can complete in a given time period. Accurately defining the appropriate performance metrics is essential for both users and developers of quantum computing systems.

For instance, Quantum volume (QV) is a key metric that quantifies the capability of a quantum computer by measuring the largest random circuit it can implement with equal width and depth [60]. It is closely tied to system performance factors such as gate error rates, qubit coherence, and connectivity. Higher quantum volumes generally indicate better overall system performance, including reduced errors and more efficient computations [60]. Achieving higher quantum volume requires improvements in high-fidelity operations, robust qubit connectivity, and advanced circuit rewriting techniques. These improvements, alongside high-quality state preparation and readout, enable quantum systems to scale up quantum volume while maintaining or increasing qubit count.

Additionally, the study in [61] highlights three critical attributes for assessing quantum computer performance: quality, speed, and scale. Quality is evaluated using quantum volume [60], while scale is determined by the number of qubits. To address speed, a benchmark for measuring Circuit Layer Operations Per Second (CLOPS) is introduced in [61]. CLOPS is a metric that indicates the number of QV circuits a quantum processing unit (QPU) can execute within a given time period. This benchmark provides insights into how both quantum and classical components contribute to overall system performance. Additionally, a procedure for measuring CLOPS and apply it to evaluate the performance of various IBM Quantum systems is also presented in [61].

As IBM's quantum processors evolve, these metrics remains a crucial benchmark for evaluating progress in near-term hardware capabilities. For detailed information on these performance metrics and their relation to overall quantum system performance, readers are directed to [60, 61].

6 The progression of IBM quantum's hardware

IBM Quantum has developed several generations of quantum computers, each contributing to the advancement of quantum computing capabilities. These systems are built with cutting-edge superconducting quantum processors based on transmon qubits, chosen for their ability to offer control and scalability [62].

Processor types are categorized based on their technological attributes, identified by a combination of family and revision [63]. The term "family" (e.g., *Falcon*) denotes the potential circuit size and complexity achievable on the chip, primarily dictated by the number of qubits and their connectivity structure. "Revisions" (e.g., r1) signify different design variants within a specific family, see Table 1. These systems represent ongoing advancements in quantum computing hardware, supporting research and development in quantum algorithms and applications. In this section, we summarize the progression of IBM Quantum's quantum processors.

6.1 Canary

The *Canary* family encompasses compact designs featuring between 5 and 16 qubits, utilizing an optimized 2D lattice where all qubits and readout resonators reside on a single layer [63]. This family has seen several revisions aimed at refining and expanding its capabilities. The original r1 design (January 2017) introduced the *Canary* series with 5 qubits, integrating resonators and qubits on a single lithography layer, marking an initial step in advancing quantum computational capabilities. Building upon this, *Canary* r1.1 (May 2017) expanded the processor's capacity, accommodating up to 16 qubits. Also, *Canary* r1.3 (December 2019), which focused on a minimalist design featuring a single qubit, aimed at fundamental quantum computing research [63].

6.2 Falcon

The *Falcon* family is tailored for medium-scale circuits, boasting a QV (quantum volume) of 128. It serves as a crucial testing ground for demonstrating performance enhancements and scalability improvements before integrating them into larger quantum devices. Native gates and operations supported by *Falcon* devices include `CX, ID, DELAY, MEASURE, RESET, RZ, SX, X, IF_ELSE, FOR_LOOP, and SWITCH_CASE.`

Within the *Falcon* family, several revisions have been developed to refine and expand its capabilities: The series commenced with *Falcon* r1 in February 2020, characterized by its 28-qubit design with independent readout and utilizing a heavy-hexagonal connectivity graph optimized for cross-resonance two-qubit gates. April 2020 saw the introduction of *Falcon* r4, which introduced multiplexed readout capabilities, improving qubit state readout efficiency compared to previous independent signal pathways. *Falcon* r5.10, released in December 2020, pioneering advanced on-chip filtering methods that laid the groundwork for faster qubit state

Table 1 Summary of the IBM Quantum's quantum processors and their progressions

No.	Processor	Qubits[a]	QV	Revisions	Update	Date	Details
1	Canary	5–16	–[b]	Canary r1	• The original r1 design introduced the *Canary* series with 5 qubits, integrating resonators and qubits on a single lithography layer, marking an initial step in advancing quantum computational capabilities	January 2017	Sec. 6.1
				Canary r1.1	• Expanded the processor's capacity significantly, accommodating up to 16 qubits	May 2017	
				Canary r1.3	• Focused on a minimalist design featuring a single qubit, aimed at fundamental quantum computing research	December 2019	
2	Falcon	27	128	Falcon r1	• The first iteration in the *Falcon* series. Featuring a 28-qubit design with independent readout and utilizing a heavy-hexagonal connectivity graph optimized for cross-resonance two-qubit gates	February 2020	Sec. 6.2
				Falcon r4	• Introduced multiplexed readout capabilities, improving qubit state readout efficiency compared to previous independent signal pathways	April 2020	
				Falcon r5.10	• Pioneering advanced on-chip filtering methods that laid the groundwork for faster qubit state readouts in subsequent revisions	December 2020	
				Falcon r5.11	• Which improved qubit state readout speed through innovative on-chip filtering techniques. Such enhancements are pivotal for demonstrating quantum error correction and facilitating mid-circuit measurements	January 2021	
				Falcon r8	• Brought enhanced coherence properties, building upon the advancements of previous version	September 2021	
3	Egret	33	512	Egret r1	• *Egret* applies tunable coupler advancements to a 33-qubit architecture, yielding in faster and more accurate (high-fidelity) two-qubit gates	December 2022	Sec. 6.3
4	Hummingbird	65	128	Hummingbird r1	• Marked the initial endeavor to support a large number (>50) of qubits on a single chip	October 2019	Sec. 6.4
				Hummingbird r2	• Leveraging improvements include readout multiplexing, efficient qubit-qubit couplers, and flip-chip technology	August 2020	
				Hummingbird r3	• A 65-qubit design with enhanced coherence properties	December 2021	

Table 1 continued

No.	Processor	Qubits[a]	QV	Revisions	Update	Date	Details
5	Eagle	127	128	Eagle r1	• Leveraging similar design elements and parameters as *Falcon* r5.11	December 2021	Sec. 6.5
				Eagle r3	• Featuring a 127-qubit processor with enhanced coherence properties while maintaining design continuity with *Eagle* r1	December 2022	
6	Osprey	433	–	–	• The *Osprey* processor, setting new benchmarks in quantum computational power. *Osprey* incorporates enhanced device packaging technologies and custom flex cabling within the cryostat, enabling higher I/O capabilities within the same wiring footprint	November 2022	Sec. 6.6
7	Heron	133–156	512	Heron r1	• This upgrade includes enhancements in signal delivery, utilizing high-density flex cabling to facilitate fast and high-fidelity control over both single-qubit and two-qubit operations	December 2023	Sec. 6.7
				Heron r2	• The processor has been re-designed to combine 156 qubits in a heavy-hexagonal lattice. It also offers a new TLS mitigation capability that manages the chip's TLS environment, enhancing overall coherence and stability. Currently accessible through the *ibm_fez* quantum computer	July 2024	
8	Condor	1121	–	–	• A quantum processor with 1121 superconducting qubits based on IBM Quantum's cross-resonance gate technology. Condor marks a significant advancement in chip design, featuring a 50% increase in qubit density	December 2023	Sec. 6.8

[a] Maximum number

[b] Value absent; not shown in the source

readouts in subsequent revisions. This version also implemented space-saving "direct-couplers" to enhance qubit coupling efficiency, crucial for scaling quantum systems. *Falcon* r5.11, launched in January 2021, further improved qubit state readout speed through innovative on-chip filtering techniques, facilitating quantum error correction and mid-circuit measurements. In September 2021, the introduction of *Falcon* r8 brought enhanced coherence properties, building upon the advancements of previous versions [63].

6.3 Egret

The *Egret* quantum processor features a QV of 512 and introduces tunable couplers on a 33-qubit platform, significantly enhancing the speed and fidelity of two-qubit gates. In December 2022, IBM Quantum launched the first iteration of the *Egret* processor, designated as r1. It demonstrated the highest QV among IBM Quantum systems, marking substantial advancements in reducing two-qubit gate error rates. The *Egret* quantum processor delivers notable improvements in gate fidelity, with many gates achieving 99.9% fidelity, while also minimizing spectator errors [63].

6.4 Hummingbird

The *Hummingbird* family features a QV of 128 and utilizes a heavy-hexagonal qubit layout, accommodating up to 65 qubits. October 2019 marked the debut of *Hummingbird* r1, representing the initial effort to support a large number (>50) of qubits on a single chip, setting the stage for subsequent advancements in quantum processor design and scalability. August 2020 saw the release of *Hummingbird* r2, featuring 65 qubits and leveraging improvements, such as readout multiplexing, efficient qubit-qubit couplers, and flip-chip technology, which collectively enhance the scalability and operational capabilities of the *Hummingbird* family. In December 2021, *Hummingbird* r3 introduced a 65-qubit design with enhanced coherence properties, reflecting advancements in quantum processing stability and performance [63].

6.5 Eagle

The *Eagle* family boasts a QV of 128 and integrates advanced packaging technologies to accommodate 127 qubits [18]. These processors employ a heavy-hexagonal qubit layout, where qubits are connected to two or three neighbors, resembling the edges and corners of tessellated hexagons [18], see Fig. 3. This layout minimizes errors from interactions between adjacent qubits, thereby enhancing processor reliability and functionality without compromising performance [16]. Native gates and operations supported include `ECR, ID, DELAY, MEASURE, RESET, RZ, SX, X, IF_ELSE, FOR_LOOP, AND SWITCH_CASE.`

In December 2021, *Eagle* r1 was introduced, leveraging similar design elements and parameters as *Falcon* r5.11. This version supports fast qubit readout and aims for comparable gate speeds and error rates [16]. In December 2022, *Eagle* r3 was
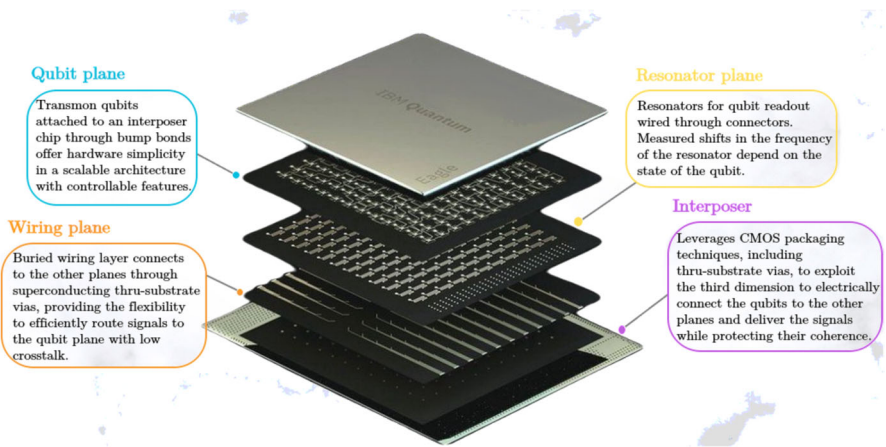
✑ Springer

Qubit plane
Transmon qubits attached to an interposer chip through bump bonds offer hardware simplicity in a scalable architecture with controllable features.

Resonator plane
Resonators for qubit readout wired through connectors. Measured shifts in the frequency of the resonator depend on the state of the qubit.

Wiring plane
Buried wiring layer connects to the other planes through superconducting thru-substrate vias, providing the flexibility to efficiently route signals to the qubit plane with low crosstalk.

Interposer
Leverages CMOS packaging techniques, including thru-substrate vias, to exploit the third dimension to electrically connect the qubits to the other planes and deliver the signals while protecting their coherence.

Fig. 3 IBM Quantum's *Eagle* processors family configuration. These processors utilize a heavy-hexagonal qubit layout, where qubits connect with two or three neighboring qubits resembling edges and corners of tessellated hexagons. This design reduces errors caused by interactions between adjacent qubits, thereby improving processor reliability and functionality while maintaining high performance

released, featuring a 127-qubit processor with enhanced coherence properties while maintaining design continuity with *Eagle* r1 [63]. Currently, *Eagle* systems are deployed at various IBM Quantum's quantum computers. The error map and layout of a quantum computer that is built based on an *Eagle* processor, such as *ibm_sherbrooke*, is depicted in Fig. 4.

6.6 Osprey

The *Osprey* quantum processor boasting 433 qubits, nearly four times the size of its predecessor, *Eagle*. *Osprey* integrates enhanced device packaging technologies and custom flex cabling within the cryostat, enabling higher I/O capabilities within the same wiring footprint. IBM Quantum unveiled the *Osprey* processor in November 2022. *Osprey* has the potential to execute complex computations far surpassing the capabilities of classical computers. For context, the number of classical bits required to represent a single state on the IBM *Osprey* processor exceeds the total number of atoms in the observable universe [63].

6.7 Heron

Heron represents a significant advancement in quantum computing, featuring a QV of 512 and incorporating innovations in signal delivery previously seen in the *Osprey* processor. With 133 qubits, *Heron* builds upon the size and capabilities of its predecessor, *Egret*, and shares a similar footprint to *Eagle*. This upgrade includes enhancements in signal delivery, utilizing high-density flex cabling to facilitate fast and high-fidelity control over both single-qubit and two-qubit operations. Native
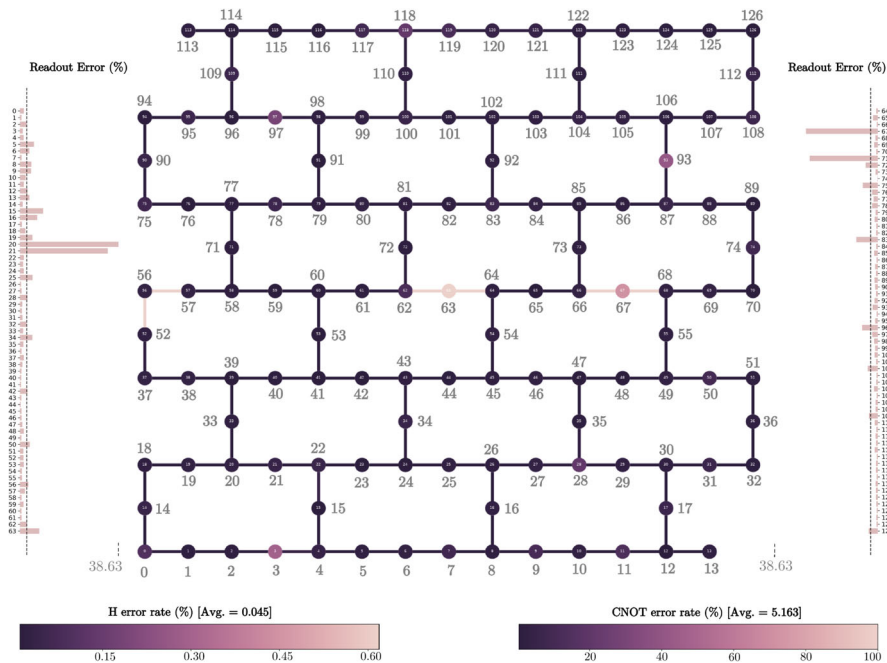
🍃 Springer

Fig. 4 Readout error map and layout of the *ibm_sherbrooke* quantum computer. This quantum system is based on an *Eagle r3* quantum processor, featuring 127 superconducting transmon qubits. Key performance metrics include median ECR error: 7.571×10^{-3}, median SX error: 2.411×10^{-4}, median readout error: 1.350×10^{-2}, median T1: 262.69 μs, and median T2: 176.67 μs, as of August 1, 2024. Regenerated under the terms of the under a Creative Commons Attribution 4.0 International License (http://creativecommons.org/licenses/by/4.0/) from [64]

gates and operations supported by *Heron* include CZ, ID, DELAY, MEASURE, RESET, RZ, SX, X, IF_ELSE, FOR_LOOP, and SWITCH_CASE.

In December 2023, *Heron* r1 was introduced, leveraging 133 qubits as the first version of *Heron*, currently accessible through *ibm_torino*. In July 2024, the processor has been re-designed to combine 156 qubits in a heavy-hexagonal lattice. It also offers a new TLS mitigation capability that manages the chip's TLS environment, enhancing overall coherence and stability. The *Heron* r2 processor, currently accessible through *ibm_fez* quantum computer [63].

6.8 Condor

In December 2023, IBM Quantum unveiled *Condor*, a groundbreaking quantum processor consists of 1121 superconducting qubits and leveraging IBM Quantum's cross-resonance gate technology [17, 65]. This technology facilitates precise two-qubit operations between superconducting qubits with fixed frequencies, known for their simplicity in implementation and resilience against noise [65].

Condor represents a leap forward in chip design, boasting a 50% increase in qubit density and notable enhancements in qubit fabrication and laminate size. Moreover, it

🖄 Springer

Fig. 5 **a** Classical crosstalk levels between *Falcon* and *Eagle* processors, shown as a quantile plot, with the ▶ median value at $x = 0$. **b** Comparison of χ (coupling strength) values for *Falcon* (Kolkata) and *Eagle* (Washington) chips, illustrating differences in readout performance. **c** Detailed comparison of κ values for Falcon (Kolkata) and Eagle (Washington) chips, further emphasizing their impact on processor performance. Adapted from [16]

integrates an impressive length of over a mile of high-density cryogenic flex I/O wiring within a single dilution refrigerator. With performance comparable to its predecessor, the 433-qubit *Osprey*, *Condor* signifies a significant milestone in quantum computing innovation. It effectively tackles scalability challenges while offering valuable insights for future hardware designs [63].

7 Performance and characteristics of IBM's quantum computers

7.1 Quantum performance progress

Looking at the evolution of IBM's quantum processors, IBM Quantum has made significant strides in improving coherence time, gate fidelity, and error rates across multiple processor generations. The leap from 5 qubits in 2016 to over 1000 qubits today (e.g., 1121-qubit *Condor*) involved iterative advancements [16]. Initially, scaling up the number of qubits was prioritized, requiring innovations in chip design and materials. Simultaneously, smaller chips were developed with high-coherence features, which were later incorporated into larger chips, such as the *Falcon*, *Hummingbird*, *Eagle*, and *Osprey* families.

Each generation focused on key performance metrics. For example, while *Eagle*'s initial coherence times lagged behind *Falcon* processors, advancements like *Falcon* r8 led to improvements in *Eagle* r3, achieving similar coherence times. IBM also worked to optimize two-qubit gate fidelities and improve readout metrics, focusing on parameters like χ (coupling strength) and κ (photon exit rate), as shown in Fig. 5, comparing Falcon and *Eagle* chips. These parallel efforts in scaling and quality have driven IBM's quantum hardware development [16]. For a deeper understanding of the performance of the *Eagle* processor, readers are encouraged to explore [16]. A comparison of three generations of chip packaging is shown in Fig. 6. This methodology allows IBM to continuously improve system performance while scaling up the qubit count, ensuring meaningful error-corrected computations are possible [15].

7.2 Evolution of quantum systems

Quantum computing hardware technology is making solid progress each year. In this changing environment, IBM Quantum is constantly at work improving the performance of quantum computers by developing the fastest, highest-quality systems with the most number of qubits [15]. IBM Quantum's quantum computing offerings have evolved to include both current and retired systems. These systems range from early developments to advanced processors with up to 433 qubits (refer to
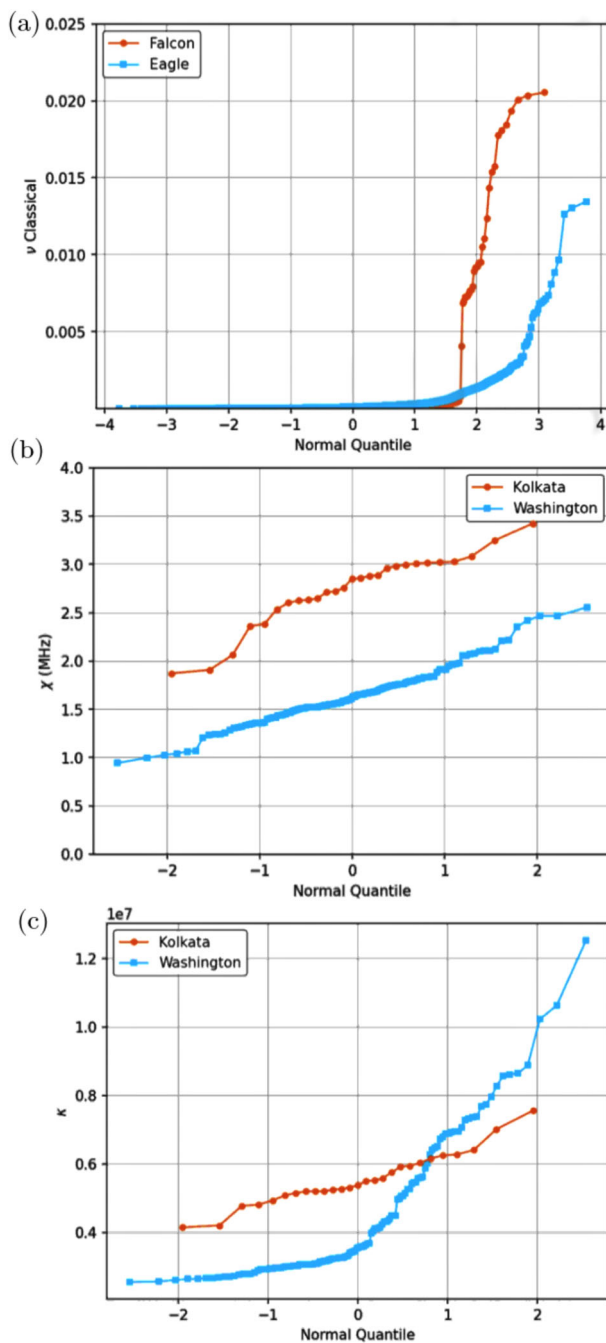
Fig. 6 Comparison of chip packaging across three generations, highlighting the evolution from Generation 1 to Generation 3. In Generation 3, a sophisticated design is introduced that enhances signal delivery, enabling the seamless integration of hundreds of qubits. This approach incorporates technologies adapted from conventional CMOS processing. Regenerated from [16]
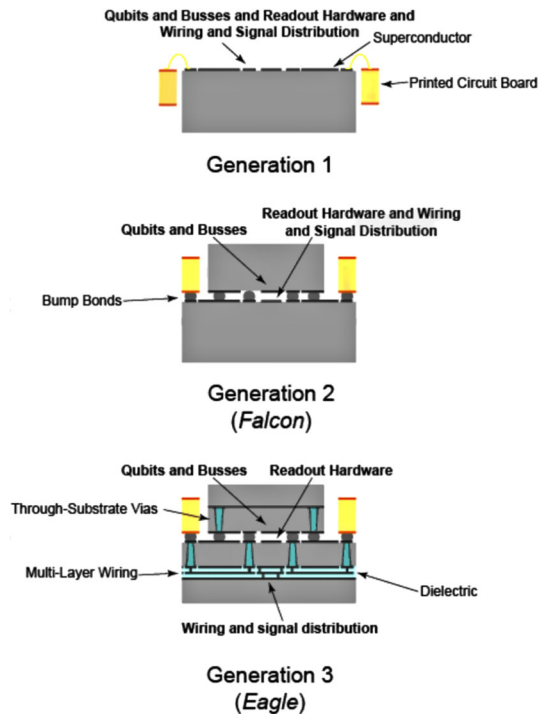
Table 2 for specific details). The journey from retired systems to the latest generations reflects IBM's continuous efforts to push the boundaries of quantum computation. For a view of the availability and details of IBM Quantum's current quantum systems, including access plans, interested readers are referred to [66].

7.3 Retired quantum systems and simulators: paving the path for future innovations

IBM's commitment to quantum computing is evident through a series of pioneering systems, some of which have since been retired. Systems such as *ibmq_5_yorktown* and *ibmq_16_melbourne*, retired on August 9, 2021. *ibmq_manhattan* followed on September 22, 2021, and earlier systems such as *ibmq_athens* and *ibmq_rome* were retired on June 30, 2021. Refer to Table 2 for a list of retired systems. These quantum systems, alongside quantum simulators, were pivotal in early quantum algorithm experimentation and have paved the way for newer generations that continue to push the boundaries of quantum computing.

This section offers detailed performance summaries for various retired IBM Quantum's quantum computers, along with some performance data from previous versions of current systems. Tables 3 to 26 provide key specifications such as coherence times (T1 and T2), qubit frequencies, gate error rates, qubit counts, basis gates, connections, and calibration dates, documented for historical and educational purposes within the literature of NISQ computing era. This enables a comparative

Table 2 List of IBM Quantum's retired quantum systems and cloud simulators

IBM Quantum quantum computers

No	Quantum System	Qubit count	Retirement date	No	Quantum System	Qubit count	Retirement date
1	ibm_algiers	27	April 30, 2024	25	ibmq_bogota	5	June 17, 2022
2	ibm_cairo	27	April 30, 2024	26	ibmq_santiago	5	June 17, 2022
3	ibm_hanoi	27	April 30, 2024	27	ibmq_casablanca	7	March 2, 2022
4	ibmq_kolkata	27	April 1, 2024	28	ibmq_sydney	27	January 11, 2022
5	ibmq_mumbai	27	April 1, 2024	29	ibmq_dublin	27	November 16, 2021
6	ibm_ithaca	65	January 24, 2024	30	ibmq_manhattan	65	September 22, 2021
7	ibm_nairobi	7	November 28, 2023	31	ibmq_5_yorktown	5	August 9, 2021
8	ibm_lagos	7	November 28, 2023	32	ibmq_16_melbourne	15	August 9, 2021
9	ibm_perth	7	November 28, 2023	33	ibmq_paris	27	June 30, 2021
10	ibm_auckland	27	November 9, 2023	34	ibmq_rome	5	June 30, 2021
11	ibmq_guadalupe	16	October 27, 2023	35	ibmq_athens	5	June 30, 2021
12	ibmq_lima	5	September 26, 2023	36	ibmq_berlin	27	December 31, 2020
13	ibmq_belem	5	September 26, 2023	37	ibmq_boeblingen	20	January 31, 2021
14	ibmq_quito	5	September 26, 2023	38	ibmq_ourense	5	January 15, 2021
15	ibmq_manila	5	September 26, 2023	39	ibmq_vigo	5	January 15, 2021
16	ibmq_jakarta	7	September 26, 2023	40	ibmq_valencia	5	January 15, 2021
17	ibm_seattle	433	September 7, 2023	41	ibmq_rochester	53	October 31, 2020
18	ibm_washington	127	June 3, 2023	42	ibmq_cambridge	28	October 31, 2020
19	ibmq_oslo	7	May 4, 2023	43	ibmq_almaden	20	August 31, 2020
20	ibmq_geneva	27	May 4, 2023	44	ibmq_singapore	20	August 31, 2020
21	ibmq_montreal	27	April 11, 2023	45	ibmq_johannesburg	20	August 31, 2020
22	ibmq_toronto	27	April 11, 2023	46	ibmq_essex	5	August 31, 2020
23	ibmq_armonk	1	July 7, 2022	47	ibmq_burlington	5	August 31, 2020
24	ibmq_brooklyn	65	June 28, 2022	48	ibmq_london	5	August 31, 2020

IBM Quantum cloud simulators

No	Quantum simulators	Qubit counts	Processor type		Retirement date
1	simulator_stabilizer	5000	Clifford simulator	–	May 15, 2024
2	simulator_mps	100	Matrix product state	–	May 15, 2024
3	simulator_extended_stabilizer	63	Extended Clifford (e.g. Clifford+T)	–	May 15, 2024
4	ibmq_qasm_simulator	32	General, context-aware	–	May 15, 2024
5	simulator_statevector	32	Schrödinger wavefunction	–	May 15, 2024

Older systems are identified with names starting with "ibmq," while newer systems use names beginning with "ibm."

Table 3 Hardware performance and qubit properties of the 433 qubit *ibm_seattle* quantum computer

System characteristics	Min	Mean	1st Quartile	Median	3rd Quartile	Stdev	StdError	Max	Unit
T1	1.318680	91.67790	66.47356	88.34887	110.75190	38.68508	1.901270	237.9175	μs
T2	4.769450	61.86490	33.40824	58.73242	84.342912	34.52344	1.696730	181.6891	μs
Frequency	0.0	4.967799	5.094863	5.181795	5.2812598	1.072827	0.051566	5.526796	GHz
Anharmonicity	−0.402713	−0.278956	−0.301865	−0.300014	−0.2974234	0.075007	0.003605	0.0	GHz
Readout assignment error	0.72	11.20224	1.970000	4.909999	10.93	20.31924	0.976480	100	$\times 10^{-2}$
Prob. meas|0⟩ prep|1⟩	0.40	7.066876	2.085	4.380	9.655	7.168634	0.352319	51.580	$\times 10^{-2}$
Prob. meas|1⟩ prep|0⟩	0.36	7.187085	1.72	4.18	9.635	8.260245	0.405969	71.64	$\times 10^{-2}$
Readout length	2000	2000	2000	2000	2000	0.0	0.0	2000	ns
ID error	0.179	45.722	0.4599	0.625	1.290	204.837	9.843	1000	$\times 10^{-3}$
$\sqrt{X}$ (SX) error	0.179	45.722	0.4599	0.625	1.290	204.837	9.843	1000	$\times 10^{-3}$
Pauli-X error	0.179	45.722	0.4599	0.625	1.290	204.837	9.843	1000	$\times 10^{-3}$
ECR Error	7.198471	109.2662	15.51089	21.54787	39.877844	264.56291	11.78457	1000	$\times 10^{-3}$
ECR Gate time	135	635	660	660	660	138.9054	6.187339	1404	ns

The processor type is *Osprey* r1. The basis gates of this machine are: ECR, ID, RZ, SX, X. With a median ECR error: 2.155×10^{-2}, a median SX error: 6.256×10^{-4}, a median readout error: 4.910×10^{-2}, a median T1: 88.35 μs, and a median T2: 58.73 μs. Accessed June 29, 2023

Table 4 Summary of hardware performance, qubit characteristics and key specifications for the 127-qubits quantum computer *ibm_sherbrooke*, featuring basis gates ECR, ID, RZ, SX, and X

System characteristics	Min	Mean	1st Quartile	Median	3rd Quartile	Stdev	StdError	Max	Unit
T1	18.19069	281.5453	212.7437	289.0375	352.64895	104.2918	9.254408	513.9483	μs
T2	1.973268	180.1907	83.12792	168.4437	258.97337	106.4481	9.445748	392.8104	μs
Frequency	4.455260	4.790289	4.731587	4.794001	4.8593516	0.109099	0.009681	5.057533	GHz
Anharmonicity	−0.32426	−0.31039	−0.31225	−0.31093	−0.309626	0.005480	0.000486	−0.27186	GHz
Readout assignment error	0.0023	1.990682	0.649999	1.0	1.98	3.338019	0.296201	27.67	$\times 10^{-2}$
Prob. meas $|0\rangle$ prep $|1\rangle$	0.0020	2.141312	0.750	1.14	2.17	4.084455	0.362436	41.44	$\times 10^{-2}$
Prob. meas $|1\rangle$ prep $|0\rangle$	0.0012	1.870131	0.460	0.82	1.95	3.596563	0.319143	32.86	$\times 10^{-2}$
Readout length	1244.444	1244.444	1244.444	1244.444	1244.444	0.0	0.0	1244.444	ns
ID error	0.552649	5.274019	1.678334	2.149589	3.233953	11.90043	1.055992	111.4219	$\times 10^{-4}$
$\sqrt{X}$ (SX) error	0.552649	5.274019	1.678334	2.149589	3.233953	11.90043	1.055992	111.4219	$\times 10^{-4}$
Pauli-X error	0.552649	5.274019	1.678334	2.149589	3.233953	11.90043	1.055992	111.4219	$\times 10^{-4}$
ECR Error	2.771444	45.41823	5.559371	7.494834	11.50235	182.0391	15.11699	1000	$\times 10^{-3}$
ECR Gate time	448	538.4691	533.3334	533.3334	533.3334	40.83243	3.402702	881.7778	ns

The processor type is *Eagle* r3, and calibration data were accessed on June 30, 2023

⚛ Springer

Table 5 Summary of hardware performance, qubit characteristics and key specifications for the 127-qubits quantum computer *ibm_washington*, featuring basis gates CX, ID, IF_ELSE, RZ, SX and X

System characteristics	Min	Mean	1st Quartile	Median	3rd Quartile	Stdev	StdError	Max	Unit
T1	30.33	99.99779	84.46	99.68	116.815	27.40558	2.43185	188.64	μs
T2	5.33	96.948	60.7	94.13	135.75	49.201	4.3658	245.74	μs
Frequency	4.766	5.064	4.985	5.017	5.1405	0.1132	0.01	5.292	GHz
Anharmonicity	−0.3249	−0.30671	−0.3086	−0.3074	−0.3056	0.0053	0.0005	−0.27711	GHz
Readout assignment error	0.180	3.000	0.54	1.25	3.27	5.25	0.47	38.39	$\times 10^{-2}$
Prob. meas|0⟩ prep|1⟩	0.22	3.17	0.73	0.14	2.91	5.34	0.47	39.56	$\times 10^{-2}$
Prob. meas|1⟩ prep|0⟩	0.00	2.831	0.16	0.9	3.67	5.36579	0.4761365	37.22	$\times 10^{-2}$
Readout length	864	864	864	864	864	0.0	0.0	864	ns
Single-qubit error	1.720	8.636	2.2	3.0	4.8	22.3	2.0	210.6	$\times 10^{-4}$
CX Error	5.542	38.352	9.05025	12.31	18.2325	141.941	8.3931	1000	$\times 10^{-3}$
Gate time	270.222	567.621	405.333	469.333	689.778	224.770	13.314	1187.556	ns

The processor type is *Eagle* r3. The system boasts 288 CX qubit connections, and calibration data were accessed on November 12, 2022

Table 6 Summary of hardware performance, qubit characteristics and key specifications for the 127-qubit quantum computer *ibm_kyiv*, featuring basis gates CX, ID, RZ, SX and X

System characteristics	Min	Mean	1st Quartile	Median	3rd Quartile	Stdev	StdError	Max	Unit
T1	44.81	299.737	233.6	302.51	367.63	101.11256	8.9723	495.91	μs
T2	13.72	160.919	63.37	122.66	223.88	118.695	10.5325	512.18	μs
Frequency	4.341	4.6202	4.539	4.613	4.7025	0.1125	0.0099	4.959	GHz
Anharmonicity	−0.36821	−0.14058	−0.31176	0	0	0.156603	0.013896	0	GHz
Readout assignment error	0.06	1.4262	0.25	0.66	1.475	2.0975	0.1861	12.67	$\times 10^{-2}$
Prob. meas$|0\rangle$ prep$|1\rangle$	0.06	1.4924	0.32	0.66	1.43	2.318	0.206	13.34	$\times 10^{-2}$
Prob. meas$|1\rangle$ prep$|0\rangle$	0.0	1.36	0.12	0.46	1.43	2.5257	0.22412	19.36	$\times 10^{-2}$
Readout length	867.556	867.556	867.556	867.556	867.556	0.0	0.0	867.556	ns
Single-qubit error	0.775	4.391	1.419	2.102	3.9875	10.509	0.9325	110.5	$\times 10^{-4}$
CX Error	1.0	1.0	1.0	1.0	1.0	0.0	0.0	1.0	
Gate time	611.556	636.445	611.556	636.4445	661.333	24.9318	1.469	661.333	ns

The processor type is *Eagle* r3. The system boasts 288 CX qubit connections, and calibration data were accessed on November 14, 2022

⁂ Springer

Table 7 Summary of hardware performance, qubit characteristics and key specifications for the 65-qubit quantum computer *ibm_ithaca*, featuring basis gates CX, ID, RZ, SX and X

System characteristics	Min	Mean	1st Quartile	Median	3rd Quartile	Stdev	StdError	Max	Unit
T1	40.3	174.392	138.31	176.95	203.13	55.1419	6.8395	359.67	μs
T2	18.45	181.374	112.77	172.63	250.73	97.732	12.122	388.69	μs
Frequency	4.542	4.738	4.657	4.732	4.814	0.0977	0.01212	4.931	GHz
Anharmonicity	−0.35381	−0.33370	−0.33511	−0.33359	−0.3316	0.00555	0.00069	−0.31597	GHz
Readout assignment error	0.54	2.4563	1.01	1.6	2.49	2.4638	0.30559	13.43	$\times 10^{-2}$
Prob. meas $\lvert 0 \rangle$ prep $\lvert 1 \rangle$	0.92	3.10369	1.64	2.44	3.66	2.73169	0.33882	18.84	$\times 10^{-2}$
Prob. meas $\lvert 1 \rangle$ prep $\lvert 0 \rangle$	0.04	1.8089	0.26	0.84	1.92	2.7354	0.3393	14.46	$\times 10^{-2}$
Readout length	4924.444	4924.444	4924.444	4924.444	4924.444	0.0	0.0	4924.444	ns
Single-qubit error	1.28	4.508	1.935	2.619	3.505	11.849	1.469	97.72	$\times 10^{-4}$
CX Error	5.189	26.145	7.19425	10.325	13.53	116.408	9.7006	1000	$\times 10^{-3}$
Gate time	512	536.889	512	536.889	561.778	24.976	2.081	561.778	ns

The processor type is *Hummingbird* r3. The system boasts 144 CX qubit connections, and calibration data were accessed on November 14, 2022

Table 8 Summary of hardware performance, qubit characteristics and key specifications for the 27-qubit quantum computer *ibmq_kolkata*, featuring basis gates CX, ID, IF_ELSE, RZ, SX and X

System characteristics	Min	Mean	1st Quartile	Median	3rd Quartile	Stdev	StdError	Max	Unit
T1	12.78	116.237	98.63	113.5	142.365	33.779	6.5008	187.18	μs
T2	17.11	89.102	43.165	72.28	118.005	57.1635	11.0011	214.92	μs
Frequency	4.869	5.08234	5.0005	5.102	5.1845	0.11219	0.02159	5.268	GHz
Anharmonicity	−0.37341	−0.34455	−0.34554	−0.34345	−0.34158	0.006158	0.001185	−0.34002	GHz
Readout assignment error	0.53	2.0348	0.8	1.25	1.735	3.0326	0.5836	16.19	$\times 10^{-2}$
Prob. meas$|0\rangle$ prep$|1\rangle$	0.62	2.1845	0.97	1.28	2	3.0407	0.5852	15.92	$\times 10^{-2}$
Prob. meas$|1\rangle$ prep$|0\rangle$	0.26	1.885	0.69	1.14	1.6	3.0727	0.5914	16.46	$\times 10^{-2}$
Readout length	675.556	675.556	675.556	675.556	675.556	0.0	0.0	675.556	ns
Single-qubit error	1.466	3.071	1.793	1.911	2.4345	3.875	0.7457	20.97	$\times 10^{-4}$
CX Error	3.807	44.957	5.3405	6.852	9.34445	185.741	24.821	1000	$\times 10^{-3}$
Gate time	195.556	426.256	320	398.222	490.667	162.254	21.682	1059.556	ns

The processor type is *Falcon* r5.11. The system boasts 56 CX qubit connections, and calibration data were accessed on November 14, 2022

🌲 Springer

Table 9 Summary of hardware performance, qubit characteristics and key specifications for the 27-qubit quantum computer *ibmq_montreal*, featuring basis gates CX, ID, RZ, SX and X

System characteristics	Min	Mean	1st Quartile	Median	3rd Quartile	Stdev	StdError	Max	Unit
T1	3.73	108.8945	88.765	103.68	135.875	44.5739	8.5783	201.49	μs
T2	3.2	87.5989	45.46	71.84	119.88	54.8127	10.5487	228.86	μs
Frequency	4.835	4.9979	4.956	5	5.054	0.0729	0.0140	5.105	GHz
Anharmonicity	−0.41989	−0.33589	−0.33825	−0.33722	−0.324475	0.0189245	0.0036419	−0.30385	GHz
Readout assignment error	0.83	2.6389	1.285	1.62	2.94	2.4865	0.4785	11.26	$\times10^{-2}$
Prob. meas$|0\rangle$ prep$|1\rangle$	1.36	2.9489	2.06	2.22	3.23	1.7696	0.3406	9.78	$\times10^{-2}$
Prob. meas$|1\rangle$ prep$|0\rangle$	0.2	2.32889	0.53	0.82	1.7	3.91839	0.75409	17.36	$\times10^{-2}$
Readout length	5201.778	5201.778	5201.778	5201.778	5201.778	0.0	0.0	5201.778	ns
Single-qubit error	1.965	3.882	2.528	3.539	5.114	1.637	0.315	6.78	$\times10^{-4}$
CX Error	5.76	13.295	7.821	10.2165	17.13	8.009	1.07009	43.78	$\times10^{-3}$
Gate time	270.222	442.921	368.00025	405.333	490.667	145.024	19.379	1059.556	ns

The processor type is *Falcon* r4. The system boasts 56 CX qubit connections, and calibration data were accessed on November 14, 2022

Table 10 Summary of hardware performance, qubit characteristics and key specifications for the 27-qubit quantum computer *ibmq_mumbai*, featuring basis gates CX, ID, IF_ELSE, RZ, SX and X

System characteristics	Min	Mean	1st Quartile	Median	3rd Quartile	Stdev	StdError	Max	Unit
T1	31.87	121.619	85.08	119.22	148.485	46.956	9.0367	223.51	μs
T2	22.37	104.237	64.5	112.75	148.515	53.239	10.24586	202.74	μs
Frequency	4.666	4.8799	4.782	4.893	4.965	0.1164	0.0224	5.076	GHz
Anharmonicity	−0.39107	−0.33315	−0.33317	−0.33129	−0.329925	0.012249	0.002357	−0.31416	GHz
Readout assignment error	1.15	2.9548	1.55	1.92	3.49	2.38318	0.45864	11.05	$\times 10^{-2}$
Prob. meas$|0\rangle$ prep$|1\rangle$	1.74	4.1319	2.35	2.74	4.22	3.1897	0.6139	15.58	$\times 10^{-2}$
Prob. meas$|1\rangle$ prep$|0\rangle$	0.54	1.7778	0.78	1.0	1.66	2.2369	0.4305	11.48	$\times 10^{-2}$
Readout length	3552	3552	3552	3552	3552	0.0	0.0	3552	ns
Single-qubit error	1.488	16.795	2.031	2.648	3.843	70.478	13.564	369.3	$\times 10^{-4}$
CX Error	5.062	88.451	7.28325	9.154	14.4975	256.875	34.326	1000	$\times 10^{-3}$
Gate time	248.889	495.746	368.00025	430.2225	584.889	210.626	28.146	1351.111	ns

The processor type is *Falcon* r5.10. The system boasts 56 CX qubit connections, and calibration data were accessed on November 14, 2022

Table 11 Summary of hardware performance, qubit characteristics and key specifications for the 27-qubit quantum computer *ibm_cairo*, featuring basis gates CX, ID, IF_ELSE, RZ, SX and X

System characteristics	Min	Mean	1st Quartile	Median	3rd Quartile	Stdev	StdError	Max	Unit
T1	41.26	104.934	76.245	94.74	117.4	45.447	8.7462	221.09	μs
T2	12.82	102.974	42.35	113.14	145.66	73.9239	14.2267	303.4	μs
Frequency	4.911	5.1289	5.045	5.133	5.2135	0.1129	0.0217	5.284	GHz
Anharmonicity	−0.34568	−0.34074	−0.342275	−0.34054	−0.33929	0.002262	0.000435	−0.33714	GHz
Readout assignment error	0.58	2.04223	0.835	1.25	1.755	3.14460	0.60518	17.01	$\times 10^{-2}$
Prob. meas$|0\rangle$ prep$|1\rangle$	0.82	2.48741	1.08	1.46	1.94	4.81937	0.92749	26.38	$\times 10^{-2}$
Prob. meas$|1\rangle$ prep$|0\rangle$	0.34	1.5970	0.61	0.88	1.55	1.8856	0.3629	7.64	$\times 10^{-2}$
Readout length	732.444	732.444	732.444	732.444	732.444	0.0	0.0	732.444	ns
Single-qubit error	1.357	7.0541	1.965	2.512	4.263	16.298	3.1366	84.63	$\times 10^{-4}$
CX Error	4.894	89.897	8.0925	10.705	19.3425	256.469	34.272	1000	$\times 10^{-3}$
Gate time	160	352.889	255.111	316.444	415.999	163.919	21.905	970.667	ns

The processor type is *Falcon* r5.11. The system boasts 56 CX qubit connections, and calibration data was accessed on November 14, 2022

Table 12 Summary of hardware performance, qubit characteristics and key specifications for the 27-qubit quantum computer *ibm_auckland*, featuring basis gates CX, ID, IF_ELSE, RZ, SX and X

System characteristics	Min	Mean	1st Quartile	Median	3rd Quartile	Stdev	StdError	Max	Unit
T1	7.85	147.03	109.66	163.14	195.335	64.8467	12.4797	263.52	μs
T2	16.27	132.9515	61.52	129.95	178.725	87.51967	16.84317	308.12	μs
Frequency	4.692	4.9573	4.879	4.97	5.0355	0.1245	0.0239	5.204	GHz
Anharmonicity	-0.35079	-0.34432	-0.34513	-0.34389	-0.342655	0.002391	0.000460	-0.34066	GHz
Readout assignment error	0.64	2.98778	0.73	0.92	1.26	6.62509	1.27499	31.28	$\times 10^{-2}$
Prob. meas$|0\rangle$ prep$|1\rangle$	0.74	3.4312	0.91	0.96	1.44	10.506	2.0219	55.64	$\times 10^{-2}$
Prob. meas$|1\rangle$ prep$|0\rangle$	0.4	2.54445	0.56	0.74	1.08	6.29405	1.21129	32.78	$\times 10^{-2}$
Readout length	757.333	757.333	757.333	757.333	757.333	0.0	0.0	757.333	ns
Single-qubit error	1.533	44.774	1.8965	2.564	3.399	216.890	41.741	1130	$\times 10^{-4}$
CX Error	4.257	117.431	5.704	8.9255	16.24	308.699	41.252	1000	$\times 10^{-3}$
Gate time	135.111	479.746	353.778	432	560.00025	258.922	34.5999	1564.444	ns

The processor type is *Falcon* r5.11. The system boasts 56 CX qubit connections, and calibration data was accessed on November 14, 2022

⚫ Springer

Table 13 Summary of hardware performance, qubit characteristics and key specifications for the 27-qubit quantum computer *ibm_hanoi*, featuring basis gates CX, ID, IF_ELSE, RZ, SX and X

System characteristics	Min	Mean	1st Quartile	Median	3rd Quartile	Stdev	StdError	Max	Unit
T1	91	175.0207	144.08	170.53	209.07	45.1389	8.6869	288.51	μs
T2	20.54	130.6507	52.285	116.41	190.995	90.4825	17.4134	349.23	μs
Frequency	4.719	4.9993	4.9195	5.003	5.0845	0.1339	0.0258	5.256	GHz
Anharmonicity	−0.34913	−0.34332	−0.345835	−0.3443	−0.34239	0.005597	0.001077	−0.31836	GHz
Readout assignment error	0.62	1.58259	0.82	1	1.47	1.81809	0.34989	9.92	$\times 10^{-2}$
Prob. meas$|0\rangle$ prep$|1\rangle$	0.64	1.6229	1.01	1.14	1.38	1.73063	0.33306	9.74	$\times 10^{-2}$
Prob. meas$|1\rangle$ prep$|0\rangle$	0.38	1.5423	0.64	0.84	1.69	1.9325	0.3719	10.1	$\times 10^{-2}$
Readout length	817.778	817.778	817.778	817.778	817.778	0.0	0.0	817.778	ns
Single-qubit error	1.275	2.5334	1.7215	1.995	2.825	1.2913	0.2485		$\times 10^{-4}$
CX Error	3.259	152.707	5.7327	8.8315	15.205	349.240	46.669	1000	$\times 10^{-3}$
Gate time	181.333	384.571	283.555	344.889	464.889	138.187	18.466	728.889	ns

The processor type is *Falcon* r5.11. The system boasts 56 CX qubit connections, and calibration data was accessed on November 14, 2022

Table 14 Summary of hardware performance, qubit characteristics and key specifications for the 27-qubit quantum computer *ibm_geneva*, featuring basis gates CX, ID, IF_ELSE, RZ, SX and X

System characteristics	Min	Mean	1st Quartile	Median	3rd Quartile	Stdev	StdError	Max	Unit
T1	52.81	299.6318	212.88	338.69	384.465	124.2378	23.90958	479.89	μs
T2	1.85	204.9359	108.215	202.21	300.63	126.6367	24.37123	458.16	μs
Frequency	4.55	4.6907	4.62	4.675	4.7485	0.09720	0.01870	4.88	GHz
Anharmonicity[a]	–	–	–	–	–	–	–	–	–
Readout assignment error	0.9	5.6267	1.56	3.38	5.105	8.5249	1.6406	42.54	$\times 10^{-2}$
Prob. meas$|0\rangle$ prep$|1\rangle$	0.58	5.7215	1.89	3.34	5.12	8.5452	1.6445	41.2	$\times 10^{-2}$
Prob. meas$|1\rangle$ prep$|0\rangle$	0.74	5.53185	1.41	2.62	5.65	8.62742	1.66035	43.88	$\times 10^{-2}$
Readout length	1600	1600	1600	1600	1600	0.0	0.0	1600	ns
Single-qubit error	1.105	69.4995	1.8595	3.014	7.352	291.345	56.0695	1518	$\times 10^{-4}$
CX Error	4.52	298	8.5007	16.250	1000	448.399	59.919	1000	$\times 10^{-3}$
Gate time	348.444	588.698	462.222	558.223	695.111	170.282	22.755	988.444	ns

The processor type is *Falcon* r8. The system boasts 56 CX qubit connections, and calibration data was accessed on November 14, 2022

[a] Missing values

Table 15 Summary of hardware performance, qubit characteristics and key specifications for the 27-qubit quantum computer *ibmq_toronto*, featuring basis gates CX, ID, RZ, SX and X

System characteristics	Min	Mean	1st Quartile	Median	3rd Quartile	Stdev	StdError	Max	Unit
T1	50.99	117.58	97.535	118.66	141.3	36.7706	7.0765	188.87	μs
T2	12.53	125.5637	76.47	117.17	172.05	62.29247	11.98819	244.9	μs
Frequency	4.915	5.08025	5.0255	5.092	5.144	0.091117	0.017535	5.226	GHz
Anharmonicity	−0.33934	−0.32899	−0.336195	−0.33432	−0.32147	0.01130	0.002175	−0.28553	GHz
Readout assignment error	0.68	3.896296	1.635	2.31	5.25	3.67038	0.70637	15.66	$\times 10^{-2}$
Prob. meas$\lvert 0 \rangle$ prep$\lvert 1 \rangle$	0.94	4.98963	2.43	3.72	7.45	3.87152	0.74507	17.9	$\times 10^{-2}$
Prob. meas$\lvert 1 \rangle$ prep$\lvert 0 \rangle$	0.28	2.80296	0.6	0.98	3.16	3.84350	0.73969	13.42	$\times 10^{-2}$
Readout length	5962.667	5962.667	5962.667	5962.667	5962.667	0.0	0.0	5962.667	ns
Single-qubit error	1.683	5.707	2.3915	3.076	3.912	8.46809	1.62969	40.90	$\times 10^{-4}$
CX Error	6.1444	14.310	7.953	9.871	18.04	10.2225	0.012227	53.510	$\times 10^{-3}$
Gate time	241.778	454.095	373.3335	451.5555	506.66675	126.725	16.934	860.444	ns

The processor type is *Falcon* r4. The system boasts 56 CX qubit connections, and calibration data was accessed on November 14, 2022

Table 16 Summary of hardware performance, qubit characteristics and key specifications for the 27-qubit quantum computer *ibm_peekskill*, featuring basis gates CX, ID, IF_ELSE, RZ, SX, X, X12, and XPRS

System characteristics	Min	Mean	1st Quartile	Median	3rd Quartile	Stdev	StdError	Max	Unit
T1	108.2	314.384	234.06	309.41	404.42	115.347	22.1986	533.37	μs
T2	122.41	297.613	196.24	283.69	394.055	124.5816	23.97574	589.01	μs
Frequency	4.627	4.949	4.8485	4.959	5.074	0.14096	0.27128	5.175	GHz
Anharmonicity	−0.38267	−0.34702	−0.34694	−0.34405	−0.34184	0.010515	0.002024	−0.33679	GHz
Readout assignment error	0.320	4.472	0.79	1.93	3.915	8.8130	1.6960	44.500	$\times 10^{-2}$
Prob. meas$|0\rangle$ prep$|1\rangle$	0.24	3.777	0.77	1.68	3.81	6.6204	1.2741	34.40	$\times 10^{-2}$
Prob. meas$|1\rangle$ prep$|0\rangle$	0.28	5.167	0.68	1.04	2.76	11.6171	2.2357	5.46	$\times 10^{-2}$
Readout length	860.444	860.444	860.444	860.444	860.444	0.0	0.0	860.444	ns
Single-qubit error	0.7588	3.408	1.3535	1.695	3.0175	5.19027	0.99887	27.460	$\times 10^{-4}$
CX Error	2.854	79.650	6.04775	7.12	10.46325	257.6373	34.42823	1000	$\times 10^{-3}$
Gate time	291.556	472.889	398.222	451.5555	547.556	99.71249	13.32464	675.556	ns

The processor type is *Falcon* r8. The system boasts 56 CX qubit connections, and calibration data was accessed on November 14, 2022

🌀 Springer

Table 17 Summary of hardware performance, qubit characteristics and key specifications for the 16-qubit quantum computer *ibmq_guadalupe*, featuring basis gates CX, ID, RZ, SX and X

System characteristics	Min	Mean	1st Quartile	Median	3rd Quartile	Stdev	StdError	Max	Unit
T1	57.230	102.93	75.893	109.370	126.923	29.1918	7.2979	156.26	μs
T2	14.040	121.45	93.09	123.255	153	47.4965	11.8741	222.27	μs
Frequency	5.038	5.246	5.15475	5.2295	5.3215	0.1227	0.0307	5.470	GHz
Anharmonicity	−0.33734	−0.3272	−0.333956	−0.33096	−0.31743	0.00832	0.00207	−0.31579	GHz
Readout assignment error	0.980	1.955	1.3425	1.56	2.5025	0.9264	0.2316	4.160	$\times 10^{-2}$
Prob. meas$|0\rangle$ prep$|1\rangle$	1.48	3.014	2.08	2.33	3.295	1.61999	0.40499	7.32	$\times 10^{-2}$
Prob. meas$|1\rangle$ prep$|0\rangle$	0.340	0.896	0.5	0.69	1.02	0.57048	0.14262	2.46	$\times 10^{-2}$
Readout length	7111.111	7111.111	7111.111	7111.111	7111.111	0.0	0.0	7111.111	ns
Single-qubit error	1.605	3.100	2.507	2.698	3.356	1.159	0.2898	5.692	$\times 10^{-4}$
CX Error (32 connections)	6.017	10.520	7.803	8.805	12.890	3.7937	0.6706	17.700	$\times 10^{-3}$
Gate time	263.111	416.4444	344.8885	384	378.222	122.9419	21.7333	775.111	ns

The processor type is *Falcon* r4P. The system boasts 32 CX qubit connections, and calibration data was accessed on November 14, 2022

Table 18 Summary of hardware performance, qubit characteristics and key specifications for the 7-qubit quantum computer *ibm_perth*, featuring basis gates CX, ID, IF_ELSE, RZ, SX and X

System characteristics	Min	Mean	1st Quartile	Median	3rd Quartile	Stdev	StdError	Max	Unit
T1	90.63	143.24	111.295	127.84	175.23	45.363	17.145	211.16	μs
T2	53.13	112.964	86.23	98.39	141.18	45.922	17.357	184.41	μs
Frequency	4.863	5.068	5.0065	5.126	5.1575	0.114577	0.043330	5.159	GHz
Anharmonicity	−0.34727	−0.34192	−0.3452	−0.34152	−0034045	0.004564	0.00175	−0.33337	GHz
Readout assignment error	0.65	1.69	1.18	1.20	1.78	1.17	0.44	4.09	$\times 10^{-2}$
Prob. meas$|0\rangle$ prep$|1\rangle$	0.72	2.311	1.2	1.24	2.27	2.31	0.87	7.28	$\times 10^{-2}$
Prob. meas$|1\rangle$ prep$|0\rangle$	0.58	1.077	0.89	1.12	1.22	0.3305	0.1249	1.62	$\times 10^{-2}$
Readout length	675.556	675.556	675.556	675.556	675.556	0.0	0.0	675.556	ns
Single-qubit error	2.965	4.020	3.5	4.0	4.6	0.79	0.3	5.005	$\times 10^{-4}$
CX Error	12.06	13.89	12.43	13.58	14.73	1.691	4.882	16.93	$\times 10^{-3}$
Gate time	284.444	444.444	346.667	398.222	593.777	132.3611	38.2094	640	ns

The processor type is *Falcon* r5.11H. The system boasts 12 CX qubit connections, and calibration data was accessed on November 13, 2022

 Springer

Table 19 Summary of hardware performance, qubit characteristics and key specifications for the 7-qubit quantum computer *ibm_lagos*, featuring basis gates CX, ID, IF_ELSE, RZ, SX and X

System characteristics	Min	Mean	1st Quartile	Median	3rd Quartile	Stdev	StdError	Max	Unit
T1	86.39	127.73	107.115	125.73	136.795	35.02391	13.23779	194.17	μs
T2	31.02	81.29857	57.145	86.10	95.235	38.40754	14.51669	147.21	μs
Frequency	4.987	5.147857	5.082	5.176	5.2115	0.1032818	0.039037	5.285	GHz
Anharmonicity	−0.34529	−0.34188	−0.343005	−0.34193	−0.34033	0.00210	0.000795	−0.33923	GHz
Readout assignment error	0.7	1.446	1.135	1.43	1.775	0.52430	0.19816	0.217	$\times 10^{-2}$
Prob. meas$\lvert 0\rangle$ prep$\lvert 1\rangle$	0.78	1.651	1.37	1.76	1.89	0.58205	0.21999	2.5	$\times 10^{-2}$
Prob. meas$\lvert 1\rangle$ prep$\lvert 0\rangle$	0.62	1.24	0.88	1.14	1.66	0.48826	0.184545	1.84	$\times 10^{-2}$
Readout length	704	704	704	704	704	0	0	704	ns
Single-qubit error	1.647	2.758	2.0525	2.656	3.108	1.01898	3.851394	4.680	$\times 10^{-4}$
CX Error(12 connections)	5.767	8.418	8.45	8.9875	9.135	1.2633	0.3647	9.182	$\times 10^{-3}$
Gate time	256	359.111	296.889	327.111	341.333	113.272	32.699	611.556	ns

The processor type is *Falcon* r5.11H. The system boasts 12 CX qubit connections, and calibration data was accessed on November 13, 2022

Table 20 Summary of hardware performance, qubit characteristics and key specifications for the 7-qubit quantum computer *ibm_nairobi*, featuring basis gates CX, ID, IF_ELSE, RZ, SX and X

System characteristics	Min	Mean	1st Quartile	Median	3rd Quartile	Stdev	StdError	Max	Unit
T1	50.59	118.86	111.95	117.71	140.235	35.09266	13.26377	159.35	μs
T2	22.72	101.59	60.995	85.62	116.565	73.53198	27.79247	247.63	μs
Frequency	5.027	5.19	5.1495	5.177	5.267	0.094361	0.035665	5.293	GHz
Anharmonicity	−0.34253	−0.34049	−0.3406	−0.3405	−0.3401	0.0011	0.0004	−0.3389	GHz
Readout assignment error	1.830	2.883	2.54	2.85	2.96	0.83	0.31	4.500	$\times 10^{-2}$
Prob. meas$|0\rangle$ prep$|1\rangle$	2.9	4.117	3.36	4.4	4.64	0.93441	0.35317	5.52	$\times 10^{-2}$
Prob. meas$|1\rangle$ prep$|0\rangle$	0.76	1.649	1.02	1.1	2.08	1.03	0.39	3.48	$\times 10^{-2}$
Readout length	5560.889	5560.889	5560.889	5560.889	5560.889	0.0	0.0	5560.889	ns
Single-qubit error	1.674	2.805	2.3	2.8	3.4	0.79	0.3	3.768	$\times 10^{-4}$
CX Error (12 connections)	6.177	11.77	7.622	9.172	1.749	5.740	1.6570	21.02	$\times 10^{-3}$
Gate time	241.778	306.9629	275.5553	295.111	320	55.48440	16.01697	426.667	ns

The processor type is *Falcon* r5.11H. The system boasts 12 CX qubit connections, and calibration data was accessed on November 13, 2022

$\underline{\textcircled{2}}$ Springer

Table 21 Summary of hardware performance, qubit characteristics and key specifications for the 7-qubit quantum computer *ibm_oslo*, featuring basis gates CX, ID, IF_ELSE, RZ, SX and X

System characteristics	Min	Mean	1st Quartile	Median	3rd Quartile	Stdev	StdError	Max	Unit
T1	57.14	116.93	79.98	128.85	131.76	51.08602	19.30869	209.04	μs
T2	31.32	78.8757	37.17	39.53	129.38	53.53095	20.23280	148.18	μs
Frequency	4.925	5.07771	4.9865	5.046	5.1405	0.135636	0.0512657	5.319	GHz
Anharmonicity	−0.3444	−0.34226	−0.34342	−0.329	−0.34203	0.00227	0.00086	−0.33763	GHz
Readout assignment error	1.040	4.31714	1.49	2.27	5.02	4.77287	1.80397	13.89	$\times 10^{-2}$
Prob. meas $|0\rangle$ prep $|1\rangle$	1.06	4.2	1.42	2.64	4.85	4.432	1.675	13.16	$\times 10^{-2}$
Prob. meas $|1\rangle$ prep $|0\rangle$	0.92	4.434285	1.41	2.20	5.24	5.12845	1.938373	14.62	$\times 10^{-2}$
Readout length	910.222	910.222	910.222	910.222	910.222	0.0	0.0	910.222	ns
Single-qubit error	2.209	3.871	2.7	3.4	4.2	1.9	0.74	7.765	$\times 10^{-4}$
CX Error	6.716	173.9	7.126	9.551	10.53	385.8677	111.3904	1000	$\times 10^{-3}$
Gate time	167.111	300.44425	246.22225	320	341.333	75.37129	21.757817	412.444	ns

The processor type is *Falcon* r5.11H. The system boasts 12 CX qubit connections, and calibration data was accessed on November 13, 2022

Table 22 Summary of hardware performance, qubit characteristics and key specifications for the 7-qubit quantum computer *ibmq_jakarta*, featuring basis gates CX, ID, IF_ELSE, RZ, SX and X

System characteristics	Min	Mean	1st Quartile	Median	3rd Quartile	Stdev	StdError	Max	Unit
T1	95.45	138.7942	116.46	136.5	161.105	32.734337	12.3724166	184.48	μs
T2	22.47	42.946	27.705	33.94	54.28	21.156	7.9964	80.24	μs
Frequency	5.014	5.1591	5.0855	5.143	5.219	0.0979	0.0346	5.301	GHz
Anharmonicity	−0.3432	−0.34067	−0.3415	−0.3411	−0.3396	0.0016	0.0005	−0.33836	GHz
Readout assignment error	1.610	2.590	2.07	2.7	3.02	0.71	8.55	3.640	$\times 10^{-2}$
Prob. meas$|0\rangle$ prep$|1\rangle$	2.14	3.211	2.9	3.0	3.52	0.75	8.98	4.5	$\times 10^{-2}$
Prob. meas$|1\rangle$ prep$|0\rangle$	1.06	1.969	1.24	1.62	2.16	1.16	0.44	4.3	$\times 10^{-2}$
Readout length	5351.111	5351.111	5351.111	5351.111	5351.111	0.0	0.0	5351.111	ns
Single-qubit error	1.753	2.342	2.0	2.0	3.0	0.50	0.20	3.371	$\times 10^{-4}$
CX Error	6.758	9.556	6.875	7.767	9.979	4.213078	1.216211	18.19	$\times 10^{-3}$
Gate time	234.667	341.33333	275.55525	302.2225	392.889	100.0622	28.88546	540.444	ns

The processor type is *Falcon* r5.11H. The system boasts 12 CX qubit connections, and calibration data was accessed on November 13, 2022

$\underline{\textcircled{2}}$ Springer

Table 23 Summary of hardware performance, qubit characteristics and key specifications for the 5-qubit quantum computer *ibmq_manila*, featuring basis gates CX, ID, IF_ELSE, RZ, SX, and X

System characteristics	Min	Mean	1st Quartile	Median	3rd Quartile	Stdev	StdError	Max	Unit
T1	102.52	137.296	129.47	132.79	152.995	25.12629	11.23682	168.75	μs
T2	23.23	57.92	70.58	40.69	70.58	29.46491	13.17711	100.37	μs
Frequency	4.838	4.9706	4.951	4.962	5.037	0.08855	0.0396	5.065	GHz
Anharmonicity	−0.34528	−0.34363	−0.34463	−0.34358	−0.34255	0.001342	0.0006	−0.34211	GHz
Readout assignment error	1.990	2.212	2.07	2.2	2.24	0.2187921	0.0978468	2.560	$\times 10^{-2}$
Prob. meas|0⟩ prep|1⟩	2.94	3.332	3.1	3.36	3.4	0.351	3.332	3.86	$\times 10^{-2}$
Prob. meas|1⟩ prep|0⟩	1.04	1.092	1.04	1.04	1.08	0.0954987	0.0427083	1.26	$\times 10^{-2}$
Readout length	5351.111	5351.111	5351.111	5351.111	5351.111	0	0	5351.111	ns
Single-qubit error	2.335	2.829	2.4	2.5	2.6	0.9	0.4	4.436	$\times 10^{-4}$
CX Error	7.053	8.156	7.1055	7.3705	8.421	1.666769	0.589292	10.83	$\times 10^{-3}$
Gate time	277.333	368	309.3335	344.889	410.6665	81.85500	28.9401143	504.889	ns

The processor type is *Falcon* r5.11H. The system boasts 8 CX qubit connections, and calibration data was accessed on November 13, 2022

Table 24 Summary of hardware performance, qubit characteristics and key specifications for the 5-qubit quantum computer *ibmq_quito*, featuring basis gates CX, ID, RZ, SX, and X

System characteristics	Min	Mean	1st Quartile	Median	3rd Quartile	Stdev	StdError	Max	Unit
T1	43.76	87.426	83.75	94.7	106.63	26.34978	11.78398	108.29	μs
T2	19.93	85.032	57.36	94.72	105.55	48.56339	21.71820	147.6	μs
Frequency	5.052	5.1838	5.081	5.164	5.3	0.123420	0.05520	5.322	GHz
Anharmonicity	−0.33508	−0.327478	−0.33232	−0.33148	−0.31926	0.007624	0.003409	−0.31925	GHz
Readout assignment error	3.510	4.430	3.58	3.58	3.99	1.721089	0.769695	7.490	$\times 10^{-2}$
Prob. meas|0⟩ prep|1⟩	5.06	6.14	5.44	5.56	5.74	1.56	0.7	8.9	$\times 10^{-2}$
Prob. meas|1⟩ prep|0⟩	1.42	2.72	1.46	1.72	2.92	1.98	0.88	6.08	$\times 10^{-2}$
Readout length	5351.111	5351.111	5351.111	5351.111	5351.111	0	0	5351.111	ns
Single-qubit error	2.858	3.761	3.00	3.8	4.4	0.809867	0.36218	4.708	$\times 10^{-4}$
CX Error	7.781	12.53	9.96275	11.755	14.3275	43.41329	1.534892	18.85	$\times 10^{-3}$
Gate time	234.667	295.111	268.44425	288	318.22225	43.17165	15.26348	369.778	ns

The processor type is *Falcon* r4T. The system boasts 8 CX qubit connections, and calibration data was accessed on November 13, 2022

Table 25 Summary of hardware performance, qubit characteristics and key specifications for the 5-qubit quantum computer *ibmq_belem*, featuring basis gates CX, ID, RZ, SX, and X

System characteristics	Min	Mean	1st Quartile	Median	3rd Quartile	Stdev	StdError	Max	Unit
T1	70.6	101	37.2	100.74	130.18	29.17987	13.04963	130.28	μs
T2	58.22	102.948	79.62	94.24	135.89	37.50387	16.77224	146.77	μs
Frequency	5.09	5.225	5.17	5.246	5.258	0.010158	0.04543	5.361	GHz
Anharmonicity	-0.33612	-0.329682	-0.33374	-0.33135	-0.33063	0.007641	0.003417	-0.31657	GHz
Readout assignment error	1.650	4.290	2.1	2.96	3.78	3.817185	1.707097	10.96	$\times10^{-2}$
Prob. meas $\lvert 0 \rangle$ prep $\lvert 1 \rangle$	2.96	7.428	3.28	4.74	6.16	7.142431	3.194193	20.0	$\times10^{-2}$
Prob. meas $\lvert 1 \rangle$ prep $\lvert 0 \rangle$	0.34	1.152	0.92	1.18	1.4	0.584226	0.261274	1.92	$\times10^{-2}$
Readout length	6158.222	6158.222	6158.222	6158.222	6158.222	0.00	0.00	6158.222	ns
Single-qubit error	1.735	26.1794	2.666	2.83	2.866	0.5289654	0.2365605	120.8	$\times10^{-4}$
CX Error	6.474	25.64	6.807	6.654	259.2925	458.93856	162.2593	1000	$\times10^{-3}$
Gate time	405.333	538.6666	433.77775	469.3335	588.44425	162.05814	57.29620	810.667	ns

The processor type is *Falcon* r4T. The system boasts 8 CX qubit connections, and calibration data was accessed on November 13, 2022

Table 26 Summary of hardware performance, qubit characteristics and key specifications for the 5-qubit quantum computer *ibmq_lima*, featuring basis gates CX, ID, RZ, SX, and X

System characteristics	Min	Mean	1st Quartile	Median	3rd Quartile	Stdev	StdError	Max	Unit
T1	23.85	87.786	58.94	98.74	126.44	45.82035	20.49148	130.96	μs
T2	19.37	100.824	26.33	130.68	150.39	37.17569	32.72517	177.45	μs
Frequency	5.03	5.16	5.092	5.128	5.247	0.112434	0.05028	5.303	GHz
Anharmonicity	−0.33574	−0.33068	−0.33447	−0.3336	−0.33124	0.007085	0.003169	−0.31835	GHz
Readout assignment error	1.790	3.672	1.95	5.86	5.69	2.060903	0.921664	6.070	$\times 10^{-2}$
Prob. meas$|0\rangle$ prep$|1\rangle$	2.52	5.2	3.04	4.18	8.82	3.314604	1.482336	9.54	$\times 10^{-2}$
Prob. meas$|1\rangle$ prep$|0\rangle$	0.86	1.724	1.06	1.54	1.84	0.972358	0.434852	3.32	$\times 10^{-2}$
Readout length	5351.111	5351.111	5351.111	5351.111	5351.111	0.0	0.0	5351.111	ns
Single-qubit error	4.736	7.642	5.723	6.948	9.381	2.734339	1.222834	11.42	$\times 10^{-4}$
CX Error	6.318	12.49	7.58475	11.1335	16.0375	6.328578	2.237490	21.37	$\times 10^{-3}$
Gate time	298.667	405.333	327.111	401.7775	487.1115	93.57069	33.08224	519.111	ns

The processor type is *Falcon* r4T. The system boasts 8 CX qubit connections, and calibration data was accessed on November 13, 2022.

Ⓐ Springer

Table 27 The up-to-date IBM Quantum's quantum computers

No.	System[a]	Qubits	QV	EPLG[b]	CLOPS[c]	T1 (μs)[d]	T2 (μs)	QPU[e]	Processor	Version	Features	Performance
1	ibm_fez	156	512	0.8%	3.8K	136.52	78.58	us-east	Heron r1	1.0.0	OpenQASM 3	Table 28
2	ibm_toronto	133	512	1.0%	3.8K	158.27	122.18	us-east	Heron r1	1.0.22	OpenQASM 3	Table 29
3	ibm_kyiv	127	128	1.8%	5.0K	257.27	111.01	us-east	Eagle r3	1.20.12	OpenQASM 3	Table 30
4	ibm_sherbrooke	127	128	1.8%	5.0K	275.67	190.58	us-east	Eagle r3	1.5.3	OpenQASM 3	Table 31
5	ibm_quebec	127	128	2.2%	5.0K	295.08	161.68	us-east	Eagle r3	1.2.8	OpenQASM 3	Table 33
6	ibm_brisbane	127	128	2.2%	5.0K	225.28	144.34	us-east	Eagle r3	1.1.33	OpenQASM 3	Table 32
7	ibm_rensselaer	127	128	2.6%	5.0K	262.14	176.61	us-east	Eagle r3	1.1.6	OpenQASM 3	Table 35
8	ibm_brussels	127	128	2.7%	5.0K	293.28	160.86	us-east	Eagle r3	1.1.13	OpenQASM 3	Table 34
9	ibm_kawasaki	127	128	3.0%	5.0K	197.23	142.23	us-east	Eagle r3	2.1.31	OpenQASM 3	Table 37
10	ibm_strasbourg	127	128	3.0%	5.0K	269.01	169.50	eu-de	Eagle r3	1.0.10	OpenQASM 3	Table 39
11	ibm_nazca	127	128	3.5%	5.0K	178.17	110.34	us-east	Eagle r3	1.0.31	OpenQASM 3	Table 38
12	ibm_kyoto	127	128	3.6%	5.0K	216.88	93.31	us-east	Eagle r3	1.2.38	OpenQASM 3	Table 36
13	ibm_osaka	127	128	3.6%	5.0K	278.37	132.37	us-east	Eagle r3	1.1.8	OpenQASM 3	Table 40
14	ibm_cleveland	127	128	5.0%	5.0K	213.58	191.65	us-east	Eagle r3	1.5.1	OpenQASM 3	Table 41
15	ibm_cusco	127	128	6.8%	5.0K	135.76	72.35	us-east	Eagle r3	1.0.40	OpenQASM 3	Table 42

[a] The information provided in this table reflects the quantum systems available at the time of writing. Given the dynamic nature of IBM's quantum computing infrastructure, systems may be updated, replaced, or retired over time

[b] Error per layered gate for a 100-qubit chain

[c] Hardware-aware circuit layer operations per second

[d] The median values of the relaxation time-T1 and the coherence time-T2, measured in microseconds (μs). Accessed July 2, 2024. except for the ibm_fez accessed 04 July 2024. Most systems support a maximum of 300 circuits and 100,000 shots

[e] QPU region

Table 28 Summary of hardware performance, qubit characteristics, and key specifications for the 156 qubit quantum computer *ibm_fez*

System parameters	Mean	StDev	Min	1st Quartile	Median	3rd Quartile	Max
T1 (μs)	137.558138	47.587586	13.834783	106.863088	136.523081	162.444316	271.626108
T2 (μs)	82.612083	46.241133	4.583184	52.180838	78.580919	111.299718	268.217025
Frequency (GHz)	0.0	0.0	0.0	0.0	0.0	0.0	0.0
Anharmonicity (GHz)	0.0	0.0	0.0	0.0	0.0	0.0	0.0
Readout assignment error	0.024617	0.033318	0.003100	0.008325	0.016300	0.032025	0.363200
Prob. measure $|0\rangle$ prepare $|1\rangle$	0.029385	0.038514	0.0	0.011650	0.020000	0.035050	0.416400
Prob. measure $|1\rangle$ prepare $|0\rangle$	0.019849	0.029431	0.0	0.004400	0.012700	0.026617	0.310000
Readout length (ns)	1560	0.0	1560	1560	1560	1560	1560
ID error	0.000443	0.000589	0.000129	0.000232	0.000288	0.000398	0.005070
The Z-axis rotation (R_Z) error	0.0	0.0	0.0	0.0	0.0	0.0	0.0
The $\sqrt{X}$ (SX) error	0.000443	0.000589	0.000129	0.000232	0.000288	0.000398	0.005070
Pauli-X error	0.000443	0.000589	0.000129	0.000232	0.000288	0.000398	0.005070

The basis gates employed by this system are CZ, ID, RZ, SX, and X. The processor type is *Heron* r2 (version 1.0.0). As of July 4, 2024, the system demonstrates a median CZ error of 2.848×10^{-3}, and a median gate time of 68 ns

Table 29 Summary of hardware performance, qubit characteristics, and key specifications for the 133 qubit quantum computer *ibm_torino*

System parameters	Mean	StDev	Min	1st Quartile	Median	3rd Quartile	Max
T1 (μs)	157.481331	71.344649	10.161401	103.099556	162.909929	215.918228	320.890662
T2 (μs)	131.875390	65.751564	14.347368	81.995644	129.917339	175.014680	314.087388
Frequency (GHz)	0.0	0.0	0.0	0.0	0.0	0.0	0.0
Anharmonicity (GHz)	0.0	0.0	0.0	0.0	0.0	0.0	0.0
Readout assignment error	0.030614	0.043730	0.005100	0.011900	0.020500	0.036600	0.433300
Prob. measure $|0\rangle$ prepare $|1\rangle$	0.036508	0.067759	0.003333	0.013600	0.022000	0.041200	0.716200
Prob. measure $|1\rangle$ prepare $|0\rangle$	0.024720	0.026747	0.002200	0.008400	0.015400	0.033200	0.187000
Readout length (ns)	1560	0.0	1560	1560	1560	1560	1560
ID error	0.000754	0.001624	0.000112	0.000241	0.000317	0.000542	0.013031
The Z-axis rotation (R_Z) error	0.0	0.0	0.0	0.0	0.0	0.0	0.0
The $\sqrt{X}$ (SX) error	0.000754	0.001624	0.000112	0.000241	0.000317	0.000542	0.013031
Pauli-X error	0.000754	0.001624	0.000112	0.000241	0.000317	0.000542	0.013031

The basis gates of this machine are CZ, ID, RZ, SX, and X. The processor type is *Heron* r1 (version 1.0.22). As of July 3, 2024, the system demonstrates a median CZ error of 4.769×10^{-3}, and a median gate time of 84 ns.

Table 30 Summary of hardware performance, qubit characteristics, and key specifications for the 127-qubit quantum computer *ibm_kyiv*

System parameters	Mean	StDev	Min	1st Quartile	Median	3rd Quartile	Max
T1 (μs)	263.380990	94.540378	25.637671	209.55451	254.456028	320.062960	576.494856
T2 (μs)	146.828103	114.200863	13.236858	57.008413	110.193349	195.220693	495.328304
Frequency (GHz)	4.619478	0.112134	4.341284	4.540540	4.612760	4.702569	4.958907
Anharmonicity (GHz)	0.0	0.0	0.0	0.0	0.0	0.0	0.0
Readout assignment error	0.015976	0.033548	0.001100	0.003450	0.006900	0.012800	0.323000
Prob. measure $|0\rangle$ prepare $|1\rangle$	0.017805	0.033056	0.001200	0.005200	0.009000	0.015600	0.287800
Prob. measure $|1\rangle$ prepare $|0\rangle$	0.014146	0.036527	0.0	0.001300	0.004000	0.010200	0.358200
Readout length (ns)	1244.444	0.0	1244.444	1244.444	1244.444	1244.444	1244.444
ID error	0.000549	0.001485	0.000105	0.000194	0.000293	0.000517	0.016190
The Z-axis rotation (R_Z) error	0.0	0.0	0.0	0.0	0.0	0.0	0.0
The $\sqrt{X}$ (SX) error	0.000549	0.001485	0.000105	0.000194	0.000293	0.000517	0.016190
Pauli-X error	0.000549	0.001485	0.000105	0.000194	0.000293	0.000517	0.016190

The basis gates employed by this system include ECR, RZ, SX, ID, and X. The processor type is *Eagle* r3 (version 1.20.12). As of July 3, 2024, the system demonstrates a median ECR error of 1.160×10^{-2}, and a median gate time of 561.778 ns.

Table 31 Summary of hardware performance, qubit characteristics, and key specifications for the 127-qubit quantum computer *ibm_sherbrooke*

System parameters	Mean	StDev	Min	1st Quartile	Median	3rd Quartile	Max
T1 (μs)	274.123442	98.517950	21.158141	224.50857	269.502295	344.268918	521.784547
T2 (μs)	189.105523	122.86363	12.393942	79.646051	183.988935	263.367610	725.093616
Frequency (GHz)	4.789996	0.109104	4.455281	4.731590	4.794027	4.859388	5.057532
Anharmonicity (GHz)	−0.310393	0.005480	−0.324263	−0.312253	−0.310932	−0.309626	−0.271864
Readout assignment error	0.028869	0.058722	0.002800	0.007900	0.012200	0.023600	0.439200
Prob. measure $\lvert 0\rangle$ prepare $\lvert 1\rangle$	0.033345	0.070388	0.003200	0.008400	0.013400	0.024300	0.483333
Prob. measure $\lvert 1\rangle$ prepare $\lvert 0\rangle$	0.024393	0.054051	0.001200	0.005500	0.009400	0.020500	0.447600
Readout length (ns)	1244.444	0.0	1244.444	1244.444	1244.444	1244.444	1244.444
ID error	0.000441	0.000791	0.000080	0.000167	0.000227	0.000349	0.006187
The Z-axis rotation (R_Z) error	0.0	0.0	0.0	0.0	0.0	0.0	0.0
The $\sqrt{X}$ (SX) error	0.000441	0.000791	0.000080	0.000167	0.000227	0.000349	0.006187
Pauli-X error	0.000441	0.000791	0.000080	0.000167	0.000227	0.000349	0.006187

The basis gates employed by this system include ECR, RZ, SX, ID, and X. The processor type is Eagle r3 (version 1.5.3). As of July 3, 2024, the system demonstrates a median ECR error of 7.400×10^{-3}, and a median gate time of 533.333 ns.

Table 32 Summary of hardware performance, qubit characteristics, and key specifications for the 127-qubit quantum computer *ibm_brisbane*

System parameters	Mean	StDev	Min	1st Quartile	Median	3rd Quartile	Max
T1 (us)	215.546208	79.938473	23.612698	151.804061	222.649128	266.129216	407.872593
T2 (us)	153.564636	82.301519	14.358729	90.089787	145.556518	218.296065	326.660536
Frequency (GHz)	4.896177	0.109272	4.609657	4.821185	4.905596	4.971761	5.117739
Anharmonicity (GHz)	−0.308664	0.005384	−0.359055	−0.309744	−0.308420	−0.307402	−0.289806
Readout assignment error	0.028724	0.046723	0.004000	0.008900	0.014100	0.023850	0.338500
Prob. measure $|0\rangle$ prepare $|1\rangle$	0.029354	0.044149	0.004600	0.009700	0.015600	0.024500	0.351000
Prob. measure $|1\rangle$ prepare $|0\rangle$	0.028094	0.059044	0.002400	0.007300	0.010800	0.020900	0.481000
Readout length (ns)	1300.00	0.0	1300.00	1300.00	1300.00	1300.00	1300.00
ID error	0.000689	0.003614	0.000077	0.000185	0.000244	0.000363	0.040644
The Z-axis rotation (R_Z) error	0.0	0.0	0.0	0.0	0.0	0.0	0.0
The $\sqrt{X}$ (SX) error	0.000689	0.003614	0.000077	0.000185	0.000244	0.000363	0.040644
Pauli-X error	0.000689	0.003614	0.000077	0.000185	0.000244	0.000363	0.040644

The basis gates employed by this system include ECR, RZ, SX, ID, and X. The processor type is *Eagle* r3 (version 1.1.33). As of July 3, 2024, the system demonstrates a median ECR error of 8.335×10^{-3}, and a median gate time of 660 ns.

Table 33 Summary of hardware performance, qubit characteristics, and key specifications for the 127-qubit quantum computer *ibm_quebec*

System parameters	Mean	StDev	Min	1st Quartile	Median	3rd Quartile	Max
T1 (us)	292.051452	112.235331	3.180864	214.685833	288.916307	358.436905	616.631699
T2 (us)	178.416351	135.865063	2.208681	65.975403	145.882121	278.439621	583.406553
Frequency (GHz)	4.910363	0.113470	4.634752	4.831137	4.901556	4.996106	5.198909
Anharmonicity (GHz)	−0.298732	0.054194	−0.329975	−0.309970	−0.308308	−0.307014	0.0
Readout assignment error	0.041901	0.079884	0.002600	0.008050	0.013000	0.028300	0.484700
Prob. measure $|0\rangle$ prepare $|1\rangle$	0.040815	0.082489	0.002800	0.008700	0.013200	0.024700	0.470200
Prob. measure $|1\rangle$ prepare $|0\rangle$	0.042986	0.089180	0.001000	0.006800	0.012400	0.027200	0.522000
Readout length (ns)	835.555556	0.0	835.555556	835.555556	835.555556	835.555556	835.555556
ID error	0.002031	0.018074	0.000088	0.000171	0.000225	0.000345	0.203685
The Z-axis rotation (R_Z) error	0.0	0.0	0.0	0.0	0.0	0.0	0.0
The $\sqrt{X}$ (SX) error	0.002031	0.018074	0.000088	0.000171	0.000225	0.000345	0.203685
Pauli-X error	0.002031	0.018074	0.000088	0.000171	0.000225	0.000345	0.203685

The basis gates of this machine are ECR, RZ, SX, ID, X. The processor type is *Eagle* r3 (version 1.2.8). As of July 3, 2024, the system demonstrates a median ECR error of 8.017×10^{-3}, and a median gate time of 593 ns.

Table 34 Summary of hardware performance, qubit characteristics, and key specifications for the 127-qubit quantum computer *ibm_brussels*

System parameters	Mean	StDev	Min	1st Quartile	Median	3rd Quartile	Max
T1 (μs)	320.440117	111.234768	39.414051	246.872003	313.847394	389.887420	608.989954
T2 (μs)	167.756680	117.414095	0.455292	65.949763	173.149154	243.485123	465.689813
Frequency (GHz)	4.800165	0.114353	4.532232	4.731179	4.798645	4.884004	5.074872
Anharmonicity (GHz)	−0.299139	0.055095	−0.380843	−0.310694	−0.309003	−0.307563	0.0
Readout assignment error	0.028740	0.033565	0.004800	0.010300	0.017200	0.034150	0.206667
Prob. measure $|0\rangle$ prepare $|1\rangle$	0.025434	0.031165	0.003400	0.010000	0.015400	0.029700	0.230000
Prob. measure $|1\rangle$ prepare $|0\rangle$	0.032045	0.042137	0.002600	0.010000	0.017000	0.037600	0.333600
Readout length (ns)	1600	0.0	1600	1600	1600	1600	1600
ID error	0.000387	0.000543	0.000086	0.000177	0.000242	0.000352	0.004047
The Z-axis rotation (R_Z) error	0.0	0.0	0.0	0.0	0.0	0.0	0.0
The $\sqrt{X}$ (SX) error	0.000387	0.000543	0.000086	0.000177	0.000242	0.000352	0.004047
Pauli-X error	0.000387	0.000543	0.000086	0.000177	0.000242	0.000352	0.004047

The basis gates employed by this system include ECR, RZ, SX, ID, and X. The processor type is *Eagle* r3 (version 1.1.13). As of July 3, 2024, the system demonstrates a median ECR error of 8.074×10^{-3}, and a median gate time of 660 ns.

$\underline{\textcircled{2}}$ Springer

Table 35 Summary of hardware performance, qubit characteristics, and key specifications for the 127-qubit quantum computer, *ibm_rensselaer*

System parameters	Mean	StDev	Min	1st Quartile	Median	3rd Quartile	Max
T1 (μs)	259.126834	101.960836	22.517959	193.211648	261.637128	329.469093	502.305781
T2 (μs)	176.992496	102.018513	0.954730	94.366764	172.220393	253.475846	470.735523
Frequency (GHz)	4.836538	0.116574	4.544908	4.763693	4.830515	4.919746	5.220783
Anharmonicity (GHz)	−0.288692	0.075452	−0.347815	−0.309668	−0.308135	−0.306593	0.0
Readout assignment error	0.021865	0.035818	0.002300	0.005550	0.008400	0.015600	0.199000
Prob. measure $|0\rangle$ prepare $|1\rangle$	0.022471	0.037413	0.002400	0.006400	0.009200	0.018900	0.207000
Prob. measure $|1\rangle$ prepare $|0\rangle$	0.021258	0.039389	0.001400	0.004100	0.007200	0.016200	0.244400
Readout length (ns)	1112.889	0.0	1112.889	1112.889	1112.889	1112.889	1112.889
ID error	0.000995	0.005936	0.000102	0.000165	0.000230	0.000336	0.065202
The Z-axis rotation (R_Z) error	0.0	0.0	0.0	0.0	0.0	0.0	0.0
The $\sqrt{X}$ (SX) error	0.000995	0.005936	0.000102	0.000165	0.000230	0.000336	0.065202
Pauli-X error	0.000995	0.005936	0.000102	0.000165	0.000230	0.000336	0.065202

The basis gates employed by this system include ECR, RZ, SX, ID, and X. The processor type is *Eagle* r3 (version 1.1.6). As of July 3, 2024, this quantum system exhibits a median ECR error: 7.580×10^{-3}, and a median gate time of 665.889 ns.

Table 36 Summary of hardware performance, qubit characteristics, and key specifications for the 127-qubit quantum computer *ibm_kyoto*

System parameters	Mean	StDev	Min	1st Quartile	Median	3rd Quartile	Max
T1 (μs)	223.401174	70.329045	0.868321	179.834966	216.880493	261.150818	425.219660
T2 (μs)	116.498508	81.507892	5.093271	50.531352	98.471325	164.392541	348.377179
Frequency (GHz)	4.966616	0.130136	4.704558	4.857412	4.959635	5.066503	5.250633
Anharmonicity (GHz)	−0.292802	0.065494	−0.312095	−0.308707	−0.307325	−0.305526	0.0
Readout assignment error	0.036971	0.052227	0.004600	0.009650	0.016400	0.041800	0.315300
Prob. measure $|0\rangle$ prepare $|1\rangle$	0.037713	0.064612	0.004000	0.009600	0.014400	0.039400	0.493400
Prob. measure $|1\rangle$ prepare $|0\rangle$	0.036229	0.047338	0.002800	0.008600	0.017000	0.046300	0.305600
Readout length (ns)	1400	0.0	1400	1400	1400	1400	1400
ID error	0.003028	0.022267	0.000106	0.000194	0.000289	0.000526	0.246250
The Z-axis rotation (R_Z) error	0.0	0.0	0.0	0.0	0.0	0.0	0.0
The $\sqrt{X}$ (SX) error	0.003028	0.022267	0.000106	0.000194	0.000289	0.000526	0.246250
Pauli-X error	0.003028	0.022267	0.000106	0.000194	0.000289	0.000526	0.246250

The basis gates employed by this system include ECR, RZ, SX, ID, and X. The processor type is *Eagle* r3 (version 1.2.38). As of July 3, 2024, the system demonstrates a median ECR error of 1.023×10^{-2}, and a median gate time of 660 ns.

Table 37 Summary of hardware performance, qubit characteristics, and key specifications for the 127-qubit quantum computer *ibm_kawasaki*

System parameters	Mean	StDev	Min	1st Quartile	Median	3rd Quartile	Max
T1 (μs)	195.343472	64.693363	0.776066	148.57249	196.852003	239.485612	344.118089
T2 (μs)	160.814823	90.323244	6.473055	94.779526	148.271693	223.492753	502.659788
Frequency (GHz)	5.241257	0.130815	4.904341	5.156160	5.239658	5.340298	5.583662
Anharmonicity (GHz)	−0.301599	0.011852	−0.365607	−0.304317	−0.302589	−0.300511	−0.206400
Readout assignment error	0.028137	0.050709	0.004600	0.008050	0.010700	0.020500	0.383600
Prob. measure $|0\rangle$ prepare $|1\rangle$	0.024430	0.031478	0.004000	0.008900	0.012400	0.022600	0.206667
Prob. measure $|1\rangle$ prepare $|0\rangle$	0.031844	0.079804	0.002200	0.006700	0.009200	0.020400	0.730400
Readout length (ns)	1112.889	0.0	1112.889	1112.889	1112.889	1112.889	1112.889
ID error	0.000320	0.000330	0.000114	0.000170	0.000247	0.000328	0.003243
The Z-axis rotation (R_Z) error	0.0	0.0	0.0	0.0	0.0	0.0	0.0
The $\sqrt{X}$ (SX) error	0.000320	0.000330	0.000114	0.000170	0.000247	0.000328	0.003243
Pauli-X error	0.000320	0.000330	0.000114	0.000170	0.000247	0.000328	0.003243

The basis gates employed by this system include ECR, RZ, SX, ID, and X. The processor type is *Eagle* r3 (version 2.1.31). As of July 3, 2024, the system demonstrates a median ECR error of 7.114×10^{-3}, and a median gate time of 586.667 ns.

Table 38 Summary of hardware performance, qubit characteristics, and key specifications for the 127-qubit quantum computer *ibm_nazca*

System parameters	Mean	StDev	Min	1st Quartile	Median	3rd Quartile	Max
T1 (μs)	185.190222	69.655015	32.25129	140.13869	178.168265	233.203341	352.943675
T2 (μs)	123.274041	78.552897	1.046602	61.592155	110.340019	176.435465	376.598767
Frequency (GHz)	5.080864	0.127984	4.769237	5.002285	5.081721	5.169752	5.382887
Anharmonicity (GHz)	−0.298594	0.046907	−0.346217	−0.307314	−0.305897	−0.304007	0.0
Readout assignment error	0.044305	0.062403	0.002900	0.011950	0.025300	0.044150	0.490000
Prob. measure $|0\rangle$ prepare $|1\rangle$	0.044364	0.056621	0.004400	0.013800	0.025600	0.046700	0.312400
Prob. measure $|1\rangle$ prepare $|0\rangle$	0.044246	0.074209	0.001400	0.010200	0.023600	0.044400	0.667600
Readout length (ns)	4000	0.0	4000	4000	4000	4000	4000
ID error	0.001259	0.005361	0.000141	0.000256	0.000360	0.000569	0.048093
The Z-axis rotation (R_Z) error	0.0	0.0	0.0	0.0	0.0	0.0	0.0
The $\sqrt{X}$ (SX) error	0.001259	0.005361	0.000141	0.000256	0.000360	0.000569	0.048093
Pauli-X error	0.001259	0.005361	0.000141	0.000256	0.000360	0.000569	0.048093

The basis gates employed by this system include ECR, RZ, SX, ID, and X. The processor type is *Eagle* r3 (version 1.0.31). As of July 3, 2024, the system demonstrates a median ECR error of 1.240×10^{-2}, and a median gate time of 660 ns.

⚛ Springer

Table 39 Summary of hardware performance, qubit characteristics, and key specifications for the 127-qubit quantum computer *ibm_strasbourg*

System parameters	Mean	StDev	Min	1st Quartile	Median	3rd Quartile	Max
T1 (μs)	292.823565	119.937196	40.243743	200.07130	287.181909	364.642999	707.960349
T2 (μs)	199.708814	128.709167	12.680931	87.916392	187.396030	290.491071	510.203219
Frequency (GHz)	4.815512	0.120955	4.536352	4.729195	4.816615	4.900868	5.107659
Anharmonicity (GHz)	−0.263911	0.107956	−0.319817	−0.309432	−0.308260	−0.305938	0.0
Readout assignment error	0.034652	0.044990	0.003600	0.010100	0.017100	0.041000	0.346300
Prob. measure $|0\rangle$ prepare $|1\rangle$	0.033777	0.052202	0.003600	0.009600	0.016200	0.037000	0.344800
Prob. measure $|1\rangle$ prepare $|0\rangle$	0.035527	0.049744	0.002400	0.009800	0.015800	0.035400	0.347800
Readout length (ns)	1600	0.0	1600	1600	1600	1600	1600
ID error	0.001408	0.008712	0.000084	0.000183	0.000244	0.000454	0.095269
The Z-axis rotation (R_Z) error	0.0	0.0	0.0	0.0	0.0	0.0	0.0
The $\sqrt{X}$ (SX) error	0.001408	0.008712	0.000084	0.000183	0.000244	0.000454	0.095269
Pauli-X error	0.001408	0.008712	0.000084	0.000183	0.000244	0.000454	0.095269

The basis gates of this machine are ECR, RZ, SX, ID, X. The processor type is *Eagle* r3 (version 1.10.11). As of July 3, 2024, the system demonstrates a median ECR error of 8.857×10^{-3}, and a median gate time of 660 ns.

Table 40 Summary of hardware performance, qubit characteristics, and key specifications for the 127-qubit quantum computer *ibm_osaka*

System parameters	Mean	StDev	Min	1st Quartile	Median	3rd Quartile	Max
T1 (μs)	275.209175	93.340756	7.717160	222.16072	278.368365	335.722431	440.616889
T2 (μs)	144.771406	99.247376	8.117184	60.099590	132.372260	213.681193	409.977824
Frequency (GHz)	4.854223	0.114444	4.568035	4.772079	4.861266	4.928279	5.128348
Anharmonicity (GHz)	−0.284977	0.079198	−0.311990	−0.308883	−0.307491	−0.306113	0.0
Readout assignment error	0.051915	0.076861	0.003500	0.011500	0.021900	0.060600	0.493100
Prob. measure $|0\rangle$ prepare $|1\rangle$	0.053071	0.082672	0.003600	0.011000	0.022600	0.058500	0.500000
Prob. measure $|1\rangle$ prepare $|0\rangle$	0.050758	0.085043	0.002000	0.010100	0.021000	0.062600	0.689600
Readout length (ns)	1400	0.0	1400	1400	1400	1400	1400
ID error	0.001470	0.006991	0.000077	0.000170	0.000250	0.000432	0.062575
The Z-axis rotation (R_Z) error	0.0	0.0	0.0	0.0	0.0	0.0	0.0
The $\sqrt{X}$ (SX) error	0.001470	0.006991	0.000077	0.000170	0.000250	0.000432	0.062575
Pauli-X error	0.001470	0.006991	0.000077	0.000170	0.000250	0.000432	0.062575

The basis gates employed by this system include ECR, RZ, SX, ID, and X. The processor type is *Eagle* r3 (version 1.1.8). As of July 3, 2024, the system demonstrates a median ECR error of 8.596×10^{-3}, and a median gate time of 660 ns.

Table 41 Summary of hardware performance, qubit characteristics, and key specifications for the 127-qubit quantum computer *ibm_cleveland*

System parameters	Mean	StDev	Min	1st Quartile	Median	3rd Quartile	Max
T1 (μs)	211.979707	72.812847	18.787932	172.508265	213.579840	256.393505	454.759059
T2 (μs)	196.083432	119.767324	14.467346	102.122094	191.647308	274.766102	523.275907
Frequency (GHz)	4.876390	0.123974	4.589666	4.795009	4.876078	4.948031	5.238570
Anharmonicity (GHz)	−0.308475	0.004577	−0.324563	−0.310648	−0.308918	−0.307588	−0.278350
Readout assignment error	0.029770	0.047776	0.004500	0.009250	0.013000	0.024600	0.323700
Prob. measure $|0\rangle$ prepare $|1\rangle$	0.026925	0.035570	0.004600	0.011100	0.014800	0.024900	0.256400
Prob. measure $|1\rangle$ prepare $|0\rangle$	0.032615	0.065273	0.003200	0.006400	0.010600	0.022000	0.391000
Readout length (ns)	1251.556	0.0	1251.556	1251.556	1251.556	1251.556	1251.556
ID error	0.000445	0.000847	0.000100	0.000202	0.000278	0.000401	0.009188
The Z-axis rotation (R_Z) error	0.0	0.0	0.0	0.0	0.0	0.0	0.0
The $\sqrt{X}$ (SX) error	0.000445	0.000847	0.000100	0.000202	0.000278	0.000401	0.009188
Pauli-X error	0.000445	0.000847	0.000100	0.000202	0.000278	0.000401	0.009188

The basis gates of this machine are ECR, RZ, SX, ID, X. The processor type is *Eagle* r3 (version 1.5.1). As of July 3, 2024, the system demonstrates a median ECR error of 9.157×10^{-3}, and a median gate time of 590.222 ns.

Table 42 Summary of hardware performance, qubit characteristics, and key specifications for the 127-qubit quantum computer *ibm_cusco*

System parameters	Mean	StDev	Min	1st Quartile	Median	3rd Quartile	Max
T1 (μs)	136.288638	63.328683	26.825990	80.328785	135.758247	184.787286	346.403520
T2 (μs)	96.987691	71.929940	2.803230	47.662439	72.346176	142.604449	346.467411
Frequency (GHz)	5.164246	0.133437	4.806652	5.071311	5.168677	5.263250	5.462529
Anharmonicity (GHz)	−0.299714	0.038185	−0.322850	−0.305927	−0.304439	−0.302885	0.0
Readout assignment error	0.060970	0.073258	0.005000	0.019450	0.038100	0.065900	0.392800
Prob. measure $|0\rangle$ prepare $|1\rangle$	0.072222	0.087468	0.007800	0.018400	0.039000	0.085767	0.429000
Prob. measure $|1\rangle$ prepare $|0\rangle$	0.049717	0.072154	0.0	0.014300	0.026000	0.049833	0.377600
Readout length (ns)	4000	0.0	4000	4000	4000	4000	4000
ID error	0.002483	0.006949	0.000138	0.000262	0.000565	0.001776	0.058174
The Z-axis rotation (R_Z) error	0.0	0.0	0.0	0.0	0.0	0.0	0.0
The $\sqrt{X}$ (SX) error	0.002483	0.006949	0.000138	0.000262	0.000565	0.001776	0.058174
Pauli-X error	0.002483	0.006949	0.000138	0.000262	0.000565	0.001776	0.058174

The basis gates employed by this system include ECR, RZ, SX, ID, and X. The processor type is *Eagle* r3 (version 1.0.40). As of July 3, 2024, the system demonstrates a median ECR error of 2.398×10^{-2}, and a median gate time of 460 ns.

☝ Springer

assessment of different IBM Quantum systems, highlighting advancements in technology over time.

7.4 The up-to-date machines' performance

This section analyzes the performance metrics of 15 up-to-date IBM Quantum's quantum machines (see Table 27)). Tables 28 to 42 summarize the hardware performance, qubit characteristics, and specifications of these quantum computers. Key parameters such as coherence times (T1 and T2), qubit frequencies, qubit anharmonicity, readout assignment error, readout length, qubit flip probabilities, as well as error rates for both single-qubit and two-qubit gates.

8 IBM quantum's software ecosystem

8.1 Qiskit

Qiskit, the software development kit for quantum information science, launched by IBM in 2017 as an open-source toolbox for quantum computing. Over the past six years, it has flourished significantly. Qiskit has been installed over 6 million times, with current installations occurring at a rate of 300,000 per month [67]. Boasting
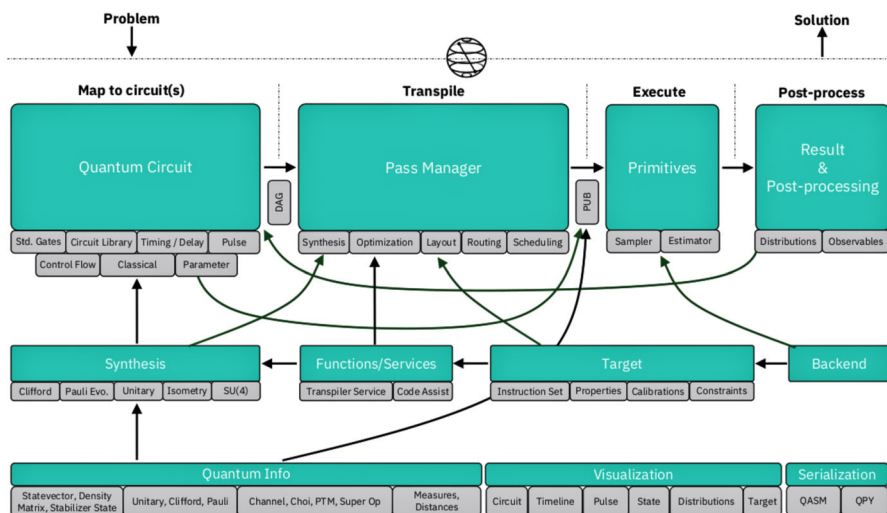
Fig. 7 Qiskit's software architecture: The quantum info module links circuits to quantum information mathematics. The transpiler optimizes circuits via a pass manager, considering ISA and constraints. Primitives run circuits on simulators or hardware, evaluating results. Visualization tools and serialization with OpenQASM and QPY format are also included. Regenerated under a Creative Commons license (https://creativecommons.org/licenses/by/4.0/) from [67]

more than 2000 forks, over 8000 contributions, and has facilitated the execution of over 3 trillion circuits [67]. By a significant margin, Qiskit stands out as the most widely-adopted quantum computing software.

Qiskit has demonstrated its effectiveness in recent studies in quantum computing, particularly in error mitigation [10]. Moreover, it played a crucial role in achieving fault-tolerant magic state preparation surpassing break-even fidelity [68], as well as in numerous significant studies involving up to 133 qubits and thousands of two-qubit entangling gates [69–78].

8.2 Qiskit patterns

Qiskit patterns, outline a structured four-step process for executing algorithms on quantum computers, aligning with its software architecture (shown in Fig. 7). Initially, classical problems are translated into quantum computations by constructing circuits that encode the specific problem. Qiskit provides a user-friendly circuit construction API capable of handling extensive circuits. Subsequently, circuits undergo transformation-referred to as transpilation-to optimize them for execution on target hardware, focusing on circuit-to-circuit rewriting rather than full compilation to classical controller instructions. Following transpilation, circuits are executed on a target backend using primitive computations. Finally, the obtained results are post-processed to derive solutions for the original problem.

Workflows may iterate through these steps, incorporating advanced patterns like generating new circuits based on results from prior batches [79], integrating quantum and classical computing in a quantum-centric supercomputing architecture [80, 81].

Fig. 8 Examples of Qiskit circuits: **a** Quantum phase estimation algorithm. **b** Entanglement distillation circuit with fallback logic for Bell state preparation. **c** Trotterized $XX + YY$ Hamiltonian simulation circuit with Pauli twirling for noise suppression. **d** GHZ state preparation circuit optimized for hardware ISA, using dynamical decoupling to reduce noise. Regenerated under a Creative Commons license (https://creativecommons.org/licenses/by/4.0/) from [67]

⌖ Springer

Complex pattern orchestration is streamlined via the Qiskit serverless framework [82].

8.3 Qiskit circuits

Quantum circuits are central to Qiskit's architecture, representing computations as sequences of instructions that can be manipulated and analyzed within the software. Qiskit defines circuits broadly, encompassing operations on both quantum and classical data. This includes standard actions like qubit operations and measurements, as well as advanced mathematical operators such as unitaries, Cliffords, isometries, and Fourier transforms. Circuits may also involve classical computations in real-time, such as applying Boolean functions to measurement outcomes, and classical control flow mechanisms like loops and branches.

Circuits can also delineate timing operations and continuous-time qubit dynamics (CTQD) using pulse-defined gates. These levels of abstraction can be combined within a single circuit, facilitating modular composition. Figure 7 provides an overview of Qiskit's architecture, highlighting its components and interactions, while Fig. 8 illustrates diverse circuit types supported by Qiskit [67]. This flexibility supports the exploration of various quantum algorithms and physical implementations.

8.4 Scale to large numbers of qubits

In quantum computing, advancing in the field requires tackling utility-scale tasks, which involve computations on a significantly larger scale. This entails working with circuits that utilize more than 100 qubits and incorporate over 1000 gates.

To demonstrate large-scale operations on IBM Quantum systems, we consider the following example, involving the generation and analysis of a 100-qubit GHZ state ($|\text{GHZ}\rangle_{100} = \frac{1}{\sqrt{2}}(|0\rangle^{\otimes 100} + |1\rangle^{\otimes 100})$) [83]. This approach leverages the Qiskit patterns workflow and concludes with the measurement of the expectation value $\langle Z_0 Z_i \rangle$ for each qubit. The process of developing a quantum program using Qiskit entails four essential steps: mapping the problem to a quantum-native format, optimizing circuits and operators, executing with a quantum primitive function, and analyzing the resulting data.

- *Mapping the Problem*. Begin by constructing a function that generates a `QuantumCircuit` specifically designed to prepare an n-qubit GHZ state. Then, apply this function to generate a 100-qubit GHZ state and collect the relevant observables for measurement.

```python
# Step 1: Mapping the problem
from qiskit import QuantumCircuit

def create_n_qubit_GHZ_circuit(n_qubits: int) -> QuantumCircuit:
    """Generates a QuantumCircuit for an n_qubit GHZ state.

    Args:
        n_qubits (int): Number of qubits in the n-qubit GHZ state

    Returns:
        QuantumCircuit: Quantum circuit that prepares the n-qubit GHZ state
    """
    if isinstance(n_qubits, int) and n_qubits >= 2:
        ghz_circuit = QuantumCircuit(n_qubits)
        ghz_circuit.h(0)
        for i in range(n_qubits-1):
            ghz_circuit.cx(i, i+1)
    else:
        raise ValueError("Invalid input: n_qubits must be >= 2")

    return ghz_circuit

# creating a 100-qubit GHZ state
n_qubits = 100
ghz_circuit = create_n_qubit_GHZ_circuit(n_qubits)
```

- Next, proceed to map to the operators of interest. In this case, the focus is on *ZZ* operators between qubits to analyze their behavior over increasing distances. The goal is to observe how expectation values become progressively less accurate (more corrupted), indicating the extent of noise present in the system.

```python
# Next, mapping to relevant operators

from qiskit.quantum_info import SparsePauliOp

# Create a list of operator strings for ZZ terms
operator_strings = ['Z' + 'I'*i + 'Z' + 'I'*(n_qubits-2-i) for i in range(n_qubits-1)]
print(operator_strings)
print(len(operator_strings))

# Create SparsePauliOp objects for each operator string
operators = [SparsePauliOp(operator) for operator in operator_strings]
```

- *Optimization for quantum hardware execution.* Optimize the problem to align with the Instruction Set Architecture (ISA) of the backend.

```python
# Step 2: Optimization for quantum hardware execution

from qiskit.transpiler.preset_passmanagers import generate_preset_pass_manager
from qiskit_ibm_runtime import QiskitRuntimeService

# Instantiate QiskitRuntimeService
service = QiskitRuntimeService()

# Find the least busy backend with at least 100 qubits
backend = service.least_busy(simulator=False, operational=True, min_num_qubits=100)

# Generate a preset pass manager for optimization
pm = generate_preset_pass_manager(optimization_level=1, backend=backend)

# Run the pass manager on the initial state preparation circuit
optimized_circuit = pm.run(ghz_circuit)

# Apply layout to operators
isa_operators_list = [op.apply_layout(optimized_circuit.layout) for op in operators]
```

- *Execution on quantum hardware*. Proceed to submit the job for execution on the quantum hardware, implement error suppression using a technique known as dynamical decoupling to mitigate errors, and adjust the resilience level to determine the degree of error resilience desired. Higher resilience levels yield more precise results but require longer processing times.

```python
# Step 3: Execution on quantum hardware

from qiskit_ibm_runtime import EstimatorOptions
from qiskit_ibm_runtime import EstimatorV2 as Estimator

# Define options for the Estimator
options = EstimatorOptions()
options.resilience_level = 1
options.optimization_level = 0
options.dynamical_decoupling.enable = True
options.dynamical_decoupling.sequence_type = "XY4"

# Create an Estimator object
estimator = Estimator(backend, options=options)

# Submit the circuit and operators list to the Estimator
job = estimator.run([(optimized_circuit, isa_operators_list)])
job_id = job.job_id()
print(job_id)
```

- *Post-processing of results*. Visualize the results through plotting after the job execution is finished. Observing the expectation value $\langle Z_0 Z_i \rangle$ decreases as i increases, indicating a deviation from the ideal scenario where all $\langle Z_0 Z_i \rangle$ values should ideally be 1 in simulation.

```python
# Step 4: Post-processing of results

import matplotlib.pyplot as plt
import numpy as np
from qiskit_ibm_runtime import QiskitRuntimeService

# Define data: Distance between the Z operators
data = list(range(1, len(operators) + 1))

# Retrieve results from the job
result = job.result()[0]

# Extract expectation values from the result
values = result.data.evs

# Normalize the expectation values relative to the first value
values = [v / values[0] for v in values]

# Plotting the graph
plt.scatter(data, values, marker='o', label='100-qubit GHZ state')
plt.xlabel('Distance between qubits $i$')
plt.ylabel(r'$\langle Z_0 Z_i \rangle / \langle Z_0 Z_1 \rangle $')
plt.legend()
plt.show()
```

For the 100-qubit GHZ state, the normalized expectation value $\langle Z_0 Z_i \rangle / \langle Z_0 Z_1 \rangle$ is crucial for understanding the quantum correlations among the qubits. Figure 9 illustrates how the signal decays with increasing distance between qubits, reflecting the presence of noise in the system. To delve deeper into quantum computing with Qiskit, and to gain more detailed insights into its impact on developers and researchers, as well as an in-depth look at how it empowers the quantum computing community, we refer readers to the recent review in [67].

9 IBM quantum partnerships and case studies

IBM's Quantum Network, comprising over 210 *Fortune* 500 companies, leading academic institutions, government agencies, start-ups, and national research labs, plays a crucial role in advancing real-world quantum applications. By collaborating with these diverse partners, IBM is tackling complex challenges in fields such as quantum chemistry, optimization, and machine learning. In this section, we explore IBM Quantum's use cases and strategic partnerships. These partnerships help bridge
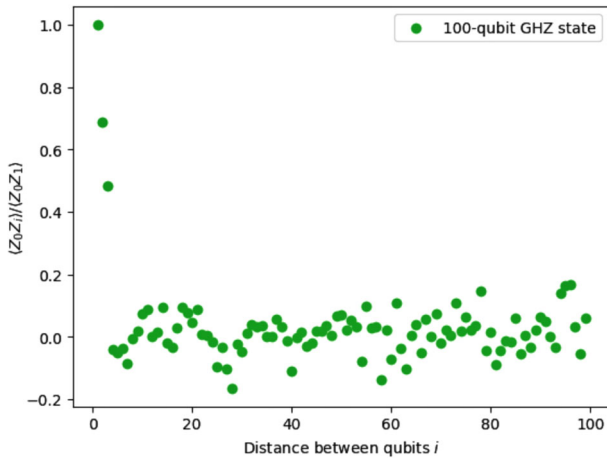
Fig. 9 Decay of normalized $\langle Z_0 Z_i \rangle / \langle Z_0 Z_1 \rangle$ expectation values for a 100-qubit GHZ state, demonstrating quantum correlations as distance between qubits increases. Reproduced from [83]

the gap between theoretical research and tangible, practical solutions, bringing us closer to achieving a quantum advantage in various industries and demonstrating the transformative potential of quantum technologies.

9.1 Boeing

Advancing aerospace material design: Boeing is collaborating with IBM Quantum to tackle the complex challenge of designing strong, lightweight materials, specifically ply composites used in aerospace applications like spacecraft, satellites, and commercial jets. These composites consist of thousands of layers of super-strong materials, each layer angled precisely to achieve optimal strength. The complexity of these designs, involving up to 100,000 variables, surpasses the capabilities of classical supercomputers.

Currently, Boeing addresses this challenge by breaking the design problem into smaller, manageable parts, a method that is effective but time-consuming and costly. However, through its partnership with IBM, Boeing is exploring quantum computing as a potential solution. In a recent experiment, they ran a 40-variable model on a quantum computer, demonstrating that quantum algorithms could efficiently solve a portion of the complex optimization problem.

While quantum computers are not yet large enough to fully solve these design challenges, the collaboration marks a significant step toward utilizing quantum computing to streamline the design of aerospace materials in the future. Boeing sees quantum technology as a critical tool that will eventually help reduce costs and improve the efficiency of material design in aerospace engineering.

9.2 CERN

Unveiling the universe's mysteries: CERN, known for its groundbreaking work in particle physics, including the discovery of the Higgs boson, is collaborating with IBM Quantum to explore new ways to analyze vast amounts of data generated by the Large Hadron Collider (LHC). The LHC produces petabytes of data per second, and analyzing this data requires a complex and powerful computational effort (1 million classical CPU cores in 170 locations across the world). Currently, classical supercomputers rely on a million CPU cores across 170 locations, but quantum computing offers a potential solution to tackle problems beyond their reach.

By applying quantum machine learning, CERN is exploring how quantum algorithms can reveal hidden patterns in LHC data. In early experiments, quantum algorithms showed promising results, even matching the performance of CERN's best classical algorithms. This signals a future where quantum computing could help uncover new physics, such as dark matter and unexplained particle behaviors, as CERN continues to push the boundaries of our understanding of the universe.

9.3 ExxonMobil

Optimizing Energy Supply Chains: ExxonMobil is collaborating with IBM Quantum to tackle some of the most complex optimization problems in global energy logistics, particularly in the transportation of liquefied natural gas (LNG). As the global population grows, so does the challenge of providing affordable, reliable, and sustainable energy. One of the major hurdles ExxonMobil faces is ensuring that LNG is transported efficiently across vast distances to meet fluctuating energy demands, while minimizing carbon emissions and environmental impacts [84, 85].

Quantum computing offers a solution by exploring optimization problems in new ways. IBM and ExxonMobil are developing quantum algorithms to model LNG shipping routes, enabling faster and more efficient solutions. As quantum technology advances, it could also help ExxonMobil with broader energy challenges like carbon capture, low-energy processing, and sustainability. ExxonMobil aims to use quantum computing to address global energy challenges, reduce costs, and improve efficiency in transporting energy. The collaboration is positioning both companies to lead in using quantum technology for the future of energy.

9.4 Cleveland clinic

Using the power of quantum to tackle key healthcare challenges: IBM and Cleveland Clinic have announced a strategic 10-year partnership to advance healthcare and life sciences through cutting-edge technologies, including quantum computing, hybrid cloud, and AI. This collaboration aims to establish the Discovery Accelerator, a platform designed to accelerate medical research and improve patient outcomes. The initiative will focus on key areas such as genomics, single-cell transcriptomics, population health, and drug discovery, with an emphasis on utilizing advanced computational technologies to generate and analyze data.

2 Springer

As part of this partnership, Cleveland Clinic received the first quantum computer fully dedicated to healthcare, the IBM Quantum *System One*, located at its Lerner Research Institute. This system will significantly enhance research capabilities and contribute to the center's Global Center for Pathogen Research & Human Health.

This collaboration aims to revolutionize healthcare discovery, potentially accelerating breakthroughs like vaccine development and the creation of personalized medicine. By integrating quantum computing with classical computing and AI, researchers hope to dramatically speed up research processes and tailor treatments more precisely to individuals' genetic profiles, moving beyond traditional trial-and-error methods.

9.5 E.ON

Tackling electrical grid complexity: E.ON, one of Europe's largest energy companies, is using quantum computing to improve energy pricing and risk management, particularly in predicting energy costs in the face of uncertain factors like weather and consumption trends. Currently, E.ON relies on Monte Carlo simulations for pricing energy derivatives, but these methods are limited by the computational power of classical supercomputers. Through its partnership with IBM, E.ON aims to harness quantum computing to solve these complex problems more efficiently, with the goal of achieving "quantum advantage"-where quantum algorithms outperform classical methods.

Together, IBM and E.ON have developed a quantum algorithm for managing weather-related risks in energy pricing. This algorithm could potentially deliver more accurate predictions for pricing and hedging decisions, benefiting both E.ON's operations and its customers by stabilizing energy costs. With advancements in quantum computing, E.ON expects this collaboration to provide future competitive advantages and greater efficiency in managing energy supply and pricing.

9.6 Mitsubishi chemical

Pursuing game-changing power sources with quantum: Mitsubishi Chemical, in collaboration with IBM Quantum, is exploring groundbreaking power sources, focusing on lithium-oxygen batteries as a potential leap forward in energy storage. While lithium-ion batteries have been the standard for electric vehicles, they remain heavy and limit vehicle performance. Lithium-oxygen batteries, however, promise to be significantly lighter and offer much higher energy densities, potentially enabling electric vehicles to travel further on a single charge.

The challenge lies in modeling the complex electrochemical reactions that occur in lithium-oxygen batteries, particularly the lithium superoxide rearrangement process. This is a task that current supercomputers struggle to handle efficiently. Quantum computers can simulate these complex reactions at a molecular level, offering insights that are impossible to achieve with classical methods.

The collaboration has already yielded successful results, including accurate computational models of the discharge process in lithium-oxygen batteries. By using quantum computing and developing new algorithms, the team is uncovering

previously unknown phenomena and accelerating the discovery of new materials and processes. These advancements could revolutionize battery technology, offering more efficient, lighter, and longer-lasting power sources for a range of industries, from automotive to energy production.

9.7 JSR, Mitsubishi chemical, and Keio University

Exploring new forms of light-emitting materials: IBM is collaborating with Mitsubishi Chemical, JSR Corporation, and Keio University to explore new forms of light-emitting materials using quantum computing. Their focus is on developing advanced Organic LEDs (OLEDs) that are more energy-efficient, flexible, and capable of producing brighter, more vibrant light without relying on rare and costly heavy metals. This innovation could lead to OLEDs with broader color spectrums, improved image quality, and even transparent, bendable displays.

The partnership aims to model and analyze complex molecular structures for OLEDs using quantum computing. Traditional methods struggle to simulate these molecules' behavior, especially as their complexity increases. By using IBM's quantum devices, the team can simulate molecular properties at an atomic and sub-atomic level, which is crucial for developing new, high-performance OLED materials.

The key scientific challenge involves understanding electron transitions within molecules-similar to bioluminescence in fireflies-where the transformation between energy states produces light. Quantum computing enables more accurate simulations of these processes, providing deeper insights into how molecules behave and interact under different conditions. Although quantum computing is still in its early stages [1], the partnership is making significant progress in refining these simulations, accelerating the path toward energy-efficient, scalable OLED technologies with vast potential for applications like flexible, large-area displays.

9.8 Mercedes-Benz

Revolutionizing electric vehicle battery technology: Mercedes-Benz is collaborating with IBM Quantum to accelerate the development of next-generation electric vehicle (EV) batteries, with a focus on lithium-sulfur (Li-S) technology. While today's lithium-ion batteries have made significant strides in powering electric cars, Mercedes-Benz envisions a dramatic leap forward in battery performance-doubling or even quadrupling capacity, improving battery life, reducing energy loss, and cutting costs. Achieving these breakthroughs could transform the automotive industry and help Mercedes reach its ambitious goal of having more than 50% of its car sales come from all-electric or plug-in hybrid vehicles by 2030.

The challenge lies in simulating complex molecular behaviors involved in battery chemistry, a task that traditional supercomputers struggle with due to the immense computational demands. Quantum computers, which operate on the same principles as the molecules they aim to simulate, offer the potential to perform these simulations more efficiently and accurately. By using quantum computing, Mercedes-Benz is

⌘ Springer

looking to streamline the research and development process, potentially accelerating the creation of viable Li-S batteries.

10 The quantum computing landscape

IBM's contributions to quantum computing are undeniably significant, but they exist within a much larger and rapidly evolving quantum computing landscape. To fully appreciate the progress being made, it is important to recognize the valuable work being done by other leading companies and research institutions, each taking different approaches to tackle the complex challenges of quantum computing. By considering these diverse contributions [86], we gain a more holistic view of the field and its potential for transformative impact across industries. As quantum computing continues to mature, collaboration, innovation, and the convergence of different technologies will be essential for achieving the long-term vision of scalable, fault-tolerant quantum computers.

10.1 The race is on

While IBM has made significant strides in quantum computing, particularly with its superconducting qubit-based systems, it is important to place these efforts within the broader quantum ecosystem. Several other companies and institutions are pursuing different quantum technologies, with their own advantages and challenges. For example, Google Quantum AI [87], a pioneer in quantum computing, utilizes superconducting qubits as well, most notably with its *Sycamore* processor [76, 77], which achieved quantum supremacy in 2019 [88]. Similarly, companies like Rigetti Computing and Oxford Quantum Circuits (OQC) also focus on superconducting qubits but are targeting different architectures and scalability solutions.

On the other hand, IonQ's trapped ion technology [89] and Xanadu's photonic approach offer alternative methods for quantum computation [90], each with distinct strengths. Trapped ion systems, such as those developed by IonQ [89], are known for their long coherence times and high precision, though scaling these systems remains a significant challenge. Photonic quantum computing [5, 6], championed by companies like Xanadu, offers potential for easier integration with existing optical technologies, though challenges remain in creating efficient photon sources and detectors [5].

Neutral atom-based quantum processors [91], such as those being developed by PASQAL and QuEra, represent another promising avenue. These systems leverage arrays of neutral atoms that can be individually controlled with lasers, enabling a more scalable architecture. While IBM's efforts are primarily focused on superconducting qubits, the development of these alternative quantum computing technologies highlights the diverse approaches being pursued globally, each with its own strengths, weaknesses, and scalability potential.

In addition to hardware diversity, cloud access has become a major trend, enabling global access to quantum resources. IBM's quantum platform, launched in 2016, was

Table 43 Major players in the quantum computing technology space

No.	Developer	Quantum hardware		
		Quantum computer	Qubit technology	Qubit count[a]
1	IBM Quantum	Condor	Superconducting	1,121
2	Rigetti Computing	Ankaa-2	Superconducting	84
3	IonQ	Forte[b]	Trapped ions	36
4	Honeywell[c]	System model H1	Trapped ions	20
5	Quantinuum[d]	System model H2	Trapped ions	56
6	Google Quantum AI	Willow	Superconducting	105
7	Xanadu	Borealis	Photonics	216
8	Oxford Quantum Circuits	OQC Toshiko	Superconducting	32
9	PASQAL	–	Neutral atom	1,103
10	QuEra	Aquila	Neutral atom	256
11	Quandela Cloud	MOSAIQ	Photonics	12
12	Alibaba Quantum[e]	–	Superconducting	11
13	Intel Quantum	Tangle Lake	Superconducting	49
14	USTC[f]	Jiuzhang	Photonics	76
15	Quantum Inspire[g]	Starmon-5	Superconducting	5

An overview of companies that have made significant strides in developing quantum hardware, including details on the type of qubit technology and the qubit count for each system. These companies are facilitating access to quantum computing resources for both academic and commercial users, with some offering cloud access to their quantum processors, while others (Amazon, Microsoft, Strangeworks, and T-Systems) adopt a reseller model for web-based services. Note that the qubit counts may change as new developments emerge in the industry.

[a]The quantum processors and their qubit numbers may change at any time, akin to a race, and may fluctuate due to advancements, new developments, or updates to their capabilities.

[b]Forte is IonQ's most powerful system to date, featuring the company's largest single-core quantum processor.

[c]Merged in Quantinuum.

[d]The newly formed quantum computing company, created from the merger of Honeywell Quantum Solutions and Cambridge Quantum, is named Quantinuum.

[e]Alibaba Quantum, the quantum computing division of Alibaba Group, discontinued its quantum computing operations in late 2023.

[f]Quantum computers, developed by The University of Science and Technology of China.

[g]Developed by QuTech at TU Delft

one of the first to provide quantum computing via the cloud. Other companies such as Rigetti, IonQ, and Microsoft have followed suit, providing access to quantum computing and fostering development of hybrid quantum-classical systems. These systems combine the power of quantum processors for complex tasks with classical systems for pre-processing and optimization, as seen in IBM's Qiskit Runtime.

As shown in Table 43, several major players in the quantum computing space are advancing different quantum technologies, ranging from IBM's superconducting qubits to other approaches such as trapped ions, photonics, and neutral atoms. It

🖄 Springer

highlights innovators that have made substantial advancements in the development of quantum hardware, providing information on the type of qubit technology employed and the corresponding qubit count for each system.

Despite the rapid progress, quantum computing faces numerous challenges that are common across the industry, including scalability, error correction, and qubit coherence. IBM's work on quantum error correction (QEC) and modular quantum processors is part of a broader industry trend toward addressing these issues (as detailed in Sect. 12), as seen with initiatives from companies like Google (see Sect. 10.2) and Rigetti (see Sect. 10.3). The challenge of achieving fault tolerance and scaling quantum systems remains a central focus for the entire quantum ecosystem. In the following sections, we provide discussions of other major players in the superconducting quantum computing space, such as Google Quantum AI and Rigetti Computing, whose advancements are shaping the future of quantum technologies. For a comprehensive overview of additional key players in the superconducting quantum computing space, readers are directed to the recent review by AbuGhanem in [86].

10.2 Google quantum AI

Google Quantum AI has made several groundbreaking advancements, particularly in quantum error correction and the pursuit of quantum computational advantage [88]. These milestones mark significant progress in overcoming the challenges inherent in quantum computing.

Google Quantum AI is focused on advancing superconducting (transmon) qubits [92, 93], which show strong potential for scalable quantum computing due to their compatibility with existing semiconductor technologies and their ability to maintain high fidelity and coherence [94, 95]. Through efforts to reduce environmental noise and enhance qubit design, Google has successfully extended qubit coherence times [96], improving their stability and reliability. As, error management [97] is a key priority for Google Quantum AI. By implementing advanced error correction methods and refining qubit designs [96, 98, 99], they have significantly reduced error rates, resulting in more accurate and stable quantum computations.

Google Quantum AI's quantum processors are at the forefront of computational technology, designed to address challenges that classical computers cannot solve [88, 100]. Notable processors developed by the company include *Foxtail* [94, 95], *Bristlecone* [101], and *Sycamore* [88]. These processors are equipped with advanced control and precision, enabling highly accurate manipulation and measurement of qubits [88, 100].

In 2019, major breakthroughs in quantum computing were made, notably in the demonstration of quantum supremacy [88]. Using a superconducting qubit processor with 54 qubits, Google Quantum AI and collaborators demonstrated the ability to create quantum states in a computational space of dimension 2^{53} (about 10^{16}) [88]. The SYC-54 processor completed this task in approximately 200 s, a process that would take roughly 10,000 years on a top-tier classical supercomputer. Additionally, the team tested the largest quantum circuit to date, consisting of 53 qubits and 20

cycles, gathering 30×10^6 samples across ten runs. The fidelity of the truncated circuits was found to be $(2.24 \pm 0.21) \times 10^{-3}$, with the average circuit fidelity estimated at no less than 0.1 [88].

In 2023, Google Quantum AI and its collaborators made significant strides toward achieving quantum computational supremacy with the SYCA-67 and SYCA-70 quantum processors, which feature 67 and 70 qubits, respectively [1, 100]. These experiments investigated the relationship between quantum dynamics and noise, revealing phase boundaries that help explain how noisy quantum devices can still improve their computational power. A major breakthrough was achieved in Random Circuit Sampling (RCS) [102, 103], with the 67-qubit processor maintaining a fidelity of 1.5×10^{-3} after 32 cycles, which involved 880 entanglement gates. This achievement marked a substantial increase in circuit complexity while preserving fidelity compared to prior work. The RCS experiment demonstrated that even with noise, the computational resources required for the 67-qubit processor exceed the capabilities of current classical supercomputers.

The Google Quantum AI team, in collaboration with other researchers, has made a significant breakthrough in quantum error correction. Their findings, outlined in [104], demonstrate impressive reductions in logical error rates relative to physical error rates across multiple Surface code implementations on superconducting quantum processors. Using an upgraded 105-qubit processor, the team successfully implemented a distance-7 code with 101 qubits and a distance-5 code with around 50 qubits. The distance-7 code achieved a logical error rate of $0.143\% \pm 0.003\%$, with a

Table 44 System parameters for Rigetti's state-of-the-art quantum processing units (QPUs), spanning from their large-scale ANKAA systems to their 9-qubit research and development devices, including ANKAA-9Q-3, ANKAA-9Q-1, ANKAA-2, ANKAA-1, and ASPEN-M-3.

Rigetti's state-of-the-art QPUs					
System parameters	ANKAA-9Q-3	ANKAA-9Q-1	ANKAA-2	ANKAA-1	ASPEN-M-3
Qubits	9	9	84	84	80
Tunable couplers	–	12	149	149	–
Median Time Duration (μs)					
T_1 Lifetime	21	16.8	14.8	10.5	23
T_2 Lifetime	24	13	8.5	1.8	23
Median Fidelity (per operation)					
Single-qubit gates	99.9%	99.9%	99.75%	99.74%	99.7%
Two-qubit gates (CZ)	–	–	–	93.3%	93.3%
Two-qubit gates (ISWAP)	99.2%	98.5%	98%	94.9%	–
Two-qubit gates (XY)	–	–	–	–	95%

The table includes key performance metrics such as qubit count, dephasing time (T_2), relaxation time (T_1), single- and two-qubit gate operation times, and gate fidelities for each of these quantum systems. ANKAA-9Q-3 was deployed on June 27, 2024.

🕊 Springer

suppression factor of approximately 2.14 ± 0.02. This code also increased qubit lifetimes by a factor of 2.4 ± 0.3 compared to the best-performing physical qubit [88, 96, 105–107]. Additionally, the data showed a clear performance scaling as the distance increased from 3 to 5 to 7, suggesting that a distance-27 code could potentially achieve a 10^{-6} error rate with 1457 physical qubits [104].

Google has developed specialized software and hardware solutions to support the creation of innovative quantum algorithms aimed at solving practical problems in the near term. One such solution is *Cirq*, a Python library designed for creating, manipulating, and optimizing quantum circuits. *Cirq* provides precise control over quantum gates and operations, enabling researchers to fully leverage both quantum computers and simulators.

As the field continues to evolve, Google Quantum AI's ongoing efforts are expected to play a pivotal role in shaping the future trajectory of quantum computing and driving the next wave of technological breakthroughs. For a comprehensive review of Google's achievements in quantum technology over the past decade (2013–2024), including detailed developments across both hardware and software domains, readers are encouraged to refer to the review by AbuGhanem in [87].

10.3 Rigetti computing

Since 2017, Rigetti Computing has been providing continuous access to its quantum computers via the cloud. With each new generation, the company has made consistent progress in increasing qubit count and enhancing operation fidelity. These advancements are bringing Rigetti closer to the pivotal moment when quantum computers are expected to surpass classical systems in performance [1].

Rigetti's quantum systems are powered by superconducting qubit-based processors, which leverage the principles of superconductivity to achieve high coherence times and fast gate operations. These processors form the foundation of Rigetti's quantum computing platform, enabling the execution of complex quantum algorithms with increasing efficiency and reliability. To date, the company has deployed a range of quantum systems, including: ANKAA-9Q-3, ANKAA-9Q-1, ANKAA-2, ANKAA-1, ASPEN-M-3, ASPEN-M-2, ASPEN-M-1, ASPEN-11, ASPEN-10, ASPEN-9, ASPEN-8, ASPEN-7, ASPEN-4, ASPEN-1, ACORN, and AGAVE.

These quantum processors are accessible via the AWS Braket Service. Additionally, Rigetti's latest innovation, the NOVERA QPU, builds on the same cutting-edge technology as its ANKAA-class systems. The NOVERA QPU, designed for high-performance applications, represents a significant leap forward, offering enhanced capabilities for solving complex computational problems.

Rigetti's quantum systems are specifically engineered to minimize errors, one of the most significant challenges in the field of quantum computing [108–112]. To address this, the company focuses on enhancing qubit coherence, gate fidelity, and error correction protocols, which are crucial for improving the reliability and scalability of quantum operations.

As detailed in Table 44, the performance characteristics of Rigetti's QPUs include key metrics such as qubit count, dephasing and relaxation times (T_2 and T_1), single- and two-qubit gate operation times, and gate fidelities. These parameters highlight the advancements made across Rigetti's quantum systems, from the large-scale ANKAA architecture to the more compact 9-qubit research and development devices.

In addition to hardware advancements, Rigetti's quantum instruction language, *Quil*, provides a high-level abstraction for programming quantum processing units (QPUs). Resembling an assembly language for quantum computing, *Quil* enables the specification of quantum circuits at both the gate and pulse levels, offering fine-grained control over quantum operations. It also integrates classical instructions and shared memory, allowing for hybrid quantum-classical algorithms.

11 IBM quantum's technology roadmap

11.1 The IBM's era of quantum utility

In 2023, an IBM and UC Berkeley groundbreaking experiment revealed a path toward practical quantum computing [10]. This experiment demonstrated that quantum computers could execute circuits beyond the capabilities of brute-force classical simulations. For the first time, IBM Quantum has hardware and software capable of running quantum circuits at a scale of 100 qubits and 3000 gates without prior knowledge of the outcomes [11].

These advancements have prompted IBM Quantum to advocate moving beyond traditional circuit models by embracing parallelism, concurrent classical computing, and dynamic circuits. IBM Quantum emphasizes the necessity of a heterogeneous computing architecture that integrates scalable, parallel circuit execution with advanced classical computation [11].

IBM Quantum's vision for the future involves quantum-centric supercomputing [80, 81]. At the IBM Quantum Summit 2023, significant updates were announced, bringing us closer to this goal, alongside an extended roadmap outlining IBM Quantum's journey toward quantum-centric supercomputing over the next decade. This will enable more advanced utility-scale work and provide a seamless development environment for IBM Quantum's users, potentially even before achieving fault tolerance [10, 11, 113, 114].

11.2 IBM quantum's hardware development

To guide IBM Quantum's mission toward achieving quantum-centric supercomputing, IBM Quantum is extending its roadmap to 2033, spanning a decade of quantum innovation. IBM's quantum computing roadmap outlines a series of critical milestones, reflecting both the progress made in quantum hardware and the tools developed to unlock the potential of quantum systems. By 2023, IBM's research and development enabled quantum computers to perform computations that were previously beyond the capabilities of classical machines, opening new possibilities

⑲ Springer
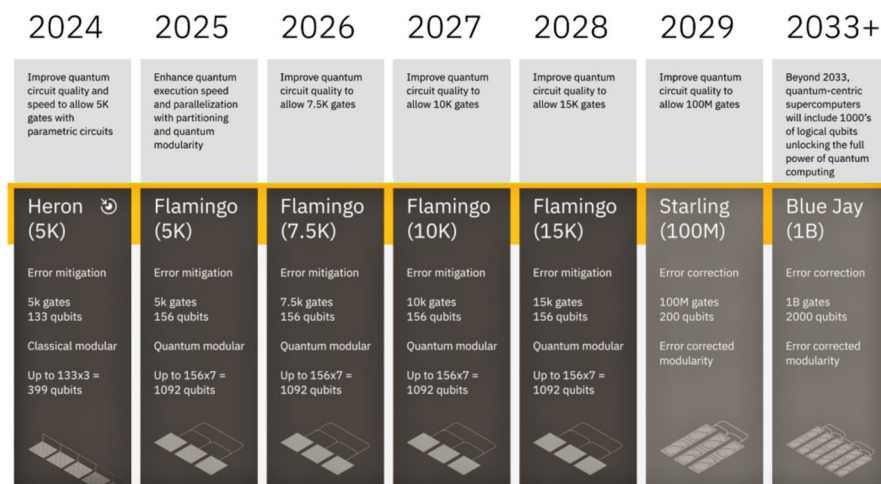
Fig. 10 IBM Quantum Hardware Development Roadmap (2024–2033+). The evolution of IBM's quantum processors from the *Canary* (5 qubits) to the *Blue Jay* processor (2000 qubits, 1 billion gates) expected in 2033 and beyond. Key milestones include advances in qubit count, gate performance, and error correction, highlighting IBM's commitment to scaling quantum computing for practical applications. The roadmap spans critical developments, including the introduction of modular processors, error-corrected systems, and the transition from benchmarking to full quantum-centric supercomputing. Adapted from [115]

for quantum applications (see Sect. 4). As the roadmap continues, the focus has expanded to include both the scaling of qubits and the complexity of quantum circuits, as measured by the number of gates that can be executed. Looking ahead to 2033, IBM is committed to delivering client-facing systems and services that leverage these advancements, with the ultimate goal of harnessing the full power of quantum-centric supercomputing. Key to this vision is the development of new tools for users to explore quantum utility, as well as the incorporation of cutting-edge techniques in machine learning and generative AI to enhance software performance.

IBM's Quantum Hardware Development Roadmap has evolved through several stages, marking key advancements in qubit count, gate fidelity, and error correction [10]. Beginning with early quantum processors from 2016 to 2019, IBM introduced the *Canary* processor (5 qubits), followed by the *Albatross* (16 qubits), *Penguin* (20 qubits), and the *Prototype* (53 qubits), each serving as stepping stones in the development of quantum technologies. In 2020–2021, IBM's *Falcon* processor emerged, with a focus on benchmarking and operating at 27 qubits. This was followed by the *Eagle* processor in 2022–2023, which continued benchmarking advancements at 127 qubits.

Looking ahead, the *Heron* processor (2024) will support up to 133 qubits, capable of executing 5000 gates. The *Flamingo* quantum processor, scheduled for deployment from 2025 through 2028, will progressively scale with qubit counts ranging from 156 qubits and 5000 gates in 2025, 7500 gates in 2026, 10,000 gates in 2027, to 15,000 gates by 2028, with different configurations each year.

In 2029, IBM plans to introduce the *Starling* processor, featuring 200 qubits and the ability to handle up to 100 million gates, with an advanced error-correction module that supports modularity [115]. By 2033 and beyond, IBM's *Blue Jay* quantum processor will reach an unprecedented milestone, with 2000 error-corrected qubits and the ability to perform 1 billion gates, paving the way for truly scalable, fault-tolerant quantum computing.

This milestone signifies a nine-order-of-magnitude increase in gate execution capability since IBM Quantum first introduced its cloud-based devices in 2016. The innovation roadmap will demonstrate the necessary technology to implement the Gross code through processors named *Flamingo*, *Crossbill*, and *Kookaburra*, utilizing l-, m-, and c-couplers, respectively [115]. Figure 10 illustrates the evolution of IBM's quantum processors from the *Canary* (5 qubits) to the *Blue Jay* processor (2000 qubits, 1 billion gates) expected in 2033 and beyond.

11.3 Detailed IBM quantum's roadmap: milestones (2016 − 2033 +)

In this section, we provide a more comprehensive view of IBM's plans for maintaining its leadership in quantum computing over the next decade. Each milestone in this roadmap is outlined in four key areas: (a) Strategy Overview, (b) Significance for clients and society, and (c) Innovations that will enable this progress, with an emphasis on (d) the delivery to clients and partners [115, 116].

1. *Run Quantum Circuits on the IBM Quantum Platform (2016–2017)* Introduced the ability to execute quantum circuits on the IBM Quantum platform, enabling practical experimentation and research on real quantum computers.
2. *Public Release of Multi-Dimensional Roadmap with Initial Focus on Scaling (2020)* Published a comprehensive multi-dimensional roadmap, with an initial emphasis on scaling quantum computing capabilities.
3. *Enhanced Quantum Execution Speed by 100x with Qiskit Runtime (2021)* Achieved a 100-fold increase in quantum execution speed by integrating Qiskit Runtime, significantly improving the efficiency of quantum algorithms.
4. *Introduced Dynamic Circuits to Enable More Complex Computations (2022)* Implemented dynamic circuits, providing the flexibility to perform more complex and adaptable quantum computations, unlocking new possibilities for quantum algorithms.
5. *Introduce Parallelization of Quantum Computations (2023)*
   (*a*) *Strategy Overview* In 2023, IBM is focused on accelerating quantum workflows by integrating parallelization into Qiskit Primitives.
   (*b*) *Significance for clients and society* Current quantum computing systems are often limited by capacity, with some user jobs taking days to complete. By implementing parallelization between Quantum Processing Units (QPUs) and integrating quantum-classical resource parallelization, IBM can provide clients with the ability to execute near-term algorithms more efficiently. This development will reduce job completion times and enhance the overall utility of quantum systems, bringing us closer to practical quantum solutions for industries such as pharmaceuticals, finance, and materials science. Significance

⁇ Springer

for clients and society:

(*c*) *The innovations that will enable this progress*

- *Middleware for task distribution* Automatically manages the distribution of tasks across available resources, ensuring that quantum computations are handled more efficiently.
- *Serverless tools* These tools will simplify the user experience by allowing clients to focus on algorithm development without worrying about managing underlying infrastructure.
- *Expanded classical resources in Qiskit Runtime* By enhancing classical computational power, IBM will speed up compilation processes, thereby optimizing the performance and resource utilization of the QPUs.

(*d*) *Delivery to clients and partners*

- IBM will connect multiple 100+ qubit *Eagle* processors using classical communication, enabling more robust and scalable quantum workflows.
- *Ahead-of-time compilation* This feature will allow for better planning of quantum jobs, maximizing the utilization of available QPUs and ensuring more efficient execution of tasks across both quantum and classical systems.

6. *Expand the Utility of Quantum Computing (2024)*
   (*a*) *Strategy Overview* IBM aims to improve the quality and speed of quantum circuits in 2024, enabling the execution of circuits with 5000 gates using parametric circuits. This advancement will allow quantum systems to tackle larger and more complex problems.
   (*b*) *Significance for clients and society* Qiskit Primitives, integrated with error mitigation techniques, will provide a solid foundation for developers. This platform will enable algorithm and application developers to focus on their workflows while maximizing the quality of quantum hardware, ultimately making quantum computing more practical and accessible for a wide range of industries.
   (*c*) *The innovations that will enable this progress:*

- *Built-in error mitigation* This technology will automatically determine the most effective method for reducing the impact of noise, improving the reliability and accuracy of quantum computations.
- *Transpiler services* AI-powered transpiler services will optimize circuit rewriting for specific hardware, ensuring that quantum circuits are as efficient as possible on available systems.
- *Watson Code Assistant* This tool will assist users in writing Qiskit code, helping them to program quantum systems more easily and efficiently.

(*d*) *Delivery to clients and partners* Multiple higher-quality 100+ qubit Heron processors will be interconnected using classical communication, providing clients with enhanced quantum capabilities and ensuring greater scalability and performance for their applications.

7. *Demonstrate Quantum-Centric Supercomputing (2025)*

   (*a*) *Strategy Overview* In 2025, IBM will prioritize improving the quality of quantum circuits, allowing for the execution of up to 7500 gates. This milestone will integrate modular processors, middleware, and quantum communication technologies to showcase the first quantum-centric supercomputer, marking a significant step forward in the integration of quantum and classical computing resources.

   (*b*) *Significance for clients and society* The abstraction layer will shift from quantum circuits to quantum functions, leveraging Qiskit patterns. This transition will make quantum computing more user-friendly and accessible.

   (*c*) *The innovations that will enable this progress*

   - *Quantum node network* A quantum node will be part of a larger network that integrates both classical and quantum communication, enabling the effective transfer and processing of information between quantum and classical systems.
   - *Resource management* A sophisticated resource management system will coordinate quantum and classical workflows, optimizing the use of both quantum processors and traditional computing resources.
   - *Qiskit libraries and APIs* Qiskit will provide libraries of quantum functions and higher-level APIs, making it easier for developers to create algorithms and applications for quantum systems.

   (*d*) *Delivery to clients and partners* Pre-built Qiskit functions and optimized libraries will be available to clients, enabling faster development of quantum algorithms. Additionally, IBM will demonstrate a 1000+ qubit Flamingo system, constructed from multiple processors and multiple chips per processor, showcasing the potential of large-scale quantum computing.

8. *Scale Quantum Computing (2027)*

   (*a*) *Strategy Overview* In 2027, IBM will scale quantum systems by improving qubits, electronics, infrastructure, and software. The focus will be on reducing the footprint, cost, and energy usage while improving the quality of quantum circuits to enable the execution of up to 10,000 gates.

   (*b*) *Significance for clients and society* Scaling quantum systems will allow users to tackle larger and more complex computations. The seamless integration of multiple computing resources will optimize workflow management, extending the computational reach and practical applicability of quantum systems for a variety of industries.

   (*c*) *The innovations that will enable this progress*

② Springer

- *Intelligent orchestration* This system will analyze workflows to determine the most efficient allocation of resources (QPUs, communication, and classical resources), ensuring that quantum tasks are handled optimally.
- *Qiskit error orchestration* Qiskit will integrate approaches to manage errors effectively, ensuring noise-free outputs and more reliable quantum computations for users.

(*d*) *Delivery to clients and partners* The performance of IBM's *Flamingo* systems will be enhanced, allowing clients to run quantum circuits with up to 10,000 gates and 1000+ qubits, enabling the execution of larger and more sophisticated quantum tasks.

9. *Deliver a Fully Error-Corrected System (2029)*
   (*a*) *Strategy Overview* In 2029, IBM will deliver a quantum system with 200 qubits, capable of running 100 million gates. This system will incorporate advanced quantum error correction techniques to ensure reliability and scalability.
   (*b*) *Significance for clients and society* With this breakthrough, users will be able to tackle large-scale problems using high-rate quantum error correction, greatly expanding the practical applications of quantum computing. This will enable clients to solve previously intractable problems across various industries, from materials science to cryptography.
   (*c*) *The innovations that will enable this progress*

   - *Novel error correction code* A new, efficient error correction code will extend the computational reach of quantum systems, enabling reliable computation at scale.
   - *Dedicated classical hardware* Low-level classical hardware will be integrated into the quantum system to support error correction, enhancing overall performance.
   - *Quantum-centric supercomputing compiler* A specialized compiler will optimize workflows for the quantum system, ensuring the most efficient execution of complex tasks.

   (*d*) *Delivery to clients and partners* The *Starling* system will be available to clients, offering a modular, error-corrected quantum-centric supercomputer with 200 qubits and the ability to run up to 100 million gates, enabling the execution of large-scale quantum applications.

10. *Deliver Quantum-Centric Supercomputers with 1000's of Logical Qubits (2030+)*
    (*a*) *Strategy Overview* Beyond 2033, IBM will deliver quantum-centric supercomputers with thousands of qubits, capable of running 1 billion gates. These advancements will unlock the full potential of quantum computing, opening the door to solving some of the most complex problems across a wide range of industries.

(*b*) *Significance for clients and society* Quantum computers running algorithms with thousands of logical qubits are expected to revolutionize industries by enabling general-purpose applications in fields such as security, chemistry, machine learning, and optimization. This will provide solutions to real-world problems that are currently out of reach for classical systems.

(*c*) *The innovations that will enable this progress*

- *Efficient logical decoding* This technology will allow 2000 qubits to function within a distributed 100,000-qubit machine, significantly enhancing the computational capacity of quantum systems.
- *Middleware for noise management* The middleware will include distributed software tools designed to manage noise-free quantum computations, enabling seamless integration with classical computing resources.
- *General-purpose quantum libraries in Qiskit* Qiskit will provide a set of libraries for general-purpose quantum computing, simplifying the development of quantum algorithms and applications for developers.

(*d*) *Delivery to clients and partners* The 100,000-qubit *Blue Jay* system will define 2000 logical qubits, capable of running a total of 1 billion gates. The middleware will integrate this system into increasingly powerful quantum-centric supercomputers, enabling clients to harness the full power of quantum computing for complex applications.

11.4 IBM quantum safe

Advancements in quantum technology highlight the need for new cryptographic methods based on mathematical challenges that are challenging for both quantum and classical computers to solve. IBM Quantum Safe aids enterprises in evaluating their cryptographic security and updating their cybersecurity strategies for the era of practical quantum computing.

IBM Quantum Safe roadmap outlines ongoing efforts to advance research in quantum-safe cryptography, collaborate with industry partners to promote adoption of post-quantum cryptographic solutions, and innovate new quantum-safe technologies. This includes "IBM Quantum Safe Explorer," a cryptographic discovery tool launched in October 2023.

12 Toward fully fault-tolerant quantum systems

Fault-tolerant quantum computing refers to the ability of a quantum computer to perform computations accurately despite the inevitable errors that arise from noise and imperfections in quantum hardware. As quantum computing continues to evolve, the goal of achieving fully fault-tolerant quantum systems becomes increasingly critical. Quantum systems inherently face challenges due to noise, decoherence, and errors arising from imperfections in quantum hardware. Overcoming these obstacles

🕊 Springer

is essential to realizing the full potential of quantum computers, which will require not only scaling systems to larger sizes, but also ensuring they remain reliable and accurate as they grow in complexity. In the following sections, we explore the key challenges and solutions that will pave the way toward fault-tolerant quantum computing, examining the progress IBM is making toward building practical, fully fault-tolerant quantum systems capable of tackling real-world problems.

12.1 Scalability challenges

While IBM has made significant strides in quantum computing, several challenges remain in developing fault-tolerant systems, particularly related to noise, error correction, and qubit connectivity [117]. One of the core limitations in IBM's current quantum architecture lies in the trade-offs of superconducting qubits when compared to other qubit types, such as trapped ions [89] or photonic qubits [5, 6].

Scalability remains another one of the most significant challenges in the development of quantum computing [14]. As quantum systems grow in size, the complexity of managing qubits, minimizing noise, and maintaining coherence increases exponentially. Quantum processors require ultra-low temperatures, precision control, and error correction to function properly, and these systems become harder to manage as qubit counts rise. Furthermore, connecting large numbers of qubits without introducing excessive error rates or cross-talk between them is a critical hurdle. As the quantum volume grows, the need for efficient qubit interactions, fault tolerance, and the ability to scale quantum systems without diminishing performance becomes increasingly difficult to achieve.

12.2 Scalability solutions

IBM Quantum is addressing scalability challenges [14] through a combination of hardware innovations, modular architectures, and advanced error correction techniques. According to IBM Quantum's development roadmap (as detailed in Sect. 11.3), the company plans to scale quantum systems by improving qubits, electronics, infrastructure, and software. The focus will be on reducing the footprint, cost, and energy consumption, while improving the quality of quantum circuits.

IBM Quantum also emphasizes modular quantum computing, where smaller quantum processors are interconnected to form a larger, cohesive system, enabling scalability without the limitations of a single processor. This modular approach will be vital for future quantum processors like *Starling* (2029) and *Blue Jay* (2033+), allowing for an increase in qubit count without sacrificing system performance. Additionally, IBM Quantum is advancing quantum error correction strategies to enhance fault tolerance, which is essential for scaling quantum computers while maintaining accuracy. As qubit counts grow, advanced error correction protocols will be necessary to maintain reliability. IBM is working on error correction methods (see Sect. 12.3) that will be essential for processors like *Starling*, supporting up to 200 qubits and enabling fault-tolerant quantum computing. Furthermore, IBM's integration of AI and classical-quantum hybrid systems improves scalability by optimizing
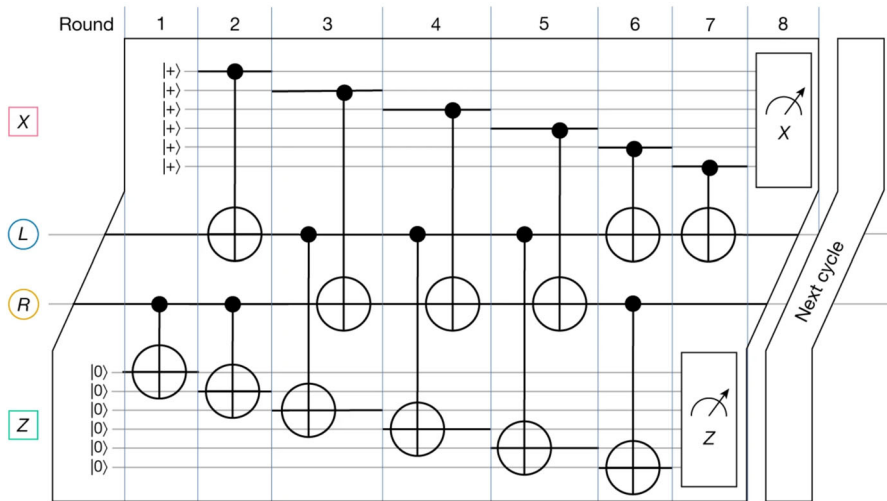
Fig. 11 The complete cycle of syndrome measurements, which involves 7-layers of CNOT gates. The circuit provides a local view, highlighting just one data qubit from each of the registers $q(L)$ and $q(R)$. The circuit is symmetric, allowing for vertical and horizontal shifts of the Tanner graph. Each data qubit interacts with 3 X-check qubits and 3 Z-check qubits via CNOT gates. Reprinted with permission under the Creative Commons Attribution 4.0 International License (http://creativecommons.org/licenses/by/4.0/) from [125]

quantum algorithms and offloading certain computations to classical systems, making the overall system more efficient.

Looking ahead, IBM is exploring quantum networking to link multiple quantum processors into distributed systems. These quantum networks will enable large-scale quantum computation by allowing processors to collaborate seamlessly, as seen in systems like *Blue Jay*, which will feature up to 2000 qubits and 1 billion gates.

As IBM Quantum moves toward quantum-centric supercomputing, the company aims to overcome the fundamental limitations of scaling quantum systems, enabling the execution of increasingly sophisticated quantum tasks with improved error resilience and faster processing speeds. Through these efforts, IBM strives to make large-scale, practical quantum computing a reality, addressing the challenges of noise, qubit connectivity, and system management as quantum systems evolve.

12.3 Quantum error correction

Currently, IBM's quantum error mitigation and quantum error correction (QEC) research focuses on developing the necessary quantum codes and modular approaches to scale quantum processors while maintaining reliability [118–122]. The company is actively working on logical qubit implementations using surface codes and other error correction schemes [97, 123, 124]. The study in [118] introduced a post-processing method for error correction, allowing a quantum computer with 127 qubits to compute the physical properties of a complex model system-something that is beyond the capability of classical computers.
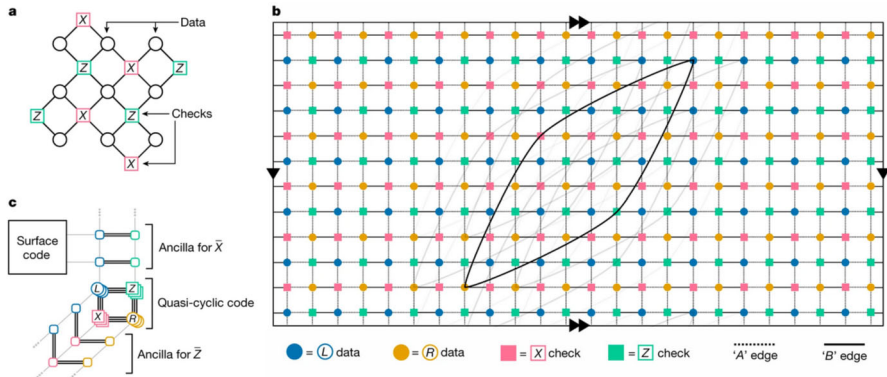
Fig. 12 Tanner Graphs of Surface and BB Codes. **a** A Tanner graph for a surface code, used for comparison. **b** The Tanner graph of a bivariate bicycle (BB) code with parameters [12, 12, 145], arranged on a torus. In this graph, data qubits (represented by blue and orange circles) are linked to check vertices by edges. Each vertex connects to 6 other vertices, with 4 of these edges being short-range (pointing in the cardinal directions, NSEW) and two being long-range, though only a few long-range edges are shown for simplicity. The graph is split into two planar subgraphs, marked by dashed and solid edges. **c** An extended Tanner graph for integrating measurement operations ($\hat{X}$ and $\hat{Z}$) with a surface code. This extension supports quantum teleportation and logical operations through load-store operations, facilitated by additional edges ('A' and 'B') within a thickness-2 architecture. Reprinted with permission under the Creative Commons Attribution 4.0 International License (http://creativecommons.org/licenses/by/4.0/) from [125]

Additionally, A recent IBM's study [125] discusses a quantum error correction protocol aimed at addressing the accumulation of physical errors [126–128], which hinder large-scale computations on current quantum computers. The proposed approach encodes logical qubits into a larger number of physical qubits, enabling error suppression to maintain computation fidelity [97]. The protocol employs (LDPC) low-density parity-check codes to achieve a notable error threshold of 0.7%, comparable to the performance of the surface code, which has been a leading error-correction method for two decades [129–132]. The method requires a specific qubit configuration, including ancillary qubits for syndrome measurement and a circuit with controlled-not gates. The study demonstrates that it is possible to preserve 12 logical qubits over nearly 1 million syndrome cycles using only 288 physical qubits, far fewer than the 3000 physical qubits the surface code would require. This work is believed to bring low-overhead fault-tolerant quantum memory closer to practical implementation on near-term quantum processors [125]. Figure 11 illustrates the complete cycle of syndrome measurements, which involves 7-layers of CNOT gates.

A quantum error-correcting code is classified as LDPC if each check operator interacts with only a small number of qubits, and each qubit is involved in a limited number of checks. Various variants of LDPC codes have been proposed, including hypergraph product codes [133], hyperbolic surface codes [134–136], balanced product codes [137], quantum Tanner codes [138, 139], and 2-block codes based on finite groups [140–143].

IBM Quantum introduces several high-rate LDPC codes designed for QEC, capable of operating with a few hundred physical qubits. These codes are optimized

for error thresholds around 0.7%, performing well in the near-threshold regime and reducing the encoding overhead by a factor of 10 compared to traditional surface codes. Importantly, the hardware requirements for implementing these codes are relatively modest, with each physical qubit only needing to interact with six neighboring qubits through two-qubit gates.

The error correction protocols developed in [125], involve efficient decoding algorithms, low-depth syndrome measurement circuits, and fault-tolerant techniques for handling individual logical qubits. While the qubit connectivity graph of these codes is not locally embeddable into a 2D grid, it can be deconstructed into 2 planar degree-3 subgraphs, making it suitable for superconducting qubit architectures. This qubit connectivity structure can be realized by arranging 2 planar layers of couplers on a chip, which aligns well with the design of superconducting qubits connected by microwave resonators.

The codes IBM develops are a generalization of "bicycle codes" [144] and are named "bivariate bicycle (BB) codes". These stabilizer codes follow the "Calderbank-Shor-Steane (CSS)" type [145, 146] and are described by 6-qubit check operators composed of Pauli X and Z operators. While similar to the 2-dimensional toric code in structure [129], the BB codes differ in that their check operators are not geometrically local and involve interactions across 6 qubits rather than four.

The BB codes are described using Tanner graphs, where each vertex represents either a data qubit or a check operator, and edges connect them based on the interactions between qubits and checks. Each BB code's Tanner graph has a vertex degree of 6 and graph thickness of two [147], meaning it can be decomposed into 2 edge-disjoint planar subgraphs (see Fig. 12). This thickness-2 connectivity is ideal for superconducting qubit systems, making the code architecture well-suited for current quantum hardware.

While superconducting qubits present certain hardware trade-offs and scaling challenges, IBM's approach-focused on error correction, modular hardware, and quantum-classical integration-is paving the way for the development of more reliable, fault-tolerant quantum systems.

12.4 Toward practical fault-tolerant quantum systems

IBM's vision for the future of quantum computing with superconducting qubits highlights the challenges and strategies necessary for overcoming them [15]. Achieving a computational advantage with quantum systems will require substantial improvements in quantum error correction to deal with challenges such as noise, qubit connectivity, and other hardware limitations [7]. In the short term, IBM sees promise in combining multiple quantum processing units (QPUs) through "circuit knitting" and enhancing performance with error suppression techniques, may enable near-term quantum advantages [1]. This approach, along with the development of heuristic quantum algorithms [15], is expected to lead to progress toward solving problems with super-polynomial speedup. Additionally, seamless integration between quantum and classical processors is central to the concept of "quantum-centric supercomputing", as a novel architecture where quantum hardware and software work in concert to deliver high-performance solutions [15]. It is specifically

designed to implement error mitigation, circuit stitching, and heuristic quantum algorithms alongside significant classical computations.

Looking further ahead, IBM's long-term plans involve leveraging higher-dimensional qubit connectivity, moving beyond simple 2D topologies, to facilitate more efficient error correction [119, 129, 138, 148–150]. They also emphasize the importance of modular architecture designs to scale QPUs and enable parallel execution of quantum circuits. Superconducting qubit architectures face several trade-offs, such as the challenge of maintaining high fidelity (99.99% or greater) while scaling. IBM is tackling these challenges with a combination of error mitigation techniques and improvements in both hardware and software to improve quantum system performance. Additionally, scaling up qubit systems introduces further complexities, such as the increased difficulty of controlling larger arrays of qubits and managing heat dissipation. To address these issues, IBM is exploring modular architectures and developing new error correction strategies, like Quantum LDPC codes [133, 151–153], which provide higher thresholds for error tolerance and improve the scalability of quantum systems.

While fault-tolerant quantum computing remains an ongoing challenge, IBM is on track to demonstrate the key principles required for building such systems. According to IBM's roadmap (Sect. 11.3), they aim to demonstrate a full fault-tolerant quantum system (quantum-centric supercomputers with thousands of logical qubits) by 2033 or later. This system will be able to perform error-corrected quantum computations at scale, potentially solving real-world problems in fields such as materials science, optimization, and cryptography.

13 Conclusion

Quantum computing is poised to revolutionize various industries, with major players like IBM Quantum driving these advancements. This study illuminates the rapid evolution and promising future of quantum computing within IBM Quantum. From pioneering quantum hardware advancements to robust software frameworks like Qiskit, IBM continues to redefine the boundaries of quantum technology.

We have delved into IBM Quantum's dynamic journey in quantum computing, providing comprehensive performance evaluations of current and retired quantum computers that illustrate their evolution and future prospects. The documented metrics underscore IBM Quantum's unwavering commitment to advancing quantum computing technology, offering a comparative framework across different systems and highlighting significant technological strides over time.

Additionally, we explored the practical applications of IBM's quantum systems across a range of industries, including airlines, banking, healthcare, insurance, life sciences, and more. Through strategic partnerships with organizations like Boeing, CERN, ExxonMobil, and Mercedes-Benz, IBM is demonstrating how quantum computing is making an impact and bridging the gap between theoretical research and real-world solutions.

As we move toward quantum-centric supercomputing and quantum-safe cryptography, IBM Quantum's trajectory promises transformative capabilities. With

ongoing innovations and collaborative efforts, IBM Quantum is poised to ushering in a new era of computing prowess, offering profound implications across scientific, industrial, and cryptographic domains.

Looking ahead, significant challenges remain in scaling quantum systems and achieving fault tolerance. These hurdles, such as cryogenics, control electronics, and error correction, must be addressed to unlock the full potential of quantum technologies. While quantum advantage in areas like optimization and quantum chemistry is anticipated, realizing fault-tolerant quantum systems will likely take several more years. Nonetheless, the progress made so far positions IBM and the broader quantum ecosystem to overcome these bottlenecks with continued innovation and collaboration.

Collaborative efforts within the quantum computing community, including strategic partnerships and open-source initiatives, will be pivotal in unlocking the full potential of quantum technologies. As a leader in the field, IBM Quantum is positioned to drive these collaborations, fostering innovation across industries, academia, and government. Moreover, substantial funding and investments at both national and international levels will be crucial in driving research, accelerating the development, scaling, and deployment of quantum technologies. IBM's ongoing leadership, alongside these collaborative efforts, will be key in realizing the transformative capabilities of quantum computing in the coming decades.

Declarations

Conflict of interest The author declares no Conflict of interest.

Ethical approval Not applicable.

Consent to participate Not applicable.

Consent for publication The author have approved the publication. This research did not involve any human, animal or other participants.

Open Access   This article is licensed under a Creative Commons Attribution 4.0 International License, which permits use, sharing, adaptation, distribution and reproduction in any medium or format, as long as you give appropriate credit to the original author(s) and the source, provide a link to the Creative Commons licence, and indicate if changes were made. The images or other third party material in this article are included in the article's Creative Commons licence, unless indicated otherwise in a credit line to the material. If material is not included in the article's Creative Commons licence and your intended use is not permitted by statutory regulation or exceeds the permitted use, you will need to obtain permission directly from the copyright holder. To view a copy of this licence, visit http://creativecommons.org/licenses/by/4.0/.

References

1. AbuGhanem M, Eleuch H (2024) NISQ computers: a path to quantum supremacy. IEEE Access 12:102941–102961
2. Dirac P (1930) The principles of quantum mechanics. Clarendon Press, Oxford
3. AbuGhanem M (2019) Properties of some quantum computing models (Master's thesis, Ain Shams University)
4. Harrow AW, Montanaro A (2017) Quantum computational supremacy. Nature 549(7671):203–209
5. AbuGhanem M (2024) Information processing at the speed of light. Front Optoelectron 17:33
6. AbuGhanem M (2024) Photonic Quantum Computers, arXiv preprint arXiv:2409.08229
7. Preskill J (2018) Quantum computing in the NISQ era and beyond. Quantum 2:79
8. Scholten TL et al (2024) Assessing the benefits and risks of quantum computers, *arXiv preprint* arXiv:2401.16317v2
9. IBM Quantum (2024) https://quantum.ibm.com/, accessed August
10. Kim Y et al (2023) Evidence for the utility of quantum computing before fault tolerance. Nature 618:500–505
11. Wendin G, Bylander J (2023) Quantum computer scales up by mitigating errors. Nature 618:462–463
12. Alvarez-Rodriguez U et al (2018) Quantum artificial life in an IBM quantum computer. Sci Rep 8:14793
13. Kandala A et al (2017) Hardware-efficient variational quantum eigensolver for small molecules and quantum magnets. Nature 549:242–246
14. Scalable manufacturing processes for quantum computing (2022) Nat Electron 5:201–202
15. Bravyi S, Dial O, Gambetta JM, Gil D, Nazario Z (2022) The future of quantum computing with superconducting qubits. J Appl Phys 132:160902
16. Dial O (2025) Eagle's quantum performance progress, 23 Mar 2022, https://www.ibm.com/quantum/blog/eagle-quantum-processor-performance. Accessed February 6
17. Castelvecchi D (2023) IBM releases first-ever 1000-qubit quantum chip, The company announces its latest huge chip - but will now focus on developing smaller chips with a fresh approach to 'error correction'. Nature 624:238
18. Ball P (2021) First quantum computer to pack 100 qubits enters crowded race. Nature 599:542
19. Underwood DL et al (2023) Using cryogenic CMOS control electronics to enable a two-qubit cross-resonance gate, arXiv:2302.11538
20. Woerner S, Egger DJ (2019) Quantum risk analysis. npj Q Inf 5:15
21. Havlíček V, Córcoles AD, Temme K, Harrow AW, Kandala A, Chow JM, Gambetta JM (2019) Supervised learning with quantum-enhanced feature spaces. Nature 567:209–212
22. Moll N, Barkoutsos P, Bishop LS, Chow JM, Cross A, Egger DJ, Filipp S, Fuhrer A, Gambetta JM, Ganzhorn M, Kandala A, Mezzacapo A, Müller P, Riess W, Salis G, Smolin J, Tavernelli I, Temme K (2018) Quantum optimization using variational algorithms on near-term quantum devices. Quantum Sci Technol 3:030503
23. Vojtech H, Córcoles Antonio D, Kristan T, Harrow Aram W, Abhinav K, Chow Jerry M, Gambetta Jay M (2019) Supervised learning with quantum enhanced feature spaces. Nature 567:209–212
24. Chemical Industry Contributes \$5.7 Trillion To Global GDP And Supports 120 Million Jobs, New Report Shows. *The European Chemical Industry Council*. March 11 (2019)

25. IBM Institute for Business value (2023) The quantum decade, Fourth edition, ISBN:978-1-7374011-9-3, IBM Corporation 2023, Armonk, NY 10504, USA
26. Coughlin T (2018) 175 Zettabytes By 2025. Forbes. November 27
27. Kandala A, Mezzacapo A, Temme K, Takita M, Brink M, Chow JM, Gambetta JM (2017) Hardware-efficient variational quantum eigensolver for small molecules and quantum magnets. Nature 549:242–246
28. Stamatopoulos N, Egger DJ, Sun Y, Zoufal C, Iten R, Shen N, Woerner S (2019) Option Pricing using Quantum Computers. arXiv:1905.02666
29. Qi G et al (2021) Applications of quantum computing for investigations of electronic transitions in phenylsulfonyl-carbazole TADF emitters. npj Comput Mater 7:70
30. Alemzadeh H, Iyer RK, Kalbarczyk Z, Raman J (2013) Analysis of safety-critical computer failures in medical devices. IEEE Secur & Privacy 11:4
31. Abbas A et al (2021) The power of quantum neural networks. Nat Comput Sci 1:403–409
32. Huang H-Y et al (2021) Power of data in quantum machine learning. Nat Commun 12:2631
33. Douglas T et al (2017) The costs and losses of wildfires: a literature review. NIST Spec Publ 1215:1–72
34. Kaku M (2023) Quantum Supremacy: How the Quantum Computer Revolution Will Change Everything. Doubleday Books, New York
35. Hang J, Wang Y, Li Y (2023) Data-driven quantum approximate optimization algorithm for power systems. Commun Eng 2:12
36. Bodenheimer T, Sinsky C (2014) From triple to quadruple aim: care of the patient requires care of the provider. Ann Fam Med 12:6
37. Denny JC, Collins FS (2021) Precision medicine in 2030-seven ways to transform healthcare. Cell 184(6):1415–1419
38. Andreyev DS, Zybailov BL (2020) Integration of flow cytometry and single cell sequencing. Trends Biotechnol 38:2
39. Shahrjooihaghighi A, Frigui H, Zhang X, Wei X, Shi B, Trabelsi A (2017) An ensemble feature selection method for biomarker discovery. In2017 IEEE International Symposium on Signal Processing and Information Technology (ISSPIT) IEEE, pp. 416-421
40. Obodoekwe N, van der Haar DT (2018) A Critical Analysis of the Application of Data Mining Methods to Detect Healthcare Claim Fraud in the Medical Billing Process. In: Boudriga N, Alouini MS, Rekhis S, Sabir E, Pollin S (eds) Ubiquitous Networking. UNet 2018. Lecture Notes in Computer Science. Springer, Cham, p 11277
41. Menden Michael P, Iorio Francesco, Garnett Mathew, McDermott Ultan, Benes Cyril H, Ballester Pedro J, Saez-Rodriguez Julio (2013) Machine learning prediction of cancer cell sensitivity to drugs based on genomic and chemical properties. PLoS ONE 8(4):e61318
42. Fogel AL, Kvedar JC (2018) Artificial intelligence powers digital medicine. npj Digital Med 1:5
43. Killian JA, Wilder B, Sharma A, Shah D, Choudhary V, Dilkina B, Tambe M (2019) Learning to Prescribe Interventions for Tuberculosis Patients Using Digital Adherence Data. arXiv:1902.01506v3
44. Quak K, Gert-Jan van Z (2019) Dynamic pricing with AI syncsinsurers with market realities: pricing automation improves speed and flexibility. IBM Institute for Business Value. https://www.ibm.com/thought-leadership/institute-business-value/en-us/report/insurance-pricing
45. Emani PS, Warrell J, Anticevic A et al (2021) Quantum computing at the frontiers of biological sciences. Nat Methods 18:701–709
46. Zambelli F, Pesole G, Pavesi G (2012) Motif discovery and transcription factor binding sites before and after the next-generation sequencing era. Brief Bioinform 14(2):225–237
47. Das R, Baker D (2007) Automated de novo prediction of native-like RNA tertiary structures. Proc Natl Acad Sci USA 104(37):14664–14669
48. Muhammed MT, Aki-Yalcin E (2019) Homology modeling in drug discovery: overview, current applications, and future perspectives. Chem Biol & Drug Des 93(1):12–20
49. Cao Y, Romero J, Aspuru-Guzik A (2018) Potential of quantum computing for drug discovery. IBM J Res Dev 62:6
50. Lyu J, Wang S, Balius TE, Singh I, Levit A, Moroz YS, O'Meara MJ, Che T, Algaa E, Tolmachova K, Tolmachev AA, Shoichet BK, Roth BL, Irwin JJ (2019) Ultra-large library docking for discovering new chemotypes. Nature 566:224–229

Springer

51. Cao Y, Romero J, Olson JP, Degroote M, Johnson PD, Kieferova M, Kivlichan ID, Menke T, Peropadre B, Sawaya NPD, Sim S, Veis L, Aspuru-Guzik A (2019) Quantum chemistry in the age of quantum computing. Chem Rev 119:19

52. Johnston SL (2007) Biologic therapies: what and when? J Clin Pathol 60(1):8–17

53. Marks C, Deane CM (2017) Antibody H3 structure prediction. Comput Struct Biotechnol J 15:222–231

54. Robert A, Kl P, Barkoutsos SW, Tavernelli I (2021) Resource-efficient quantum algorithm for protein folding. npj Quantum Inf 7:38

55. Mishra A, Shabani A (2019) High-Quality Protein Force Fields with Noisy Quantum Processors. arXiv:1907.07128

56. Callaway E (2020) It will change everything': DeepMind's AI makes gigantic leap in solving protein structures. Nature 588:203–204

57. Harwood S, Gambella C, Trenev D, Simonetto A, Bernal Neira DE, Greenberg D (2021) Formulating and solving routing problems on quantum computers. IEEE Trans Q Eng 2(3100118):1–17

58. Phillipson F, Chiscop I (2021) Multimodal container planning: a QUBO formulation and implementation on a quantum annealer. In: International Conference on Computational Science. Springer International Publishing, Cham, pp. 30-44

59. Martin P (2022) Cost of supply chain disruptions in selected countries 2021. *Statista*

60. Cross AW, Bishop LS, Sheldon S, Nation PD, Gambetta JM (2019) Validating quantum computers using randomized model circuits. Phys Rev A 100:032328

61. Wack A, Paik H, Javadi-Abhari A, Jurcevic P, Faro I, Gambetta JM, Blake R (2021) Johnson, Scale, Quality, and Speed: three key attributes to measure the performance of near-term quantum computers, arXiv:2110.14108

62. Chow J et al (2014) Implementing a strand of a scalable fault-tolerant quantum computing fabric. Nat Commun 5:4015

63. Processor types, IBM Quantum documentation, https://docs.quantum.ibm.com/guides/processor-types, accessed July (2024)

64. AbuGhanem M (2025) Characterizing Grover search algorithm on large-scale superconducting quantum computers. Sci Rep 15:1281

65. Sheldon S, Magesan E, Chow J, Gambetta J (2016) Procedure for systematically tuning up cross-talk in the cross-resonance gate. Phys Rev A 93:060302(R)

66. Quantum processing units, IBM Quantum platform, https://quantum.ibm.com/services/resources, accessed July (2024)

67. Javadi-Abhari A et al (2024) Quantum computing with Qiskit, *arXive preprint*arXiv:2405.08810

68. Gupta RS et al (2023) Encoding a magic state with beyond break-even fidelity. *arXiv preprint*arXiv:2305.13581

69. AbuGhanem M, Eleuch H (2024) Two-qubit entangling gates for superconducting quantum computers. Results Phys 56:107236

70. Farrell RC et al (2024) Quantum Simulations of Hadron Dynamics in the Schwinger Model using 112 Qubits. *arXiv preprint*arXiv:2401.08044

71. AbuGhanem M et al (2024) Fast universal entangling gate for superconducting quantum computers. Elsevier, SSRN, Rochester, p 4726035

72. Farrell RC et al (2024) Scalable circuits for preparing ground states on digital quantum computers: The schwinger model vacuum on 100 qubits. PRX Q 5:020315

73. AbuGhanem M (2024) Full quantum process tomography of a universal entangling gate on an IBM's quantum computer, *arXiv preprint*arXiv:2402.06946

74. Montanez-Barrera JA, Michielsen K (2024) Towards a universal QAOA protocol: Evidence of quantum advantage in solving combinatorial optimization problems. *arXiv preprint*arXiv:2405.09169

75. Yu H et al (2023) Simulating large-size quantum spin chains on cloud-based superconducting quantum computers. Phys Rev Res 5(1):013183

76. AbuGhanem M, Eleuch H (2024) Full quantum tomography study of Google's Sycamore gate on IBM's quantum computers. EPJ Q Technol 11(1):36

77. AbuGhanem M (2025) Experimental characterization of Google's Sycamore quantum AI on IBM's quantum computers. Elsevier, SSRN, Rochester, p 4299338

78. Zhang V, Nation PD (2023) Characterizing quantum processors using discrete time crystals. *arXiv preprint*arXiv:2301.07625

79. Cerezo M et al (2021) Variational quantum algorithms. Nat Rev Phys 3(9):625–644

80. Alexeev Y et al (2024) Quantum-centric supercomputing for materials science: a perspective on challenges and future directions. Futur Gener Comput Syst 160:666–710

81. Robledo-Moreno J et al (2024) Chemistry Beyond Exact Solutions on a Quantum-Centric Super-computer. *arXiv preprint*arXiv:2405.05068

82. Faro I et al (2023) Middleware for quantum: An orchestration of hybrid quantum-classical systems. *In 2023 IEEE International Conference on Quantum Software (QSW)* 1-8. IEEE

83. Scale to large number of qubits, IBM Quantum documentation, https://docs.quantum.ibm.com/guides/hello-world#scale-to-large-numbers-of-qubits, accessed July (2024)

84. AbuGhanem M et al (2024) Comparative characterization of entropy and heat transfer in carbon-based magnetohydrodynamic Cross nanofluids flowing through PTSCs: advancing thermal applications for solar-powered aircraft. Int J Model Simul. https://doi.org/10.1080/02286203.2023.2301211

85. AbuGhanem M, Raafat PB, Ibrahim FN (2024) An in-depth comparative analysis of entropy generation and heat transfer in micropolar-Williamson, micropolar-Maxwell, and micropolar-Casson binary nanofluids within PTSCs. Zeitschrift für Angewandte Mathematik und Mechanik 104: e202300912

86. AbuGhanem M (2025) Superconducting quantum computers: who is leading the future?. Available at SSRN: https://papers.ssrn.com/sol3/papers.cfm?abstract_id=5177748

87. AbuGhanem M (2024) Google Quantum AI's Quest for Error-Corrected Quantum Computers, arXiv: 2410.00917

88. Arute F et al (2019) Quantum supremacy using a programmable superconducting processor. Nature 574(7779):505–510

89. Chen J-S, Nielsen E, Ebert M, Inlek V, Wright K, Chaplin V, Maksymov A, Páez E, Poudel A, Maunz P, Gamble J (2024) Benchmarking a trapped-ion quantum computer with 30 qubits. Quantum 8:1516

90. Madsen LS, Laudenbach F, Askarani MF et al (2022) Quantum computational advantage with a programmable photonic processor. Nature 606:75–81

91. Bluvstein D, Levine H, Semeghini G et al (2022) A quantum processor based on coherent transport of entangled atom arrays. Nature 604:451–456

92. Wallraff A et al (2004) Strong coupling of a single photon to a superconducting qubit using circuit quantum electrodynamics. Nature 431:162–167

93. You JQ, Nori F (2011) Atomic physics and quantum optics using superconducting circuits. Nature 474:589–597

94. Kelly J, Barends R, Fowler A et al (2015) State preservation by repetitive error detection in a superconducting quantum circuit. Nature 519:66–69

95. Barends R, Shabani A, Lamata L et al (2016) Digitized adiabatic quantum computing with a superconducting circuit. Nature 534:222–226

96. Acharya R et al (2023) Suppressing quantum errors by scaling a surface code logical qubit. Nature 614:676–681

97. Shor PW (1995) Scheme for reducing decoherence in quantum computer memory. Phys Rev A 52: R2493

98. Swingle B (2018) Unscrambling the physics of out-of-time-order correlators. Nat Phys 14:988–990

99. Babbush R, McClean JR, Newman M et al (2021) Focus beyond quadratic speedups for error-corrected quantum advantage. PRX Q 2:010103

100. Morvan A, Villalonga B, Mi X, Mandrà S et al (2023) Phase transition in Random Circuit Sampling. *arXiv preprint*arXiv:2304.11119

101. Kelly J (2018) A Preview of Bristlecone Google's New Quantum Processor, Google Quantum AI Lab

102. Boixo S, Isakov SV, Smelyanskiy VN, Babbush R, Ding N, Jiang Z, Bremner MJ, Martinis JM, Neven H (2018) Characterizing quantum supremacy in near-term devices. Nat Phys 14(6):595–600

103. Fisher MPA, Khemani V, Nahum A, Vijay S (2023) Random quantum circuits. Annu Rev Condens Matter Phys 14(1):335–379

104. Acharya R et al (2024) Quantum error correction below the surface code threshold, arXiv:2408.13687

105. Sivak VV et al (2023) Real-time quantum error correction beyond break-even. Nature 616:50–55

106. Ofek N et al (2016) Extending the lifetime of a quantum bit with error correction in superconducting circuits. Nature 536:441–445

Ⓐ Springer

107. Ni Z et al (2023) Beating the break-even point with a discrete-variable-encoded logical qubit. Nature 616:56–60
108. Bal M, Murthy AA, Zhu S et al (2023) Systematic improvements in transmon qubit coherence enabled by niobium surface encapsulation, arXiv:2304.13257v2
109. Arrasmith A, Patterson A, Boughton A, Paini M (2023) Development and Demonstration of an Efficient Readout Error Mitigation Technique for use in NISQ Algorithms, arXiv:2303.17741v2
110. Daniel A, Maxime D, Bram E, Reagor Matthew J, Dalla Torre Emanuele G (2023) Navigating the noise-depth tradeoff in adiabatic quantum circuits. Phys Rev B 107:125127
111. Dupont M, Evert B, Hodson MJ et al (2023) Quantum Enhanced Greedy Solver for Optimization Problems, arXiv:2303.05509
112. Reagor MJ, Bohdanowicz TC, Rodriguez PD, Sete EA, Zeng WJ (2022) Hardware optimized parity check gates for superconducting surface codes, arXiv:2211.06382
113. Xu Q et al (2023) Constant-Overhead Fault-Tolerant Quantum Computation with Reconfigurable Atom Arrays, arXiv preprint arXiv:2308.08648v1
114. Bravyi S et al (2024) High-threshold and low-overhead fault-tolerant quantum memory. Nature 627:778–782
115. Development & Innovation Roadmap, IBM Quantum, https://www.ibm.com/quantum/assets/IBM_Quantum_Development_&_Innovation_Roadmap.pdf, accessed August (2024)
116. IBM Quantum's technology roadmap, https://www.ibm.com/roadmaps/quantum.pdf, Accessed August (2024)
117. AbuGhanem M (2025) A Toffoli gate decomposition via echoed cross-resonance gates, arXiv:2501.02222 [quant-ph]
118. Kim Y, Wood CJ, Yoder TJ et al (2023) Scalable error mitigation for noisy quantum circuits produces competitive expectation values. Nat Phys 19:752–759
119. Temme K, Bravyi S, Gambetta JM (2017) Error mitigation for short-depth quantum circuits. Phys Rev Lett 119:180509
120. Li Y, Benjamin SC (2017) Efficient variational quantum simulator incorporating active error minimization. Phys Rev X 7:021050
121. Kandala A et al (2019) Error mitigation extends the computational reach of a noisy quantum processor. Nature 567:491–495
122. Endo S, Benjamin SC, Li Y (2018) Practical quantum error mitigation for near-future applications. Phys Rev X 8:031027
123. van den Berg E, Minev ZK, Kandala A et al (2023) Probabilistic error cancellation with sparse Pauli-Lindblad models on noisy quantum processors. Nat Phys 19:1116–1121
124. Chamberland C, Zhu G, Yoder TJ, Hertzberg JB, Cross AW (2020) Topological and subsystem codes on low-degree graphs with flag qubits. Phys Rev X 10:011022
125. Bravyi S, Cross AW, Gambetta JM et al (2024) High-threshold and low-overhead fault-tolerant quantum memory. Nature 627:778–782
126. Wu Y, Wang S-T, Duan L-M (2018) Noise analysis for high-fidelity quantum entangling gates in an anharmonic linear Paul trap. Phys Rev A 97:062325
127. Boguslawski MJ et al (2023) Raman scattering errors in stimulated-Raman-induced logic gates in ^{133}Ba^{+}. Phys Rev Lett 131:063001
128. Houck AA et al (2008) Controlling the spontaneous emission of a superconducting transmon qubit. Phys Rev Lett 101:080502
129. Kitaev AY (2003) Fault-tolerant quantum computation by anyons. Ann Phys 303:2–30
130. Bravyi SB, Kitaev AY (1998) Quantum codes on a lattice with boundary. arXiv:quant-ph/9811052
131. Dennis E, Kitaev A, Landahl A, Preskill J (2002) Topological quantum memory. J Math Phys 43:4452–4505
132. Fowler AG, Stephens AM, Groszkowski P (2009) High-threshold universal quantum computation on the surface code. Phys Rev A 80:052312
133. Tillich J-P, Zémor G (2013) Quantum LDPC codes with positive rate and minimum distance proportional to the square root of the blocklength. IEEE Trans Inf Theory 60:1193–1202
134. Breuckmann NP, Terhal BM (2016) Constructions and noise threshold of hyperbolic surface codes. IEEE Trans Inf Theory 62:3731–3744
135. Higgott O, Breuckmann NP (2021) Subsystem codes with high thresholds by gauge fixing and reduced qubit overhead. Phys Rev X 11:031039

136. Higgott O, Breuckmann NP (2024) Constructions and performance of hyperbolic and semi-hyper-bolic floquet codes. PRX Q 5:040327
137. Breuckmann NP, Eberhardt JN (2021) Balanced product quantum codes. IEEE Trans Inf Theory 67:6653–6674
138. Panteleev P, Kalachev G (2022) Asymptotically good quantum and locally testable classical LDPC codes. In: Proceedings of the 54th Annual ACM SIGACT Symposium on Theory of Computing, pp. 375-388
139. Leverrier A, Zémor G (2022) Quantum Tanner codes. In Proceedings *2022 IEEE 63rd Annual Symposium on Foundations of Computer Science* (FOCS), IEEE. pp. 872-883
140. Kovalev AA, Pryadko LP (2013) Quantum kronecker sum-product low-density parity-check codes with finite rate. Phys Rev A 88:012311
141. Panteleev P, Kalachev G (2021) Degenerate quantum LDPC codes with good finite length performance. Quantum 5:585
142. Wang R, Lin H-K, Pryadko LP (2023) Abelian and non-Abelian quantum two-block codes. arXiv:2306.16400
143. Lin H-K, Pryadko LP (2024) Quantum two-block group algebra codes. Phys Rev A 109:022407
144. MacKay DJC, Mitchison G, McFadden PL (2004) Sparse-graph codes for quantum error correction. IEEE Trans Inf Theory 50:2315–2330
145. Steane A (1996) Multiple-particle interference and quantum error correction. Proc R Soc London A Math Phys Eng Sci 452:2551–2577
146. Calderbank AR, Shor PW (1996) Good quantum error-correcting codes exist. Phys Rev A 54:1098
147. Tremblay MA, Delfosse N, Beverland ME (2022) Constant-overhead quantum error correction with thin planar connectivity. Phys Rev Lett 129:050504
148. Bombín H (2015) Single-shot fault-tolerant quantum error correction. Phys Rev X 5:031043
149. Campbell ET (2019) A theory of single-shot error correction for adversarial noise. Q Sci Technol 4:025006
150. Kubica A, Vasmer M (2021) Single-shot quantum error correction with the three-dimensional sub-system toric code, arXiv preprint arXiv:2106.02621
151. Breuckmann NP, Eberhardt JN (2021) Quantum low-density parity-check codes. PRX Q 2:040101
152. Gallager R (1962) Low-density parity-check codes. IRE Trans Inf Theory 8:21–28
153. Gottesman D (2014) Fault-tolerant quantum computation with constant overhead. Quant Inf Comput 14:1338–1372

Terms and Conditions

Springer Nature journal content, brought to you courtesy of Springer Nature Customer Service Center GmbH ("Springer Nature").

Springer Nature supports a reasonable amount of sharing of research papers by authors, subscribers and authorised users ("Users"), for small-scale personal, non-commercial use provided that all copyright, trade and service marks and other proprietary notices are maintained. By accessing, sharing, receiving or otherwise using the Springer Nature journal content you agree to these terms of use ("Terms"). For these purposes, Springer Nature considers academic use (by researchers and students) to be non-commercial.

These Terms are supplementary and will apply in addition to any applicable website terms and conditions, a relevant site licence or a personal subscription. These Terms will prevail over any conflict or ambiguity with regards to the relevant terms, a site licence or a personal subscription (to the extent of the conflict or ambiguity only). For Creative Commons-licensed articles, the terms of the Creative Commons license used will apply.

We collect and use personal data to provide access to the Springer Nature journal content. We may also use these personal data internally within ResearchGate and Springer Nature and as agreed share it, in an anonymised way, for purposes of tracking, analysis and reporting. We will not otherwise disclose your personal data outside the ResearchGate or the Springer Nature group of companies unless we have your permission as detailed in the Privacy Policy.

While Users may use the Springer Nature journal content for small scale, personal non-commercial use, it is important to note that Users may not:

1. use such content for the purpose of providing other users with access on a regular or large scale basis or as a means to circumvent access control;

2. use such content where to do so would be considered a criminal or statutory offence in any jurisdiction, or gives rise to civil liability, or is otherwise unlawful;

3. falsely or misleadingly imply or suggest endorsement, approval , sponsorship, or association unless explicitly agreed to by Springer Nature in writing;

4. use bots or other automated methods to access the content or redirect messages

5. override any security feature or exclusionary protocol; or

6. share the content in order to create substitute for Springer Nature products or services or a systematic database of Springer Nature journal content.

In line with the restriction against commercial use, Springer Nature does not permit the creation of a product or service that creates revenue, royalties, rent or income from our content or its inclusion as part of a paid for service or for other commercial gain. Springer Nature journal content cannot be used for inter-library loans and librarians may not upload Springer Nature journal content on a large scale into their, or any other, institutional repository.

These terms of use are reviewed regularly and may be amended at any time. Springer Nature is not obligated to publish any information or content on this website and may remove it or features or functionality at our sole discretion, at any time with or without notice. Springer Nature may revoke this licence to you at any time and remove access to any copies of the Springer Nature journal content which have been saved.

To the fullest extent permitted by law, Springer Nature makes no warranties, representations or guarantees to Users, either express or implied with respect to the Springer nature journal content and all parties disclaim and waive any implied warranties or warranties imposed by law, including merchantability or fitness for any particular purpose.

Please note that these rights do not automatically extend to content, data or other material published by Springer Nature that may be licensed from third parties.

If you would like to use or distribute our Springer Nature journal content to a wider audience or on a regular basis or in any other manner not expressly permitted by these Terms, please contact Springer Nature at

onlineservice@springernature.com